Lysosomal degradation of insulin granules promotes β-cell failure in type 2 diabetes

Adrien Pasquier

UNIVERSITÉ DE STRASBOURG

ÉCOLE DOCTORALE DES SCIENCES DE LA VIE ET DE LA SANTÉ

IGBMC

THÈSE présentée par :

Adrien PASQUIER

soutenue le : **08 Novembre 2016**

pour obtenir le grade de : **Docteur de l'université de Strasbourg**

Discipline/ Spécialité : Biologie moléculaire et cellulaire

Lysosomal degradation of insulin granules promotes β-cell failure in type 2 diabetes

THÈSE dirigée par :

M. RICCI Romeo Professeur, Université de Strasbourg

RAPPORTEURS :

M. SAFTIG Paul Professeur, Université de Kiel, Allemagne

M. DONATH Marc Professeur, Université de Bâle, Suisse

AUTRE MEMBRE :

Mme SUMARA Izabela DR2, CNRS

Acknowledgements

I first would like to thanks the committee members for accepting to review my thesis and coming to my defence.

I would like thanks Prof. Romeo Ricci, for giving me the opportunity to work in his team. Your support and patience were really valuable for me who came from a different background. I learn a lot in your lab, scientifically and humanly. I would like to emphasize the constant passion that drive both your work and hobbies, which is exemplary and contagious. Thanks a lot.

J'aimerais ensuite remercier Eric Erbs pour son aide précieuse, les très bons moments, et ses conseils avisés. Je n'oublierai pas le partage de nos points de vue sur des sujets plus ou moins scientifiques mais à chaque fois très importants.

My acknowledgements also go to Alexander Goginashvili who is now in San Diego. Thank you for setting up the project and always give positive and constructive inputs in the numerous skype discussion we had and will have on this project.

I would like to say a big 谢谢 to Zhirong Zhang for teaching me the new CRISPR/Cas9 technique which I am sure will be of great use in a near future. Your determination and kindness were great models for me.

J'aimerais aussi remercier les étudiants que j'ai pu encadrer, David Kaiser et surtout Victor Aubert sans qui le projet n'aurait pas pu aller aussi loin, bonne chance à Caen !

My thoughts also go to the people who formed me at the beginning, Joelle Morvan and Helmuth Gehart. I would also like to thanks all the member of the lab, Gergö for the great help with the mice and the football game, Yan Fan for the delicious tea and Olga for the tiramisu. Thank you also to the members of the Sumara lab.

A big thank to my former Italo-Canadian flat mate Marco Incarbone, who is definitely the alpha male (after Matumbo). Say hi to Marion!

Un grand merci à ma famille pour votre soutien et encouragements, ça a beaucoup compté dans les moments difficiles et les périodes de doutes. Moi + !

Infine, il mio pensiero va a Vale. Condividere la mia vita con te è la mia più grande fonte di felicità !

Table of contents

Acknowledgements 2
Table of contents 3
Figure list 6
Annexes list 7
Introduction 9
I. Glucose sensing and homeostasis at the organismal level 10
A. Pancreatic islets and glucose homeostasis 11
B. The α-cells and glucagon 12
1. Glucagon secretion: Molecular mechanisms 13
2. Glucagon signalling 13
C. The β-cells and insulin 15
1. Canonical Insulin secretion mechanisms 15
2. Potentiation of insulin secretion by incretins 15
3. Other mechanisms regulating insulin secretion 16
4. Neuronal control of insulin secretion 17
5. Insulin granule biogenesis 17
6. Insulin signalling pathway 18
II. Nutrient sensing and homeostasis at the cellular level 20
A. Lipid and glucose sensing 21
1. Lipid sensing 21
2. Glucose sensing 22
B. AMPK and energy sensing 23
1. AMPK activation 23
2. Effects of AMPK activation 24
C. mTORC1 and amino acid sensing. 27
1. mTORC1 activation 28
2. Effects of mTORC1 activation 30
D. ULK1 and macroautophagy 32
1. Macroautophagy molecular regulation 32
1. Autophagy in a disease context 35
E. Lysosomes as a regulatory hub for nutrient sensing 36
III. Nutrient sensing controls pancreatic β-cell function 36

A. Lysosomal degradation of insulin granules in pancreatic β-cells 38
B. PKD functions in pancreatic β-cells 39
IV. T2DM and pancreatic β-cells 40
Aim of the project 42
Material and Methods 43
I. Materials 44
II. Methods 44
A. Mouse maintenance and experimentation 44
B. Molecular cloning and knock-in cell line generation 45
C. Cell lines and transfections 46
D. Isolation of pancreatic islets 47
E. Cell lysis 47
F. Western blot 47
G. qPCR analysis 47
H. Immunofluorescence 48
I. Histochemistery 48
J. Colocalisation analysis 49
K. Transmission electron microscopy (TEM) 49
L. α-cells isolation 50
M. Statistical analysis 50
Results 51
I. Targeting of insulin granules to CD63-positive compartments is increased in diabetic β-cells 52
A. Pancreatic β-cells from diabetic BTBR *ob/ob* mice contain numerous Granule-Containing Lysosomes (GCLs) 52
A. Dramatic changes in CD63 expression and localization in diabetic β-cells 54
B. Generation of a double knock-in INS1 cell line expressing CD63-DsRed and Phogrin-eGFP 57
C. Insulin granules are targeted to CD63 compartments in double knock-in INS1 cells in response to glucolipotoxicity stress 60
D. Diabetic conditions inhibit autophagic flux and autophagosome formation 61
E. Inhibition of lysosomal degradation and autophagy by BafA1 enhances co-localization of CD63 and phogrin 64

F. mTOR is recruited to CD63-positive compartments during glucolipotoxicity challenge 66
G. Knock-down of CD63 restores insulin granules in response to a glucolipotoxic stress 67
II. PKD inhibition contributes to β-cell failure in diabetes 67
A. PKD1 expression is reduced upon onset of diabetes 67
B. PKD1 inhibition increases co-localisation of CD63-positive compartments and insulin granules 69
C. CD63 knock-down partially rescues insulin content in PKD1 depleted INS1 cells 70
D. PKD inhibition *in vivo* leads to faster onset of diabetes in our murine model 71
III. PKD1 activation leads to restoration of the insulin content and improved glucose homeostasis in mice. 73
A. p38δ inhibition activates PKD 74
B. PKD activation *in vivo* delays onset of diabetes 74
C. PKD activation increases insulin granules levels in normal and diabetic human islets 75
IV. LIMP2 is highly expressed in alpha-cells. 76
Discussion 79
References 89
Annexes 101
Résumé 121
Résumé en anglais 121

Figure list

Figure 1 : Pancreatic islets are at the centre of glucose homeostasis in mammals. 12
Figure 2 : The interplay between pancreatic islets and other metabolic tissues. 19
Figure 3 : AMPK is pivotal in the regulation cellular metabolism. 27
Figure 4 : mTORC1 regulation at the lysosomal membrane..... 29
Figure 5 : Molecular mechanisms governing macroautophagy.. 33
Figure 6: Proposed Mechanisms for Reciprocal Regulation of mTORC1 and AMPK at the Cytoplasmic Surface of the Lysosome. 37
Figure 7 : SINGD inhibits autophagy and is controlled by PKD. 39
Figure 8. Colocalisation analysis scheme using the Colocalisation Threshold plugin from Fiji. 49
Figure 9. BTBR *ob/ob* mice become severely obese and diabetic 8 weeks after birth. 52
Figure 10. Increased numbers of GCLs in β-cells of diabetic mice. 53
Figure 11. Expression of LAMP1 is unchanged, while LAMP2 expression is slightly decreased in β-cells of diabetic islets 55
Figure 12. CD63 staining is strongly enhanced in diabetic β-cells. 56
Figure 13. mRNA and protein levels of CD63 are enhanced in a diabetic context. 56
Figure 14. Increase in co-localisation between CD63 and insulin upon glucolipotoxic stress. 57
Figure 15. Generation of CD63-DsRed single knock-in INS1 cells. 58
Figure 16. Generation of CD63-DsRed/Phogrin-eGFP double knock-in INS1 cells. 59
Figure 17. Increase in colocalisation between CD63-Dsred and Phogrin-GFP upon glucolipotoxic stress. 61
Figure 18. Autophagic flux is decreased in diabetic β-cells. 62
Figure 19 : LC3B-GFP dots decrease under glucolipotoxic conditions. 63
Figure 20. Autophagic flux is decreased in INS1 cells under glucolipotoxic conditions. 63
Figure 21 : Glucolipotoxic treatment decreases the levels of LC3B II. 64
Figure 22. Bafilomycin A1 treatment enhanced formation of CD63 and phogrin double positive structures. 65
Figure 23. mTOR is recruited to CD63-positive structures upon glucolipotoxic conditions. . 66
Figure 24. CD63 knock-down leads to restoration of insulin content under glucolipotoxic conditions. 68
Figure 25. PKD1 levels are decreased in diabetic islets and INS1 cells. 69

Figure 26. PKD inhibition led to increased co-localisation between CD63-DsRed and Phogrin-GFP..... 70
Figure 27. Knock-down of CD63 restores abundance and localisation of insulin granules in PKD1-depleted cells..... 71
Figure 28. *In vivo* inhibition of PKD led to acceleration of diabetes..... 72
Figure 29. Inhibition of PKD *in vivo* led to increased GCL formation..... 73
Figure 30. RA treatment activates PKD1 in human islets..... 74
Figure 31. Inhibition of p38δ *in vivo* delayed diabetes development in BTBR ob/ob mice..... 75
Figure 32. RA treatment increases insulin content in human islets from non-diabetic as well as diabetic donors. 76
Figure 33. LIMP2 is higly expressed in α-cells. 77
Figure 34. LIMP2 is highly expressed in insulin-negative cells in the periphery of murine islets. 77
Figure 35 : LIMP2 co-localises with glucagon in glucagon granules..... 78
Figure 36 : Lysosomal Insulin granule degradation mechanisms.. 84

Introduction

To properly function, every system needs energy or at least the possibility to extract it from a given source. For living organisms, nutrients represent the principal energy source. Nutrients are simple organic compounds which produce energy through biochemical reactions. The most common nutrients in our organism are glucose and related sugars, amino acids as well as lipids (Efeyan et al., 2015). As complete lack of nutrients would be detrimental, every species have developed mechanisms for nutrient sensing and storing to ensure sufficient nutrient availability during nutrient scarcity. During a period of abundant nutrients, they will be stored. Conversely, during a period of nutrient depletion, nutrient stocks can be mobilized. Unicellular organisms are directly exposed to nutrients from the extracellular environment. In multicellular organisms, blood circulation guarantees nutrient delivery to different organs/cells after food intake. Specialized organs/cells will provide energy for other cells that do not have the capacity to store and mobilize nutrients during fasting. This requires tight regulation and coordination at the organismal level. In humans, nutrient and energy homeostasis are regulated by hormonal cues that induce multiple signalling pathways in target cells. Dysregulation of these mechanisms are at the origin of metabolic disorders, which increasingly become a major health burden in the world-wide population. The mechanisms involved in nutrient sensing and storing at the organismal level in mammals will first be discussed in this chapter; the focus will then be shifted to cellular mechanisms governing nutrient sensing; the third chapter will cover nutrient sensing and responses in pancreatic β-cells and finally the fourth chapter will address how the latter mechanisms in β-cells may contribute to a predominant metabolic disease, type 2 diabetes (T2D).

I. Glucose sensing and homeostasis at the organismal level

In mammals, nutrients are extracted from the food along the gastrointestinal (GI) track. After being broken down into small molecules by digestive enzymes, nutrients cross the intestinal lining and reach the blood stream where they can be distributed among organs. To ensure proper functioning, the organism needs to maintain a steady delivery of nutrients to different organs also when they are not available. It is therefore important to stock newly absorbed nutrients during food ingestion for later use when food is scarce. Several organs such as adipose tissue,

muscle and liver, are capable of storing nutrients during feeding and of mobilizing them during fasting. Nutrients are delivered to organs through the blood stream allowing for sensing nutrients and the energy status at different levels. The regulatory network of energy homeostasis is comprised of several peripheral organs including the intestinal tract, the liver, the brain, the muscle, the bone, the adipose tissue as well as the pancreas. Among other nutrients such as fatty acids or vitamins, the regulation of glucose levels in mammals and humans is critical and has been extensively studied. Importantly, aberrant glycaemia is a hallmark of diabetes mellitus, a severe metabolic disorder leading to several life-threatening complications.

A. Pancreatic islets and glucose homeostasis

The blood glucose level, also called glycaemia, needs to be kept at a constant level. In humans, optimal glycaemia, or euglycaemia, is comprised between 70mg/dL and 100mg/dL before a meal. Glycaemia higher than 100 mg/dL is called hyperglycaemia. Glycaemia under 70mg/dL is called hypoglycaemia. After food intake, the body is exposed to a hyperglycaemic phase and blood glucose needs to be decreased. Conversely, upon a long period of fasting the body experiences a hypoglycaemic phase and glycaemia needs to increase. Almost a century ago it has been demonstrated that pancreatectomy (removal of the pancreas) in dogs, resulted in severe hyperglycaemia and diabetes, suggesting that this organ is absolutely crucial to maintain normal glucose homeostasis.

The pancreas is composed of two parts, the exocrine pancreas, which represent ~98% of the organ and is responsible for the secretion of the digestive enzymes into the GI track. 1-2% of the organ is composed of the endocrine part consisting of pancreatic islets, also called islets of Langerhans (named after their discovery by Paul Langerhans), which secrete major regulating hormones into the blood stream. The pancreatic islets are composed of five different cell types secreting specific hormones: the α cells (15-20% of the islet cells) which secrete glucagon, the β-cells (~65-80% of the islet cells) which co-secrete insulin, amylin and C-peptide, the γ cells (~3-5% of the islet cells) which secrete pancreatic polypeptide (PP), the δ cells (~3-10% of the islets cells) which secrete somatostatin and finally the ε cells (~<1% of the islet cells) which secrete ghrelin (Röder et al., 2016).

Glucose homeostasis is controlled by the two main hormones insulin and glucagon. Upon hyperglycaemia the pancreatic β-cells secrete insulin into the blood stream. Insulin stimulates glucose uptake into muscle and adipose tissue. At the same time, it induces the conversion from glucose into glycogen, a short-term energy storage product, in the liver by a process called

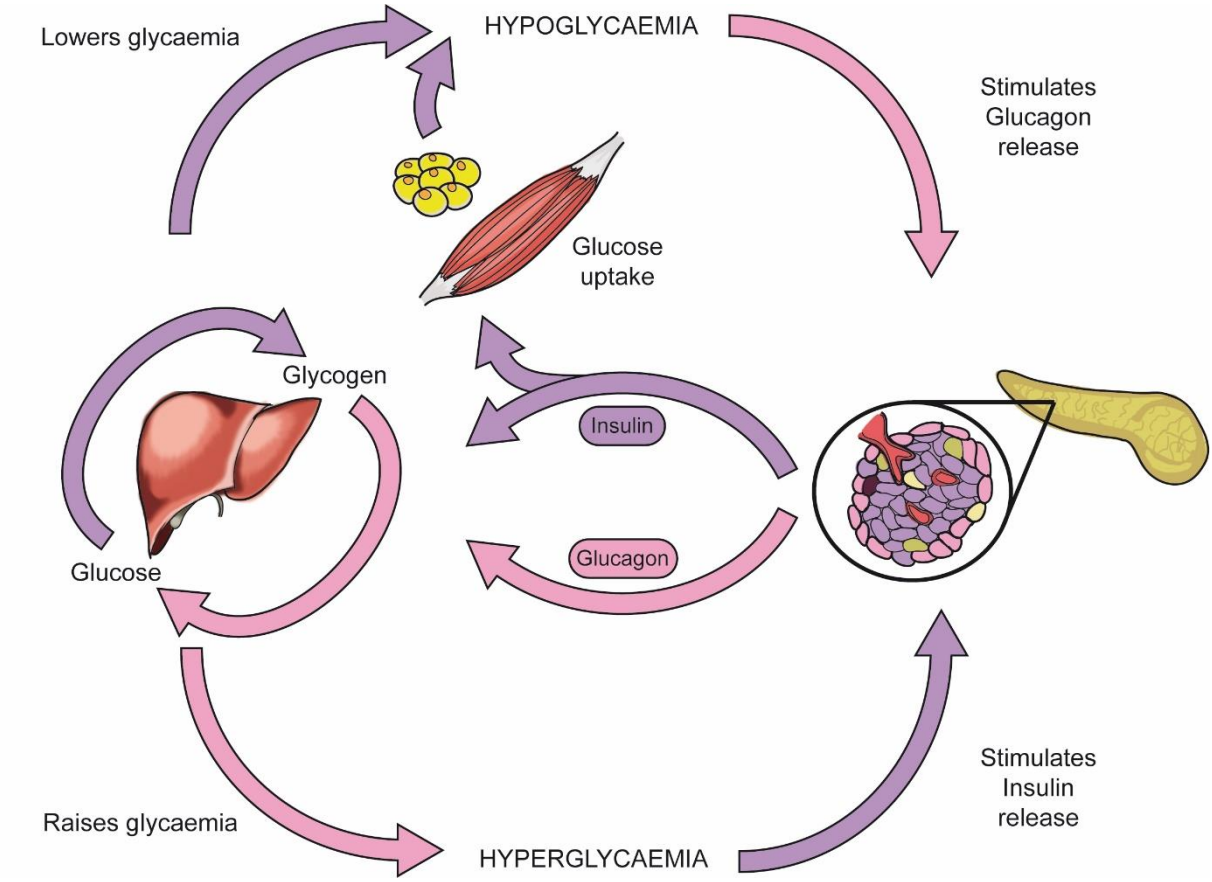

Figure 1 : Pancreatic islets are at the centre of glucose homeostasis in mammals. In the pancreatic islets, the β-cells (purple) secrete insulin in response to increased blood glucose levels (hyperglycaemia). Insulin secreted in the blood stream binds to the insulin receptor (InsR) on muscle cells, adipocytes and hepatocytes. Binding to its receptor triggers signalling pathways inducing cellular glucose uptake. In hepatocytes, insulin triggers storage of glucose in the form of glycogen through glycogenesis. Conversely, upon low blood glucose levels (hypoglycaemia) the α-cells (pink) secrete glucagon into the blood stream. Upon its binding to its receptor (GCGR) on hepatocytes, glucagon activates signalling pathways stimulating the breakdown of glycogen into glucose (glycogenolysis) and *de novo* synthesis of glucose through gluconeogenesis

glycogenesis. Through these actions, insulin decreases blood glucose levels. On the other hand, hypoglycaemia induces the secretion of glucagon into the blood stream from pancreatic α-cells. Glucagon stimulates the breakdown of glycogen into glucose by a process called glycogenolysis and *de novo* synthesis of glucose from non-carbohydrate substrates by gluconeogenesis in the liver, allowing restoration of euglycaemia (Figure 1).

B. The α-cells and glucagon

As mentioned above, the α-cell is the principal source of glucagon, a 29 amino acid peptide hormone, which is secreted at low concentrations under euglycemic conditions. Glucagon

secretion dramatically rises upon hypoglycaemia in order to restore glycaemia by triggering release of glucose from the liver (Campbell and Drucker, 2015). Glucagon is derived from a 160 amino acid pro-glucagon polypeptide encoded by the *GCG* gene. The polypeptide is then cleaved by the pro-hormone convertase 2 (PC2), which is preferentially expressed in α-cells, mainly into glucagon and into the Major proglucagon fragment (MPGF). Proglucagon is directly sorted into dense-core vesicles, indicating that cleavage occurs inside vesicles after leaving the Trans-Golgi-Network (TGN) (McGirr et al., 2013).

1. Glucagon secretion: Molecular mechanisms

Secretion of glucagon is promoted via the action of voltage-dependent sodium (Na^+) and calcium (Ca^{2+}) channels, which maintain action potentials during times of low glucose. Depolarization increases the Ca^{2+} influx and subsequent glucagon secretion, which is supported by the activity of ATP-sensitive potassium (K_{ATP}) channels. As glucose levels rise, secretion of glucagon is inhibited through the elevation of cytosolic ATP, blockade of K_{ATP} channels and termination of the Na^+-induced and Ca^{2+}-induced action potentials. This process inhibits Ca^{2+} influx and terminates glucagon secretion (Habegger et al., 2010).

Glucagon secretion is also regulated through paracrine signals. Insulin and somatostatin through binding on their respective receptors on the α-cell membrane strongly inhibit glucagon release. Glucagon secretion is also inhibited by Zn^{2+} ions and GABA that are co-secreted with insulin.

Neuronal stimulation from both branches of the autonomic nervous systems can also regulate glucagon secretion. The parasympathetic innervation impacts on glucagon secretion upon fasting by stimulating the α-cells. The sympathetic system has been involved in regulation of both α- and β-cells. Noradrenaline can bind to the β2-adrenergic receptor on the α-cells and stimulate glucagon secretion while it inhibits insulin secretion by binding to the α2-adrenergic receptor on the β-cells, thus resulting in amplified glucagon secretion (Thorens, 2014)((Jiang and Zhang, 2003).

2. Glucagon signalling

Upon its secretion in the blood stream, glucagon binds to its target cell through the Glucagon receptor (GCGR), a G-protein coupled receptor. GCGR is present on cells of most metabolic organs including liver, brain, adipose tissue and pancreatic islets.

Binding of glucagon elicits a conformational change of its receptor and subsequent activation of the G-proteins Gsα and Gq. Activation of Gsα leads to the activation of the adenyl cyclase, increase of cyclic AMP (cAMP) levels, and subsequent activation of protein kinase A (PKA).

On the other hand, activation of Gq leads to the activation of phospholipase C, generation of inositol 1,4,5-triphosphate, and subsequent release of intracellular calcium from the ER (Magliarelli 2014, thesis).

In hepatocytes, PKA signalling activates glycogen phosphorylase, which phosphorylates glycogen, increasing the breakdown of glycogen into G6P. Glucagon signalling also leads to the increase of G-6-Pase activity, which enhances conversion of G6P into glucose. Overall, glucagon signalling promotes glycogenolysis, the breakdown of glycogen into glucose (Jiang and Zhang, 2003). The opposite pathway of glycogenolysis, glycogenesis is inhibited by glucagon signalling through phosphorylation and inhibition of the glycogen synthase (GS) enzyme. In addition to glycogen catabolism, glucagon signalling reverses the metabolism of glucose, by inhibiting glycolysis and favouring the opposite pathway, gluconeogenesis. Activated PKA can phosphorylate the PFK2/FBPase-2 polypeptide at Serine 36 leading to inhibition of PFK2 and activation of FBPase-2. This in turn reduces intracellular levels of F(2,6)P2, thereby relieving the inhibition of FBPase-1 and promoting gluconeogenesis. By reducing the levels of F(2,6)P2, the activity of PFK1 is also reduced decreasing glycolysis. The activation of PKA also results in phosphorylation and nuclear localization of cAMP Response Element Binding protein (CREB). Once phosphorylated in the liver, CREB binds to the cAMP response elements of target genes, resulting in recruitment of coactivators, such as hepatic nuclear factor 4α (HNF-4α), peroxisome proliferator-activated receptor γ coactivator 1-α (PGC-1α) and the glucocorticoid receptor to induce transcription of gluconeogenic genes such as Phosphoenolpyruvate carboxykinase (PEPCK). In addition to this well-described pathway, glucagon has also been implicated in signalling via 5'-AMP-activated protein kinase (AMPK) and mitogen-activated protein kinase (MAPK)-dependent manner (Habegger et al., 2010).

In addition to its canonical role in glucose homeostasis, Glucagon has been shown to regulate lipid homeostasis by regulating triacylglycerol (TAG) levels in the liver as well as cholesterol and lipolysis in white adipose tissue. It is also involved in thermogenesis in the brown adipose tissue. Finally the GCGR is highly expressed in the Central Nervous System, and Glucagon signalling has been reported to play an important role in food intake behaviour (Habegger et al., 2010).

The opposite hormone of glucagon is insulin, which is secreted by the neighbouring β-cells in the pancreatic islets. In comparison to α-cells, the β-cells have been a lot more studied and more information related to their function are available.

C. The β-cells and insulin

Except for a small production in the neurogliaform cells in the brain (Molnár et al., 2014), the pancreatic β-cells are the major source of insulin in mammals. Because of its important hypoglycaemic effect, insulin needs to be secreted at the right moment and at the right dose, which necessitates intricate mechanisms.

1. Canonical Insulin secretion mechanisms

Insulin is secreted outside the β-cells and into the blood stream upon a raise in the glycaemia. Upon acute post-prandial hyperglycaemia, glucose enters β-cells through the bidirectional Glucose Transporter 2 (GLUT2) and is phosphorylated by the glucokinase (GK) trapping it inside the cell. Phosphorylated glucose then enters the glycolytic pathway, which modifies it into pyruvate which is then transported to mitochondria. Pyruvate is then metabolized into acetyl-CoA that enters the TCA cycle. ATP is directly generated during glycolysis and the TCA cycle. Furthermore, NADH and NADH/FADH2 produced during glycolysis and the TCA cycle, respectively are used to produce ATP through the electron transport chain. ATP production decreases the ADP/ATP and AMP/ATP ratios. This closes the ATP-sensitive K^+ channel, trapping K^+ inside the β-cell resulting in depolarization and subsequent opening of the voltage-dependent Ca^{2+} channel VDCC. This provokes Ca^{2+} entry, which promotes insulin granule fusion with the plasma membrane and release of its content to the blood stream or in the extracellular space within the islet where it can fulfil paracrine or autocrine actions. However, the current view in the field is that this canonical pathway acts in concert with numerous secondary pathways which are triggered by metabolic coupling factors (MCFs). Nutrients processed in metabolic pathways produce co-products that are used as signalling cues to trigger auxiliary pathways. The MCFs can be categorised into two groups: the effectory MCFs (EMCFs) which are responsible for the initiation of insulin secretion or the regulatory MCFs (RMCFs) which only modulate insulin secretion. Those MCFs have been extensively reviewed in Prentki et al., 2013.

2. Potentiation of insulin secretion by incretins

Insulin release is fine-tuned and potentiated by signals emerging from other nutrient sensing tissues. For example, incretins released from the gut have gained a lot of attention. The gut is the first organ to be in contact with nutrients upon food absorption and digestion. Despite this fact, it was long considered as an organ exerting digestion of food only (Badman and Flier,

2005). However, enteroendocrine cells residing in the gut can secrete hormones to the blood stream that are important in energy homeostasis. The L cells residing mainly in the ileum and colon secrete glucagon like peptide 1 (GLP1), one of the two members of the incretin family. This hormone, derived from the pre-pro-glucagon polypeptide through cleavage by the PC1 enzyme, is secreted in response to nutrients such as free fatty acid (FFA) or carbohydrates. Among other important functions, GLP-1 stimulates secretion of insulin from pancreatic islets while inhibiting secretion of glucagon by binding to its GPCR receptor (GLP1R). GLP1 levels are tightly controlled through its fast degradation by the dipeptyl peptidase IV (DPP4) resulting in half-life of only two minutes in the blood circulation.

Glucose-dependent insulinotropic polypeptide (GIP), the second member of the incretin family, is like GLP1 rapidly inactivated by DPP4 (half-life is 4-5min). GIP is secreted by the K cells in response to an increase in glucose and fat in the guts and strongly promotes insulin secretion from the pancreatic islets by binding to GIPR.

GLP-1 and GIP can enhance insulin secretion in a glucose stimulation-dependent manner by binding to their respective receptors present on the β-cells surface. The GLP1R and GIPR are GPCR receptors. Receptor binding of their specific agonist leads to the activation of the adenylyl cyclase protein (AC) and production of cyclic AMP (cAMP) (and pyrophosphate) which activates protein kinase A (PKA) upon low cAMP increase, or the exchange protein directly activated by cAMP (EPAC) upon high cAMP increase. Activation of PKA leads to closure of K_{ATP} and facilitation of membrane depolarization. PKA also leads to inhibition of the delayed rectifying K_v channel, a negative regulator of insulin secretion, resulting in prolongation of action potentials (Yabe and Seino, 2011). PKA and EPAC also promote mobilization of intracellular Ca^{2+} stocks from the Endoplasmic Reticulum (ER), which increases the fusion of the insulin granule with the plasma membrane. Increased Ca^{2+} levels also induce transcription of the insulin gene (Seino et al., 2010)(Yabe and Seino, 2011).

Finally the prototypical cholecystokinin hormone (CCK), secreted inside the gut lumen by the I cells from the duodenum and jejunum, can also promote the secretion of insulin (Badman and Flier, 2005).

3. Other mechanisms regulating insulin secretion

Paracrine signalling also affects release of insulin from β-cells. Upon binding to its receptor SSTR2 on the β-cell membrane, somatostatin secreted by the δ-cells attenuates insulin secretion.

Adiponectin, an adipokine secreted by the adipose tissue, increases insulin secretion (Röder et al., 2016). Leptin, the other prominent adipokine, has been shown to regulate insulin level but rather indirectly through action in the Central Nervous System (CNS) by activating the proopiomelanocortin (POMC) and inhibiting the Agouti related protein and the Neuropeptide Y (AgR/NPY) neurons (Begg and Woods, 2013). Finally the adipokine/myokine Interleukine 6 (IL-6) was shown to enhance GLP-1 secretion, indirectly increasing insulin secretion from the β-cells (Röder et al., 2016).

4. Neuronal control of insulin secretion

Insulin release is also amplified by neuronal signals coming from the brain. However, these signals are rather secondary and sustain insulin secretion triggered by glucose, as glucose sensing by the brain is delayed in comparison to the peripheral organs. Pancreatic islets, including both β- and α-cells, are highly innervated by both branches of the autonomic nervous system: the sympathetic and parasympathetic nervous system. The parasympathetic innervation allows for local release of acetylcholine, which binds to the muscarinic receptor m3AchR present on the surface of the β-cells and is involved in the potentiation of insulin secretion. The parasympathetic nervous system is also involved in the cephalic phase of insulin release (CIPR), which is triggered by the gustatory machinery on the tongue and prepare the body for glucose increase subsequent to food intake (Just et al., 2008). Moreover, the parasympathetic nervous system regulates pancreatic β-cell expansion during the neo-natal development. Sympathetic innervation has also been involved in the setting up of the islet architecture during development (Borden et al., 2013). It also blunts insulin secretion via the release of Neuropeptide Y (NPY) on the β-cells (Thorens, 2014)(Röder et al., 2016). Overall, insulin secretion is tightly regulated as its release into the organism has massive metabolic consequences.

5. Insulin granule biogenesis

Compared to glucagon, insulin biogenesis has been more studied. Insulin is first synthesized as a pre-pro-insulin precursor on the ribosome of the Rough Endoplasmic Reticulum (RER), and is cleaved to proinsulin during its translocation into the lumen of the RER. Subsequently, proinsulin molecules pass through RER and Golgi to the Trans-Golgi network (TGN) to be packed inside special vesicles, the so-called insulin secretory granules. Insulin secretory granules serve as a compartment where maturation of proinsulin to insulin occurs through coordinated activity of endopeptidases (Goginashvili 2015, thesis). While the distal mechanism involving insulin granule secretion via fusion with the plasma membrane have been extensively

studied, the biogenesis of insulin granules at the TGN is less known. My laboratory made several important discoveries in this context which will be discussed later in the following sections.

6. Insulin signalling pathway

Insulin is released into the blood stream reaching different target organs. Upon its binding to its receptor, InsR, insulin activates the insulin pathway. The InsR is a member of the tyrosine kinase receptor family and is widely expressed on the cell surface of almost all organs including the brain and islet cells. It can bind insulin, Insulin-like growth factor 1 (IGF1) and IGF2. Upon binding of insulin on its extracellular α subunit, the InsR dimerizes putting in close localization its intracellular β-subunits, allowing the autophosphorylation of the InsR which creates new docking sites for substrate proteins such as insulin receptor substrate 1 (IRS1), IRS2 or Src homology 2 domain containing transforming protein (SHC). The InsR can then phosphorylate bound substrates, recruiting additional substrates. The InsR activates mainly two major cellular pathways: the PI3K-Akt pathway that impacts on glucose uptake, lipid metabolism, glycogen synthesis and gluconeogenesis and the MAPK pathway which plays a role in protein synthesis, growth, survival and differentiation. The actual outcome of insulin receptor activation depends on the expression of downstream signalling modules in the stimulated cell. Therefore, the responses to insulin differ depending on which tissue is targeted (Gehart et al., 2010).

In the liver, as opposed to glucagon, insulin binding upon its receptor activates glycolysis and glycogenesis. Insulin stimulates glycolysis by increasing the expression of the hepatic glucokinase gene (GK). Insulin inactivates the glycogen phosphorylase (GP) and the glycogen synthase (GS) through the PI3K-Akt pathway, which in turn activates glycogen synthase (Röder et al., 2016) in order to favour glycogenesis. Insulin also represses the expression of the PEPCK gene by disrupting CREB association with RNA pol II. Expression of the G-6-Pase gene through forkhead transcription factor (Foxo1) is attenuated by PKB/Akt-mediated phosphorylation of Foxo1 and exclusion of the latter from the nucleus.

In muscle and adipose tissue, insulin promotes glucose uptake through GLUT4. PI3K recruitment and activation at the plasma membrane generates PI(3,4,5)P3 recruiting the phosphoinositide-dependent kinase 1 (PDK1). PDK1 phosphorylates and activates PKB/Akt and atypical Protein Kinase C (aPKC), which promotes the translocation of the GLUT4 receptor to the membrane (Sandoval et al., 2007)(Khan and Pessin, 2002).

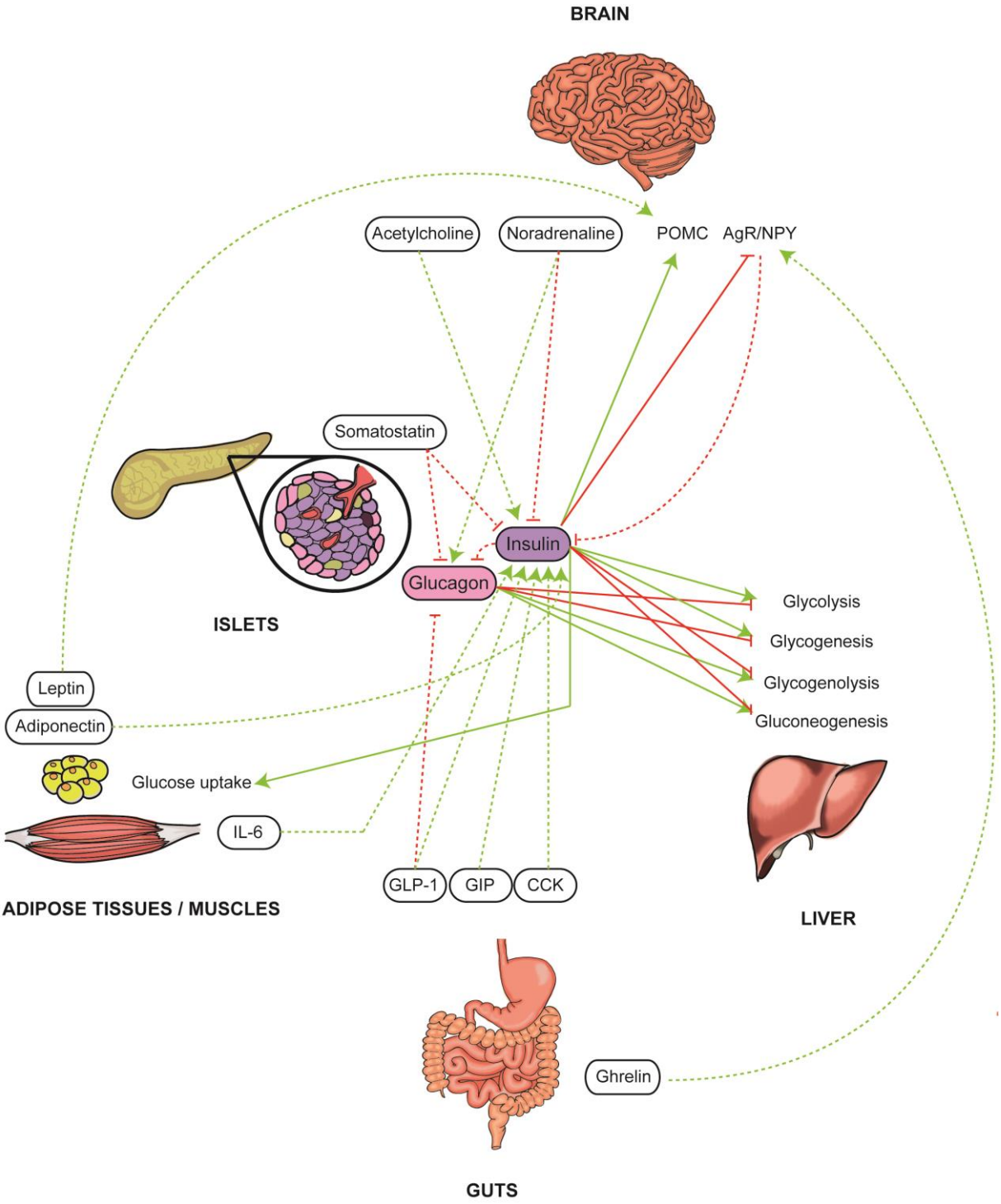

Figure 2 : The interplay between pancreatic islets and other metabolic tissues. The full green arrow represents functions of insulin or glucagon that activate indicated processes. The red line highlights functions of insulin or glucagon that inhibit indicated processes. The dashed green arrows show effects of indicated factors promoting insulin and or glucagon actions functions. The red dashed lines show effects of indicated factors inhibiting the action of insulin and/or glucagon. Details are explained in the text above.

Finally, insulin together with leptin are the main hormones feeding the CNS with information about the nutrient status and energy homeostasis of the organism, the so-called adiposity signals (Porte et al., 2005), (Sandoval et al., 2007). Both leptin and insulin can cross the blood-brain barrier and bind on their respective receptors. The InsR is highly expressed in the arcuate nucleus of the hypothalamus. There it activates the POMC neurons, which produce and release the α-melanocyte-stimulating hormone (α-MSH) that is involved in the energy expenditure and weight loss, overall exerting an anorectic effect (Sandoval et al., 2007). Another population of neurons is present in the arcuate nucleus, the AgRP/NPY producing neurons. They are orexigenic neurons, meaning they promote food intake and are inhibited upon insulin signalling (Röder et al., 2016).

The pancreatic islets are centrally involved in the regulation of glucose homeostasis. Their complex interplay with other central organs trough hormonal cues, neuropeptides or cytokines allows the organism to react accordingly to changes in nutrient availability and to optimally use the stored energy in times when nutrients are sparse. In the next part, I will focus on nutrient sensing mechanisms occurring at the cellular level highlighting the main molecular players in this context. The links between cellular metabolism and organismal metabolism will also be discussed.

II. Nutrient sensing and homeostasis at the cellular level

Once nutrients are delivered to the cells via the vasculature, they can be used and processed by the cell to derive energy. The sensing of a particular nutrient may involve direct binding of the molecule to its sensor, or occur by an indirect mechanism relying on the detection of a surrogate molecule that reflects nutrient abundance (Efeyan et al., 2015). Lipids and glucose levels can be directly monitored by specific sensors, some examples will be discussed in the first part of this chapter. During energy depletion, the cell can sense a decrease in the energy stock and react accordingly by decreasing their energy consuming pathways and promoting the energy producing one through the activation of a central cellular metabolism player which will be discussed in the second part of this chapter. Conversely, during nutrient abundance, the cells adapt their metabolism to expand and proliferate through the activation of another key

metabolic player which will be discussed in the third part. Upon starvation, cells can trigger a self-cannibalistic process to generate *de novo* nutrients, which will be discussed in the fourth part of this chapter. Finally the lysosome, an organelle common to several nutrient and energy sensors will be discussed in the last part of this chapter.

A. Lipid and glucose sensing

1. Lipid sensing

Lipids are nutrients characterized by their hydrophobic carbon backbones and can be used for energy storage and membrane biosynthesis. The cells process lipids in several metabolic pathways to derive energy and their sensing is important for cells to monitor their resource status. However lipid sensing at the cellular level is unclear to a large extent (Efeyan et al., 2015). The most studied lipids are free fatty acids (FFA) and cholesterol.

a) Free fatty acid sensing

FFA sensing can occur at the extracellular space through their binding to G-protein coupled receptors (GPCR) anchored at the plasma membrane. The two most studied receptors are GPR40 and GPR120 (Efeyan et al., 2015). In the pancreatic β-cells, FFA binding to GPR40 was shown to increase glucose stimulated insulin secretion in the blood (Itoh et al., 2003). FFA binding to GPR120 is involved in Glucagon-like peptide 1 (GLP-1) release from the enteroendocrine cells (Hirasawa et al., 2004). Moreover, GPR120 FFA binding at the plasma membrane of adipocytes also leads to the activation of the PI3K-Akt pathways, leading to subsequent glucose uptake from the adipocytes (Young Oh et al., 2010). GPR120 total knock out mice develop severe obesity under a high fat diet, and dysregulation of the *GPR120* gene is a feature in obese human patients (Ichimura et al., 2012). In addition to GPCRs, Cluster of Differentiation 36 (CD36) (also known as FAT) receptor has been implicated in direct binding and uptake of intestinal luminal fatty acids (Efeyan et al., 2015).

b) Cholesterol sensing

Cholesterol sensing is better known and strongly relies on regulation of the Sterol regulatory element binding protein 1 (SREBP1) (Brown and Goldstein, 1986). Cholesterol can be derived from the diet or can be synthetized *de novo* by the cells. It is necessary for membrane fluidity and generation steroid-related metabolites. Upon its presence in the lipid bilayer, it binds to the SREBP1 cleavage activity protein (SCAP), which forms a dimer with the SREBP1 protein

(Brown et al., 2002). Cholesterol binding promotes the complex interaction with the Insulin induced gene (INSIG) anchor protein, trapping it in the ER membrane (Yang et al., 2002). Upon cholesterol removal from SCAP due to cholesterol decrease, the SCAP/SREBP1 dissociates from INSIG and shuttles to the Golgi apparatus where the cytoplasmic N-terminal SREBP1 peptide is cleaved off. This allows for nuclear translocation of the cleaved peptide, where it can regulate genes involved in the cholesterol biosynthesis pathway. When the cholesterol levels raise up again, retention of INSIG in the SCAP/SREBP1 complex prevents cleavage of the N-terminus leading to inhibition of cholesterol biosynthesis (Radhakrishnan et al., 2008). SREBP1 can be regulated by another master regulator of nutrient sensing, mTORC1 which will be detailed in the following sections. Inhibition of mTORC1 led to a decrease in expression and processing of SREBP1, leading to a decrease of the transcription of the cholesterol regulating genes (Laplante and Sabatini, 2012).

2. Glucose sensing

Glucose sensing is crucial for mammalian cells as its metabolism is at the centre of energy homeostasis. Because glucose sensing can differ a lot from one cell type to another, I will mainly focus in this part on the general glucose sensing mechanisms common to many cell types.

a) Glucose entry and GLUT2 sensing

The GLUT2 protein is a sensor of extracellular glucose levels and is present on the plasma membrane of enterocytes, kidney epithelial cells, pancreatic β-cells, hepatocytes and in neurons from the CNS (Thorens, 2014). In contrast to other GLUT proteins (like GLUT4 in the adipocyte and skeletal muscles), GLUT2 has a low affinity towards glucose. Its K_m, an inverse measure of affinity, is around 20mM while K_ms of GLUT1 and GLUT4 are around 1mM and 5mM, respectively (Efeyan et al., 2015). GLUT2 allows for efficient transport of glucose across the plasma membrane only under hyperglycaemia while the others GLUTs are active even during low glycemic conditions. Once inside the cell, glucose encounters a second sensor: the glucokinase.

b) Glucokinase sensing

Glucokinase (GCK) catalyses the first step in the storage and consumption of glucose, glycogen synthesis and glycolysis, and its function constitutes a simple, direct intracellular nutrient-sensing mechanism that controls systemic glucose homeostasis. Like all hexokinases, GCK

phosphorylates glucose to make glucose-6-phosphate (G6P) trapping it inside the cytoplasm, but unlike the other isozymes, only GCK functions as a glucose sensor because of its low affinity towards glucose (Efeyan et al., 2015). As GLUT2, GCK is only active under high glucose concentrations. GCK is expressed in hepatocytes, pancreatic β-cells as well as hypothalamic neurons.

In addition to direct mechanisms, glucose and lipid sensing can occur indirectly through sensing consumption of the main energy source Adenosine triphosphate (ATP) that is predominantly derived through lipid and glucose catabolism.

B. AMPK and energy sensing

Nutrients are taken up by cells and converted into energy by a series of metabolic pathways among which glycolysis or the Krebs cycle are the most prominent ones. The main cellular energy carrier in the cell is ATP which delivers its energy through its hydrolysis into Adenosine Diphosphate (ADP) and phosphate or into Adenosine monophosphate (AMP) and pyrophosphate. Because ATP is the source of energy for most cellular processes, cells need to keep their ATP proportion higher than ADP or AMP, in other words their AMP/ATP and ADP/ATP ratios need to be kept low. Cells can monitor their energetic status by sensing changes in AMP/ATP and ADP/ATP ratios. AMP-activated protein kinase (AMPK) is a principal player common to all eukaryotic cells, which can sense changes in those ratios.

1. AMPK activation

AMPK is a heterotrimeric protein complex formed by a catalytic α subunit and the regulatory β and γ subunits. The AMPK complex is phosophorylated at threonine 172 by the Ca2+/calmodulin-dependent protein kinase kinase-β (CamKKβ) (Woods et al., 2005) or the Liver kinase B1 (LKB1) (Shackelford and Shaw, 2009). ATP, ADP or AMP directly bind on the AMPK γ subunit. When ATP levels are optimal, the γ subunit binds two ATPs and one AMP. Binding to additional AMP prevents dephosphorylation of AMPK and promotes allosteric activation of the phosphorylated kinase (Hardie, 2014). Binding to AMP also promotes threonine 172 phosphorylation by LKB1, via the Axin scaffold protein, which triggers interaction of AMPK with LKB1 (Zhang et al., 2013). AMPK activation thus occurs upon ATP depletion, through the binding of AMP. *In vivo,* the AMP/ATP and ADP/ATP ratio can raise because of decrease ATP production originating from defects in the metabolic pathways or

shortage in nutrient supply happening for instance during ischemia, hypoxia or hypoglycaemia (Hardie, 2014). The AMP/ATP and ADP/ATP can also raise because of higher consumption of ATP, happening for example in muscle cells during exercise. AMPK has been shown to be activated by 5-Aminoimidazole-4-carboxamide ribonucleoside (AICAR), an analog of AMP frequently used to test AMPK gain-of-function.

2. Effects of AMPK activation

AMPK is a cellular energy regulator. Upon its activation, it enhances catabolic pathways to restore the depleted ATP levels, and inhibits anabolic pathways to prevent further ATP consumption, until the energy balance is recovered. It has been shown to regulate numerous downstream targets regulating metabolic processes involved in glucose, protein and lipid metabolism as well as mitochondrial biogenesis and autophagy.

a) AMPK and glucose metabolism

AMPK has a major role in glucose metabolism. First, AMPK can directly regulate glucose entry inside cells by regulating the glucose transporter proteins. In hepatocytes, AMPK activation increases glucose uptake by increasing GLUT1 translocation to the plasma membrane. It does so by phosphorylating the Thioredoxin-interacting protein (TXNIP) on Serine 308, accelerating TXNIP degradation. TXNIP induces clathrin-dependent internalisation of GLUT1 through direct binding with GLUT1 and also decreases GLUT1 mRNA transcription through an unknown mechanism. Phosphorylation by AMPK enhances it degradation and leads to restoration of GLUT1 translocation to the plasma membrane and *GLUT1* transcription (Wu et al., 2013). In skeletal muscle cells, AMPK regulates translocation of GLUT4 in a similar way (Kurth-Kraczek et al., 1999) through phosphorylating TBC1 domain family member 1 (TBC1D1) on Serine 237 and 596. TBC1D1 is a Rab-GTPase activating protein (GAP), which prevents GLUT4 translocation to the plasma membrane. Upon its phosophorylation by AMPK, it is sequestered by binding to a 14-3-3 scaffold protein, inactivating its inhibitory function towards GLUT4 (Pehmøller et al., 2009). AMPK activity can also increase *GLUT4* transcription by phosphorylating the Histone Deacetylase 5 (HDAC5) on Serine 259 and 458, which triggers HDAC5 binding to the scaffold protein 14-3-3 trapping it in the cytoplasm. This leads to the recovery of H3 acetylation and *GLUT4* transcription (McGee et al., 2008).

Second, AMPK regulates the glycolytic pathway. In parallel to PKA-mediated glucagon responses in hepatocytes (see previous section), AMPK phosphorylates the PFK2/FBPase-2 polypeptide at Serine 466, activating PFK2 and leading to the production of Fructose-2,6-

biphosphate (F(2,6)P2). F(2,6)P2 is known to allosterically stimulate the PFK1 enzyme a key component of the glycolysis pathway which converts Fructose-6-phosphate (F-6-P) into Fructose-1,6-biphosphate (F(1,6)P2) and finally into pyruvate (Marsin et al., 2000). In monocytes, Serine 461 of PFK2 is also phosphorylated by AMPK during hypoxic stress (Marsin et al., 2002).

As mentioned above, the opposite pathway of glycolysis is gluconeogenesis. AMPK inhibits gluconeogenesis through phosphorylation of the class II HDACs (HDAC4,5 and 7), trapping them in the cytoplasm. Normally, class II HDACs translocate to the nucleus where they can recruit HDAC3, which deacetylates the FOXO1 transcription factor promoting the expression of the *G6PC* gene, which encodes the G-6-Pase catalytic unit. G-6-Pase is responsible for dephosphorylation of glucose-6-phosphate, the last step of gluconeogenesis. By trapping class II HDACs in the cytoplasm, AMPK prevents G-6-Pase transcription and dephosphorylation of glucose-6-phosphate (Mihaylova et al., 2011). Finally, AMPKα2 directly phosphorylates Glycogen Synthase (GS) on Serine 7 decreasing glycogen synthesis in muscle cells (Habets et al., 2008)(Jørgensen et al., 2004).

b) AMPK and lipid metabolism

AMPK promotes fatty acid uptake into cardiac myocytes via translocation of vesicles containing the fatty acid transporter CD36 to the plasma membrane. However, the precise mechanisms remains unknown (Habets et al., 2008). Activation of AMPK with AICAR, leads to enhanced fatty-acid oxidation in muscle to regenerate the ATP stocks (Merrill et al., 1998). AMPK is thought to regulate β oxidation by inhibiting acetyl-CoA carboxylase 2 (ACC2) at Serine 221. ACC2 produces malonyl-CoA on the mitochondriat surface, which is an inhibitor of carnitine palmitoyltransferase 1 (CPT1). CPT1 is responsible for the transport of long chain fatty acids into the mitochondria. Therefore its inhibition prevents β oxidation, overall AMPK thus promotes β oxidation (Muoio et al., 1999)(O'Neill et al., 2012). Conversely, AMPK shuts down the ATP consuming pathways involved in lipid storage and synthesis. In the liver and muscle AMPK inhibits the mitochondrial isoform of *sn*glycerol-3-phosphate acyltransferase (GPAT), the enzyme which catalyses the initial and committed step in glycerolipid biosynthesis. GPAT inhibition decreases the *de novo* synthesis of Triacylglycerol (TAG) and phospholipids (Muoio et al., 1999). AMPK also decreases lipogenesis (fatty acid synthesis) by phosphorylating SREBP1c on Serine 372. This phosphorylation prevents SREBP1c cleavage and translocation of the cleaved peptide to the nucleus, inhibiting the transcription of the lipogenic enzymes (Li et al., 2011). Finally HMGR is the rate-limiting enzyme for isoprenoid

and cholesterol synthesis and a substrate for AMPK. The catalytic activity of HMGR is inhibited by phosphorylation of Serine 872 by AMPK (Clarke and Hardie, 1990).

c) AMPK and protein metabolism

Protein degradation can also be a source of energy. One process governing protein degradation is autophagy. This process, I will describe in details in the following sections. Herein, I cover AMPK-dependent autophagy regulation. Shortly, AMPK can trigger autophagy by activation of the master regulator Unc51-like kinase (ULK1) through phosphorylation of multiple serines (Egan et al., 2010) (Kim et al., 2011).

Conversely, protein biosynthesis is inhibited by AMPK. TIF-IA, the RNA Pol I-associated transcription factor that transmits external signals to the nucleolar transcription machinery, is targeted by a variety of protein kinases that phosphorylate it at multiple sites. Upon glucose depletion and AMPK activation, TIF-1A is phosphorylated on Serine 635, leading to a decrease in RNA Pol1-dependent transcription and rRNA biosynthesis (Hoppe et al., 2009). AMPK also inactivates mammalian target of Rapamycin complex 1 (mTORC1), another major master regulator of cellular metabolism, which will be discussed in the following paragraph. AMPK regulates mTOR by at least two mechanisms: first, through activation of the mTORC1 inhibitory protein complex TSC2 through phosphorylation of Threonine 1227 and 1345 (Inoki et al., 2003), and second by direct phosphorylation of the mTORC1 Raptor subunit on Serine 792 leading to its binding to 14-3-3 and the inactivation of mTORC1 (Gwinn et al., 2008). Further details will be provided in the next paragraphs.

d) AMPK and mitochondria

Finally AMPK promotes mitochondrial biogenesis by activating key transcriptional factors through phosphorylation. Increasing mitochondrial biogenesis increase ATP production in long-term. AMPK was shown to phosphorylate the transcriptional coactivator PGC-1α on Threonine 177 and Serine 538 which is thought to promote its docking on transcription factors leading to the increase in transcription of important genes involved in mitochondrial biogenesis such as NRF2, PDK4 or MCAD (Jäger et al., 2007). PGC-1α-dependent transcriptional activity is also regulated through its deacetylation by the SIRT1 protein (Lagouge et al., 2006). AMPK can regulate SIRT1 activity by modulating the NAD+ cellular levels by enhancing beta-oxidation. Moreover, Canto et al demonstrated that PGC-1α phosphorylation was necessary for SIRT1 deacetylation (Cantó et al., 2009) placing AMPK in the centre of regulation of

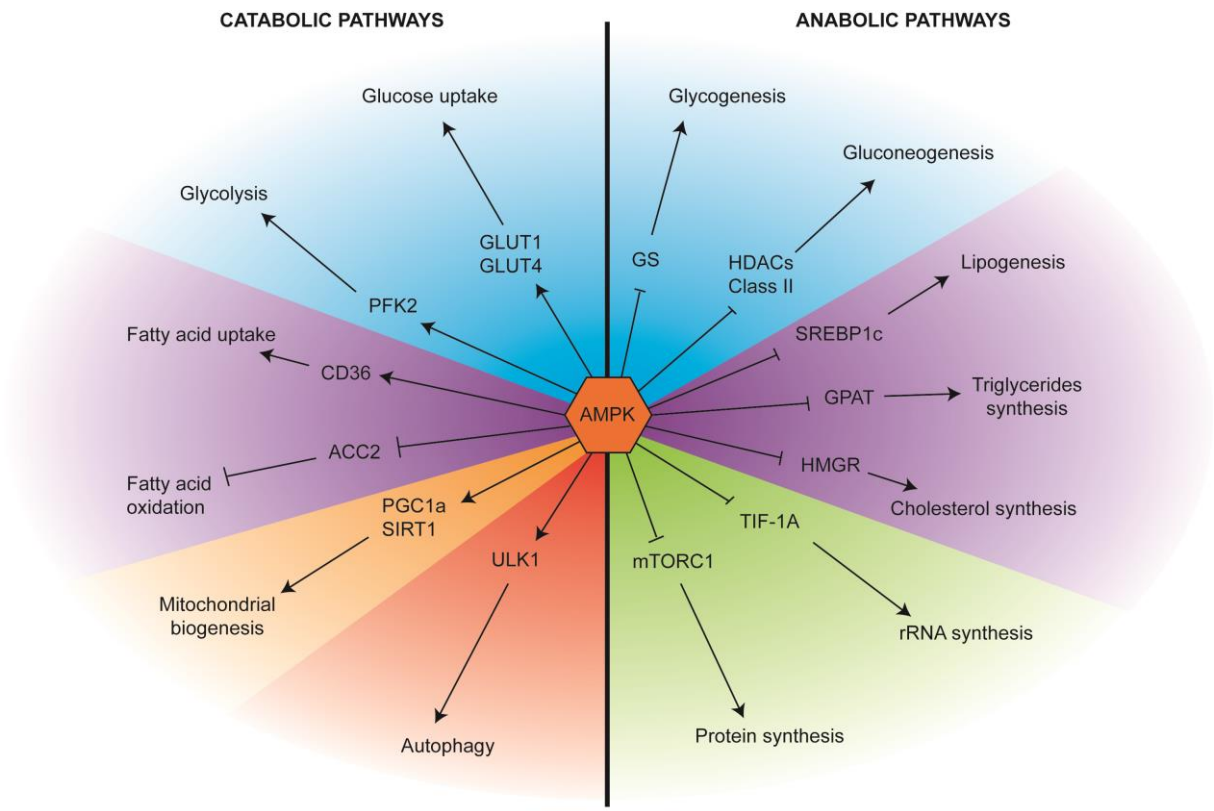

Figure 3 : AMPK is pivotal in the regulation cellular metabolism. Upon activation of AMPK, catabolic pathways are promoted, while anabolic pathways are inhibited. Different types of nutrients are depicted with different colours: blue is used to highlight glucose metabolism, purple is used to indicate lipid metabolism and green is used to show protein metabolism. Mitochondrial regulation and autophagy are shown in orange and red, respectively. The arrows indicate process stimulation, while bar-headed lines indicate process inhibition (Derived from Hardie et al 2012).

mitochondrial biogenesis. Conversely, AMPK regulates mitochondrial degradation through the control of autophagy (mitophagy) via ULK1 phosphorylation and mTORC1 inhibition.

Overall, AMPK is a master regulator of cellular metabolism upon energy depletion and is activated to restore the ATP stocks by activating catabolic pathways and inhibiting anabolic ones. On the contrary to AMPK, some pathways need to be activated when resources are abundant to switch on the anabolic pathways necessary for cell growth and proliferation. As previously mentioned, the master protein complex at the centre of this regulation is mTORC1.

C. mTORC1 and amino acid sensing.

The mammalian Target of Rapamycin (mTOR) is the central serine/threonine kinase involved in amino acid sensing, the building blocks for proteins. It can be part of two major complexes, mTORC1 with the accessory protein Raptor and mTORC2 with the accessory protein Rictor.

From the two complexes, only mTORC1 is responsive to amino acid fluctuations. mTORC1 activation by amino acids is achieved through its translocation to the lysosomal membrane where resides the small GTPase Ras homolog enriched in brain (Rheb) protein which activates mTORC1 through direct interaction.

1. mTORC1 activation

The mTORC1 translocation occurs with the help of the Ras-related GTP binding proteins (Rag proteins). This protein family is composed of four small GTPases: RagA, B, C and D, which form the heterodimers RagA/B and RagC/D. The heterodimers stay at the lysosomal membrane through binding to a scaffold complex, the Ragulator complex, which is composed of 5 proteins: p18, p14, MP1, HBXIP and C7orf59. The localisation of RagA/B and C/D is not dependent on amino acid stimulation or GTP/GDP loading (Sancak et al., 2010). The activity of the small GTPases Rheb and Rag is regulated by GTP Exchange Factors (GEFs) (which activates the small GTPases) and GTPase Activating Proteins (GAPs) (which switch them off). The identification of the small GTPase regulators involved in mTORC1 activation or recruitment has become a subject of great interest. When RagA/B is loaded with GTP and RagC/D is loaded with GDP the interaction with the mTOR accessory protein Raptor is enhanced, leading to the recruitment of mTORC1 to the lysosomal membrane (Kim and Kim, 2016). One known regulating GEF for RagA/B is the Ragulator complex, which directly interact with Rags (Bar-Peled et al., 2012). A further level of regulation was uncovered with an inside-out mechanism at the lysosomes involving the vacuolar H^+ATPase (v-ATPase). Upon amino acid accumulation in the lysosomal lumen, an activating signal is transmitted via the v-ATPase to activate the GEF activity of Ragulator on RagA. Upon RagA-GTP loading, the Rag-Ragulator interaction weakens and mTORC1 is recruited to the lysosomal membrane (Bar-Peled et al., 2012). One GAP for the RagA/B complex is the GATOR complex, which is composed of 2 subcomplexes GATOR1 and GATOR2. For the RagC/D complex one GAP identified is the folliculin (FLCN) - FLCN interacting protein (FNIP) complex.

mTORC1 activity is not only controlled by amino acids. An increase in glucose also promotes the recruitment of mTORC1 by the Rag GTPases to the lysosomal membrane, promoting its activation (Efeyan et al., 2015). Growth factors (InsR/IGF-1), stress, energy status (AMPK) and oxygen can also modify mTORC1 activity (Laplante and Sabatini, 2012). The TSC1/2 protein complex relays signals coming from most of these pathways and was described as a central hub for mTOR regulation (Huang and Manning, 2008). The TSC complex acts as a GAP

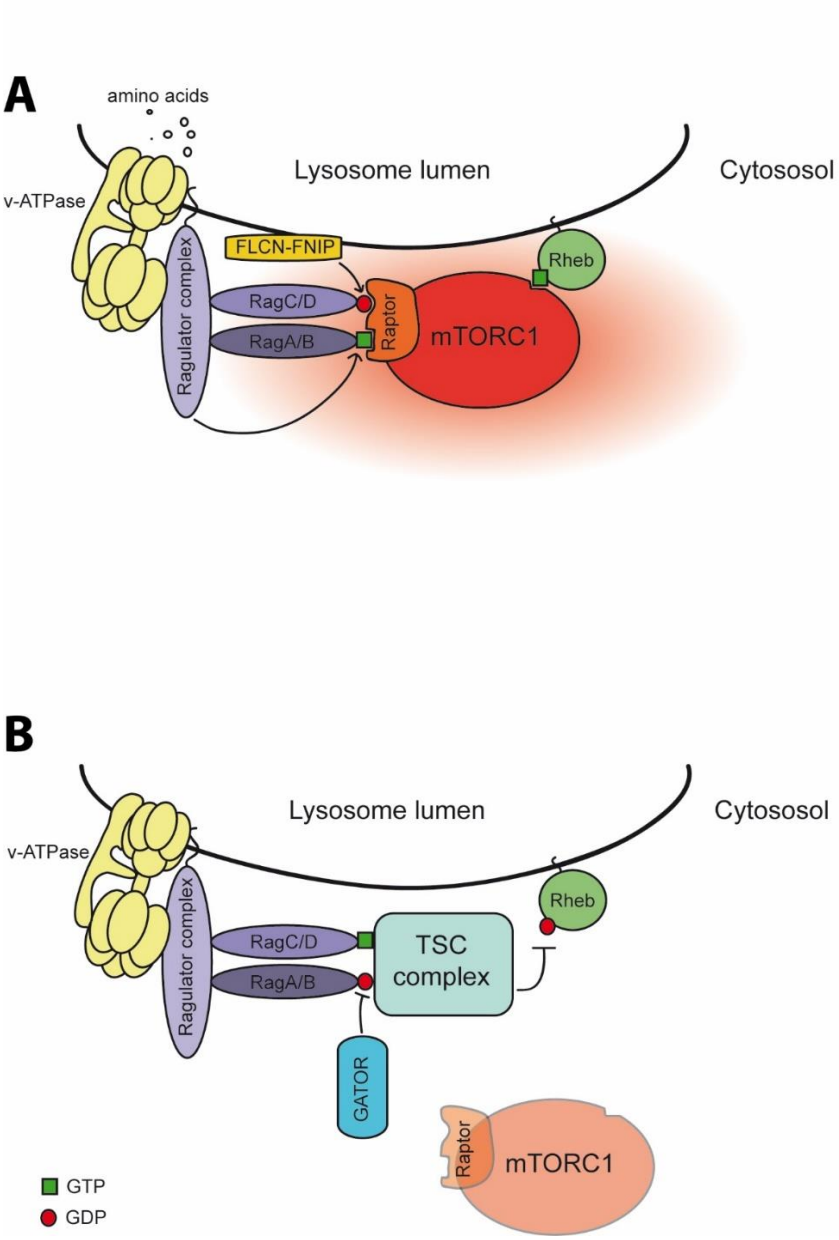

Figure 4 : mTORC1 regulation at the lysosomal membrane. (A) The presence of amino acids inside the lysosome is sensed by the v-ATPase, which transmits it to the Ragulator complex, activating its GEF activity on RagA. Concomitantly, the FLCN-FNIP complex binds GDP to the Rag C/D complex. This conformation of the Rags is optimal for their binding to the Raptor subunit of the mTORC1 recruiting it to the lysosomal membrane. At the lysosome, the Rheb protein activates mTOR. **(B)** On the contrary, upon amino acids depletion inside the lysosome, the v-ATPase is inactive and the Rag conformation is inversed by the action of other GAPs such as the GATOR1/2 complexes. This inhibits interaction of Raptor with Rags releasing mTORC1 to the cytoplasm and increasing recruitment of TSC1/2 complex which inhibits Rheb activity, fully switching off mTORC1 activation.

for Rheb, replacing the GTP by a GDP. Upon amino acids decrease, RagA loses it GTP to a GDP and RagC/D replaces its GDP to a GTP allowing the recruitment of TSC2 to the lysosome

and efficiently inhibiting the mTORC1 recruitment and activation (Demetriades et al., 2014). TSC2 is removed from lysosomal membrane upon insulin stimulation and subsequent Akt phosophosrylation of TSC2 (Menon et al., 2014). Full removal of TSC2 is needed to restore full activation of mTORC1 upon amino acids stimulation. It was recently reported that mTORC1 could still be activated by Leucine and glutamine in the absence of the RagA/B and Ragulator indicating that the canonical activation mechanism was not the only one and suggesting that different amino acids could activate mTORC1 by different means (Jewell et al., 2015).

2. Effects of mTORC1 activation

a) mTORC1 and protein metabolism

mTORC1 is crucial in protein synthesis at several levels. Translation initiation is regulated by active mTORC1 through the direct phosphorylation of eukaryotic translation initiation factor 4 (eIF4E)-binding protein 1 (4E-BP1) removing it from the eIF4E protein. This removal alleviates the inhibition of the eIF4F complex assembly leading to the start of capped mRNA translation (ma 2009). In parallel, active mTORC1 can phosphorylate S6K1 leading to a cascade of phosphorylation events on numerous transcription initiation factors, including eIF4B, leading to the increase of mRNA biogenesis (Ma and Blenis, 2009). Active mTORC1 was also shown to increase protein biogenesis not only by initiating transcription/translation but also by enhancing the activity of ribosomes. The mTORC1 dependent-phosphorylation of the transcription factor TRIM24 (TIF-1A) leads to its binding with RNA Polymerase I (PolI), resulting in increased rRNA transcription and subsequent expression (Mayer et al., 2004). Maf1, an RNA polymerase III repressor, was shown to be phosphorylated in a mTORC1-dependent manner, preventing its inhibitory effect and thus triggering the production of 5s rRNA and tRNA (Kantidakis et al., 2010).

b) mTORC1 and lipid metabolism

mTORC1 is also essential for lipid synthesis because of its capacity to regulate the SREBP-1 transcription factor and the phosphatidic acid phosphatase Lipin1. As I outlined it in the previous section, the SREBP-1 transcription factor is normally maintained at the Endoplasmic Reticulum (ER) by a short signal sequence, however upon an mTORC1-dependent mechanism it can cleave off its ER-retaining sequence and translocate to the nucleus where it initiates transcription of several genes which encode proteins involved in the *de novo* synthesis of fatty

acids and cholesterol (Laplante and Sabatini, 2009). mTORC1 can directly phosphorylate Lipin1 blocking it in the cytoplasm. When Lipin1 is dephosphorylated and in the nucleus, it prevents the expression of SREBP-1 dependent genes and decreases SREBP-1 levels (Peterson et al., 2011).

c) mTORC1 and macro-autophagy

Finally, mTORC1 inhibits a process called macro-autophagy, which will be discussed in the next section, through phosphorylation of its master regulator, the Unc51-like kinase (ULK1). mTORC1 can also regulate this process by controlling its final step, the lysosomes. Lysosome biogenesis depends on a set of genes belonging the Coordinated lysosomal expression and regulation (CLEAR) gene group. mTORC1 can inhibit the transcription of these genes through phosphorylation of Transcription factor EB (TFEB), which promotes its binding to the scaffolding protein 14-3-3 trapping it inside the cytoplasm (Settembre et al., 2011).

d) mTORC1 deregulation is linked with numerous diseases

Deregulation of mTORC1 has been reported to play a role in cancer and tumour progression through alteration of the 4E-BP1/eIF4E pathway and protein biosynthesis. Increases in lipid synthesis is a hallmark of proliferating cancer cells and has been shown to be mediated through mTORC1 and SREBP1 signalling (Laplante and Sabatini, 2012). Because mTORC1 is also controlling autophagy, it impacts on tumour growth and progression. Finally, mTORC1 has also been shown to play an important role in metabolic regulation in different organs. In the hypothalamus, mTORC1 activation reduces the expression of the orexigenic peptides NPY and AgRP through a yet unknown mechanism that involves S6K1. In adipose tissue, mTORC1 activation promotes adipogenesis by activating PPARγ. High circulating nutrients and cytokines promote mTORC1 activity in obesity, which inhibits insulin signaling and causes insulin resistance through various mechanisms. In skeletal muscle, mTORC1 plays a crucial role in regulating protein synthesis, mitochondrial biogenesis, and oxidative metabolism. Muscle contractions increase mTORC1 activity. In the liver, mTORC1 activation reduces ketone body production by inhibiting PPARα activity. mTORC1 also promotes hepatic lipogenesis by activating SREBP1. mTORC1 activity is elevated in obesity and overfeeding, which promotes hepatic insulin resistance, gluconeogenesis, and lipogenesis. Finally, in the pancreas, mTORC1 regulates β-cell mass by promoting β-cell growth and proliferation. mTORC1 is also important for insulin production and secretion. Obesity and nutrient overload

drives mTORC1 activity in β-cells. Sustained activation of mTORC1 ultimately cause β-cell apoptosis by inhibiting Akt signaling. The loss of β-cells favors progression towards diabetes.
As previously mentioned, mTORC1 inhibits the macroautophagy upon phosphorylation of its master regulator ULK1. The next section will describe more in details the mechanisms regulating cellular processes in response to nutrient starvation.

D. ULK1 and macroautophagy

Autophagy represents a housekeeping processes which allows the cells to get rid of their own components, such as defective organelles like mitochondria or peroxisomes, bulk cytoplasm and aggregated proteins or to get rid of infectious agents through lysosomal degradation. Importantly most of the cells also use autophagy to maintain their energy homeostasis upon starvation by generating *de novo* nutrients from older components (Bento et al., 2016).
Three main types of autophagy have been reported in eukaryotes, microautophagy, which degrade proteins through direct engulfment of cargo by the lysosomes, Chaperoned-mediated autophagy (CMA) which requires the Hsc70 containing complex and translocation of the cargo through a LAMP2A channel and finally macroautophagy, a complex multistep process involving numerous regulators. Most of the factors involved in macroautophagy are proteins forming complexes (Yang et al., 2013). Because macroautophagy has been shown to be involved in a panel of human diseases and is central in cellular nutrient homeostasis, I will mainly focus the following chapter on the latter.

1. Macroautophagy molecular regulation

Macroautophagy (hereafter referred to as autophagy) is always active at a low basal level. The pathway is kept low thanks to active inhibition of ULK1 by mTORC1 through phosphorylation of the ULK1 at Serine 757. Phosphorylation prevents its interaction with AMPK (Bento et al., 2016). ULK1 normally resides in the Autophagy related complex 1 (ATG1) composed of ULK1, FAK family kinase-interacting protein of 200kDA (FIP200), ATG101 and ATG13. Upon inhibition of mTORC1, starvation or rapamycin treatment, mTORC1-dependent phosphorylation is inihibited, while AMPK phosphorylates ULK1 on Serine 317 and 777 leading to derepression of autophagy initiation (Kim et al., 2011). It is important to understand that mTORC1 inhibition upon starvation is also dependent on AMPK activation. Hence, the three kinases AMPK, mTOR and ULK1 represent major enzymes at the heart of cellular nutrient homeostasis. Active ULK1 is necessary for the recruitment of the Class III PI3K

complex I, composed of Beclin1 (BECN1), Vacuolar protein sorting 34 (VPS34, also known as PI3K catalytic subunit 3), VPS15 and Autophagy related 14 (ATG14), to the phagophore initiation site to induce vesicle nucleation.

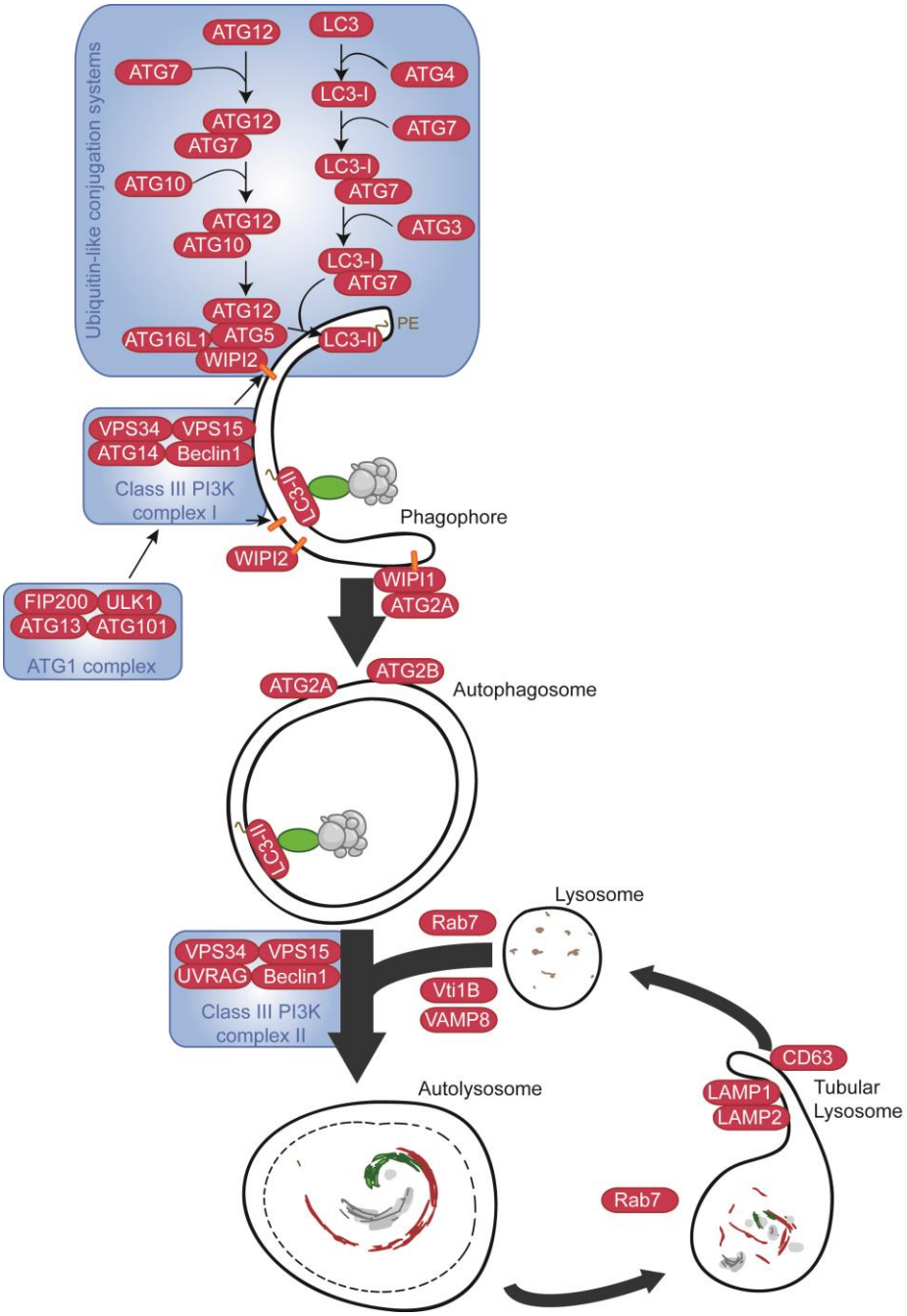

Figure 5 : Molecular mechanisms governing macroautophagy. See details in the text. PI3P are shown as red rectangles. Adaptor proteins are shown as green ovals. Aggregates to be degraded are depicted in grey. Derived from Bento *et al.* 2016.

The phagophore is a U-shape double membrane whose edges extend, by vesicle elongation, to finally join and form the autophagosome. The class III PI3K complex 1 produce phosphatidylinositol 3-phosphate (PI(3)P) which can induce positive curvature upon their insertion into the membrane thanks to their inversed conical shape (Bento et al., 2016). Moreover the formation of PI(3)P-enriched membrane favours the recruitment of the PI(3)P-binding protein of the WD repeat domain phosphoinositide-interacting protein (WIPI) family which are implicated in the formation of autophagosomes. WIPI2 mediates recruitment of the ATG16L1-ATG5/12 complex to the phagophore which is responsible for LC3 lipidation needed for its insertion into the phagophore membrane. Lipidated LC3, bound to phosphatidylethanolamine (PE, and commonly denominated LC3-II), is the end product of the autophagy ubiquitin-like conjugation system. One part starts with ATG12, an ubiquitin-like protein which, like ubiquitin, covalently attaches to substrates via the carboxyl group of its C-terminal glycine (Bento et al., 2016). It binds to the ATG7 E1-like activating enzyme, which activates ATG12 and transfers it to ATG10, an E2-like enzyme which will perform the conjugation with ATG5 making the ATG5/12 sub-complex which associates with ATG16L1 to form the ATG16L1-ATG5/12 complex. On the other part, cytoplasmic LC3 interacts with the ATG4 protein which removes its C-term arginine residues exposing the following glycine residue, which causes the recruitment of the E1-like activating enzyme ATG7 first to form LC3-I. The E2-like enzyme ATG3 binds to LC3-I and with the help of the ATG16L1-ATG5/12 complex mediates the lipidation of LC3-I, which becomes LC3-II and inserts inside the phagophore membrane (Bento et al., 2016) (Nakatogawa, 2013). The PE conjugation of LC3 leads to a visible down shift of the LC3 band in immunoblot analysis, which is commonly used to assess autophagy. LC3-II insertion in the membrane of the phagophore is important for recruitment of targets for their degradation as it serves as an anchor for adaptor proteins such as sequestome 1 (SQSTM1 also known as p62), Neighbour of BRCA1 Gene 1 (NBR1) or the NIX protein. These adaptors bind on one side the component to be degraded and on the other side LC3-II. The recruitment of extra membrane needed for the elongation of the phagophore is accomplished by the mATG9 protein. The origin of these extra membranes is still unclear and debated between three alternative models, the assembly model which consider that the membranes are from different origins, the maturation model which considers that the membrane come from an autophagogome dedicated platform and a third model, which is a combination of the two previous models (Bento et al., 2016).

Once the phagophore has engulfed the components to be degraded, each ends fuses together to form the double membrane autophagosome. This process is poorly understood so far but it probably involves ATG2A, ATG2B and WIPI1 as their knockdowns leads to the increase of unclosed phagophores inside the cell. (Bento et al., 2016)(Velikkakath et al., 2012).

The autophagosome then fuses with lysosomes to form the autolysosome, leading to degradation of the autophagosome content by release of the lysosomal degradative enzymes in an acidic environment. The fusion can happen only when the autophagosome is completely closed and thus is tighly regulated. Three class of proteins have been implicated in the autophagosome-lysosome fusion process, Rab GTPase, tethering proteins and SNAREs. Among them Rab7 has been involved in several events. Rab7 participates to the autophagosome movement by recruiting the kinesin motor proteins. Rab7 plays an important role in the Homotypic fusion and vacuolar protein (HOPS) tethering complex. Finally SNARE proteins, which were shown to be involved in endosome-lysosome fusion, such as VAMP8 and Vti1B, are also involved in the autophagosome-lysosome fusion (Furuta et al., 2010).

When the degradation is complete inside the autololysosome, the lysosomes regain their original identity by a process called Autophagic lysosome reformation (ALR) by forming tubules positive for the lysosomal associated membrane protein 1 (LAMP1) and LAMP2. This process controlled by mTORC1 also requires Rab7, clathrin and the AP2 complex (Rong et al., 2012)(Perera and Zoncu, 2016).

2. Autophagy in a disease context

In cancer, autophagy exerts both tumour suppressing and promoting functions. Mice deficient for essential components of autophagy have accelerated rates of spontaneous tumour development due to the loss of the housekeeping function of autophagy. Loss of autophagy promotes accumulation of protein aggregates, damaged mitochondria and reactive oxygen species, which are believed to enhance DNA damage and mutations. In post-mitotic cells, autophagy prevents accumulation of defective mitochondria (through mitophagy) and intracytoplasmic aggregate-prone proteins such as the Tau protein or Huntingtin in neurons. On the other hand, tumour cells which are poorly vascularised have been shown to be dependent on autophagy as nutrients coming from the blood are reduced. Finally autophagy has also been involved in ageing by increasing organismal fitness through inhibition of cell death (apoptosis and necrosis) and reduction of oncogenic transformation. On a more systemic scale, autophagy may also contribute to the clearance of intracellular pathogens and the function of antigen-

presenting cells, reduce inflammation, or improve the function of neuroendocrine circuits (reviewed in (Rubinsztein et al., 2011).

E. Lysosomes as a regulatory hub for nutrient sensing

The lysosomes are considered to constitute an organelle platform for nutrient dependent intracellular signalling (Perera and Zoncu, 2016). Proper mTORC1 binding to Rags at the lysosomal membrane is necessary for mTORC1 activation and leads to major changes in signalling and in transcription promoting cell growth and proliferation. The activation of AMPK and ULK1 also depends on lysosomes because their activities are modulated by mTORC1. As I mentioned above, mTORC1 activity is also controlled by AMPK which can phosphorylate the Raptor subunit or the upstream inhibitor TSC1/2 complex which dissociates mTORC1 from the lysosomal membrane (Alers et al., 2011). Interestingly, a recent study strengthens this idea. It was shown that the recruitment of AMPK to the lysosomal membrane occurs via attachment of the Axin-LKB1 complex with members of the Ragulator complex (Zhang et al., 2014). Localization of three important kinases at the lysosomal membrane highlights the important role of lysosomes in nutrient homeostasis.

In this part, I have described numerous effects of these three kinases more generally in cellular metabolism. But their regulation might be distinct in specialized cells. In the next section, I will address their regulation in pancreatic β-cells, which are at the centre of glucose homeostasis through insulin secretion.

III. Nutrient sensing controls pancreatic β-cell function

As explained above, pancreatic β-cells heavily rely on nutrient metabolism to activate their main function: insulin secretion. For this reason, glucose metabolism in β-cells exerts unique functions (Prentki et al., 2013). As opposed to most others cells, pancreatic β-cells activate glucose metabolism only by substrate availability and do not require additional neuronal or hormonal stimulation thanks to their low-affinity glucose transporter GLUT2 and to glucose phosphorylating activity of GCK (Otonkoski et al., 2007). The major nutrient sensor AMPK have been extensively studied in pancreatic β-cells and in the diabetic context in the beginning of the 2000's. However most of the outcomes derives from pharmacological studies leading to contradictory results. The overall tendency is that AMPK chronic activation is rather deleterious

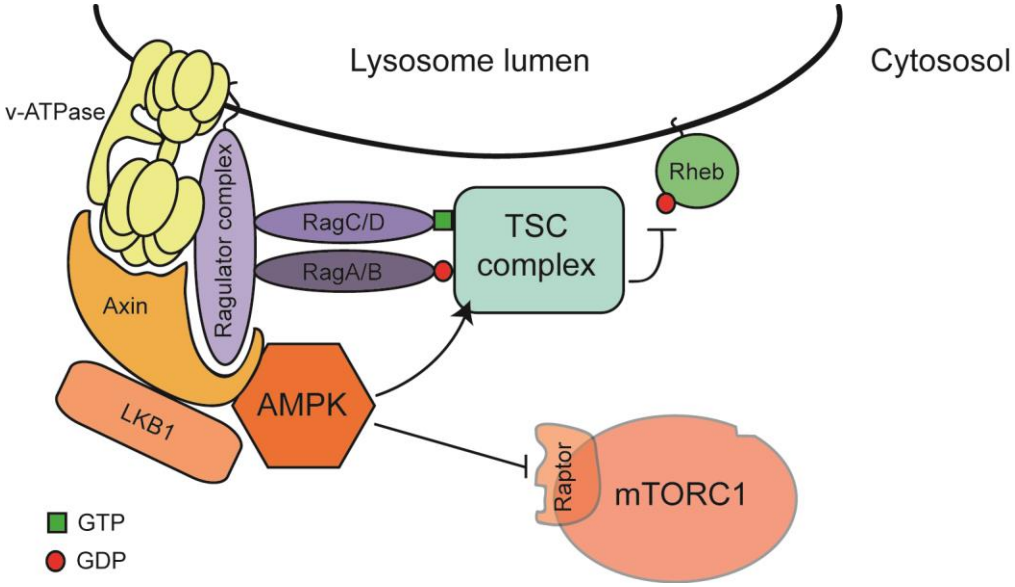

Figure 6: Proposed Mechanisms for Reciprocal Regulation of mTORC1 and AMPK at the Cytoplasmic Surface of the Lysosome. The model is based on Bar-Peled and Sabatini (2014) and Zhang et al. (2014). Lack of nutrients causes Ragulator to recruit the axin:LKB1 complex, and elevated AMP recruits AMPK to this complex. LKB1 phosphorylates and activates AMPK, which then dissociates from the complex to phosphorylate downstream targets. Two of these targets are Raptor and the TSC1:TSC2 complex. Phosphorylation of Raptor by AMPK, coupled with conversion of $RagA^{GTP}$:$RagC^{GDP}$ to $RagA^{GDP}$:$RagC^{GTP}$, may promote the dissociation of mTORC1 from the lysosome. Phosphorylation of the TSC1:TSC2 complex appears to increase its Rheb-GAP activity, thus converting Rheb:GTP to the inactive Rheb:GDP form, although the exact mechanism remains unclear.

because it inhibits glucose stimulated insulin secretion while promotes β-cell failure (Fu et al., 2013). This is in contradiction with the systemic effect of AMPK activation, which is beneficial in a diabetic context. Recently, autophagy inhibition has been implicated in the failure of pancreatic β-cells during metabolic stress. Its housekeeping function was shown to be important to allow the cell to process the massive insulin amount needed to answer insulin resistance. Deletion of crucial autophagic gene in pancreatic islets *in vivo* led to increase onset of diabetes (Lee, 2014). Autophagy inhibition by palmitate-dependent mTORC1 activation promoted apoptotic cell death and β-cell death (Choi et al., 2008). Finally autophagy is important to clear the IAPP formation which is important in triggering the diabetes in human (Rivera et al., 2014) (Kim et al., 2014) (Shigihara et al., 2014) (Osório, 2014). Because of their unique roles in organismal glucose homeostasis β-cells do not rely on the same metabolic pathways. For instance, during their development, the pancreatic β-cells actively repress the expression of the Lactate dehydrogenase enzyme (LDH), which convert the lactate into pyruvate, and the Monocarboxylate transporter (MCT1 also known as SLC16A1) at the plasma membrane, which

allows the transport of lactate and pyruvate inside the cells. Low expression of MCT and LDH is requisite to the specificity of glucose in insulin secretion, protecting the organism from undesired hypoglycemic actions of pyruvate and lactate during exercise and other catabolic states (Otonkoski et al., 2007)(Ishihara et al., 1999). Our team discovered a new cellular mechanism that is specific and is required for β-cells to cope with nutrient deprivation without triggering insulin release (Goginashvili et al., 2015).

A. Lysosomal degradation of insulin granules in pancreatic β-cells

Most of the cells in mammals trigger autophagy upon fasting and nutrient deprivation. We recently discovered that β-cells employ a very distinct and so far unknown mechanism to adapt to nutrient depletion. In contrast to other mammalian cells, autophagy in β-cells is not a predominant response upon nutrient deprivation (Goginashvili et al., 2015). Instead of autophagy, starved β-cells induce lysosomal degradation of newly generated (nascent) secretory insulin granules in the vicinity of the Golgi, a process we termed starvation-induced insulin granule degradation (SINGD). This discovery was done using immunofluorescence analysis with antibodies targeted against lysosomes and insulin granules, coupled with Correlative Light Electron Microscopy (CLEM) as well as fractionation analysis (Goginashvili et al., 2015). This process was independent of the canonical molecular machinery of autophagy. Surprisingly the autophagosome formation in pancreatic β-cells was shown to be basally high under normal nutrient conditions (Goginashvili et al., 2015). This is explained by the necessity of having an efficient housekeeping mechanism in cells that chronically process high amount of insulin. Moreover the triggering of autophagy was also shown to trigger insulin secretion even upon hypoglycemic glucose concentrations. This explains why autophagy is not used in pancreatic β-cells upon fasting, as this would promote insulin secretion and be extremely damageable for the whole organism during a fasting period (Goginashvili et al., 2015).

By degrading their nascent granules, the ones preferably secreted, pancreatic β-cells can recover nutrients and maintain their energy homeostasis. The insulin granule fusion with lysosomes was shown to activate mTORC1 leading to the inhibition of autophagy. Mechanistically, we found that nutrient depletion in β cells also decreased activation of Protein Kinase D (PKD) at the Golgi and that inactivation of PKD activity triggered constitutive induction of SINGD. Hence, β-cells employed a PKD-dependent mechanism to adapt to nutrient availability coupling autophagy flux to secretory function. Interestingly, Golgi-mediated degradation has more

recently been described in yeast cells incapable to induce autophagy due to deletion of crucial autophagy genes, ATG5 and ATG7 (Yamaguchi et al., 2016). This process might be closely related to SINGD as the same study demonstrated that β cells lacking these genes can induce Golgi-mediated degradation of insulin granules under low nutrient conditions.

B. PKD functions in pancreatic β-cells

PKD1 is calcium/calmodulin dependent serine/threonine kinase which can bind to lipid membranes from the TGN and plasma membrane. In mice and pancreatic β-cell lines, its activity have been shown to be dependent of its upstream kinase p38δ which inhibits it through the phosphorylation of the S397 and 401 (Sumara et al., 2009). Upon p38δ deletion, the activity of PKD1 remains high, and pancreatic insulin levels are higher and islet secrete more in response to glucose stimulation (Sumara et al., 2009). Interestingly p38δ is almost exclusively expressed in the pancreas (Sumara et al., 2009). In addition PKD1 has been shown to regulate transport carrier formation at the TGN in cells by enhancing the activity of lipid modifying proteins such Phosphatidylinositol 4 kinase β (PI4KIIIβ) which converts PI into PI(4)P at the TGN (Hausser et al., 2005). Generation of PI(4)P leads to the recruitment of both the Ceramide

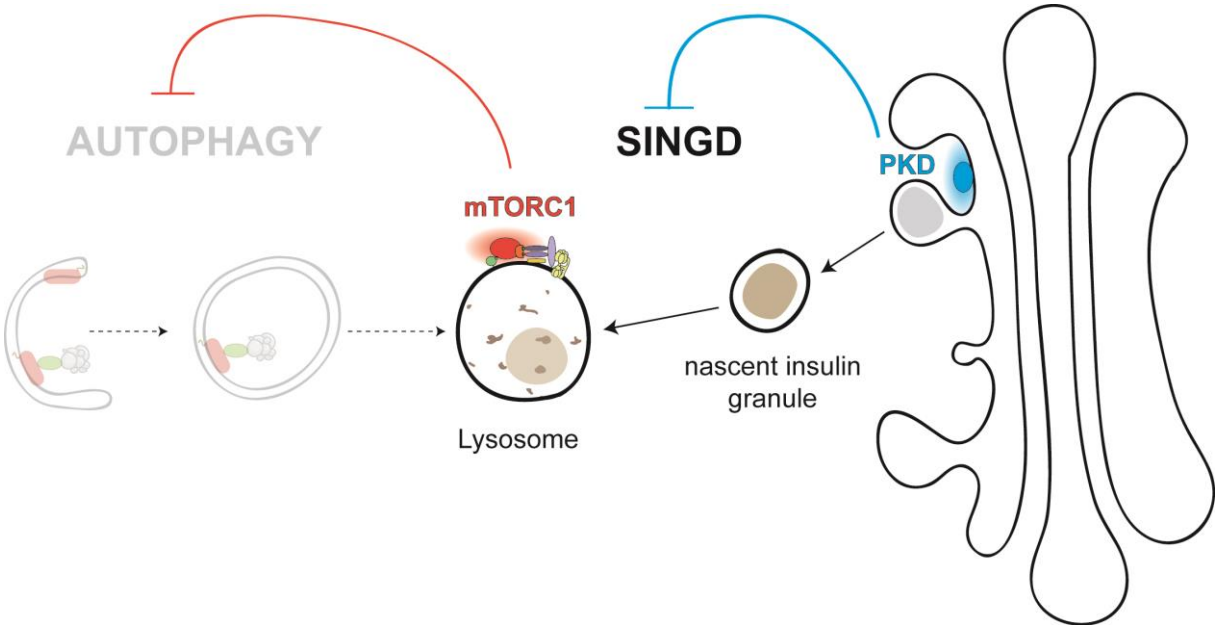

Figure 7 : SINGD inhibits autophagy and is controlled by PKD. Upon starvation in pancreatic β-cells, nascent insulin granules are directly targeted to the lysosomes where they are degraded. This recruits and activates mTORC1, inhibiting autophagy. Silencing of PKD leads to increased SINGD while its activation leads to decreased GCLs formation, implying that PKD controls SINGD.

transfer protein (CERT) which shuttles ceramides from the endoplasmic reticulum to the TNG, and the Oxysterol binding protein (OSBP) which is involved in sterol transfer and sensing. Both of this proteins can be phosphorylated by PKD1 leading to a decrease in their activity and binding with the TGN membrane (Malhotra and Campelo, 2011). PKD has been shown to be recruited at the TGN also via its interaction with Arf1 protein (Malhotra and Campelo, 2011). Moreover PKD1 activity impacts directly on insulin granule biogenesis through the control of the BAR-domain containing protein Arfaptin-1, which controls the proper release of the insulin granule from the TGN only upon its full maturation by binding to the vesicle neck (Gehart et al., 2012). PKD1 phosphorylates Arfaptin-1 inducing a conformational change and its release in the cytoplasm, leaving the way free for Arf1 and other scission related proteins. PKD1 silencing or inhibition has been shown to be damageable for both insulin secretion and total insulin content inside the β-cells (Sumara et al., 2009)(Goginashvili et al., 2015). Upon fasting PKD1 activity was shown to dramatically drop, in parallel to autophagy (Goginashvili et al., 2015).

Because SINGD and PKD1 activity were shown to play a role in insulin levels in the pancreatic β-cells during fasting, we wondered if this mechanism was important during metabolic disorder, the main one being type 2 diabetes, where insulin and pancreatic β-cells impairments have critical impact.

IV. T2DM and pancreatic β-cells

Diabetes Mellitus is a metabolic disease characterised by chronic hyperglycaemia resulting from poor insulin action, poor secretion or the combination of both. Chronic hyperglycaemia leads to several complications including retinopathy, nephropathy, neurophathy, as well as macrovascular alterations (Fowler, 2008). While type 1 diabetes (T1D) is caused by the autoimmune destruction of the pancreatic β-cells, type 2 diabetes (T2D) is a metabolic dysbalance characterised by hyperglycaemia in an insulin resistance context and a relative lack of insulin (Kumar et al 2015). T2D is a multifactorial disease having its origin both in genetics and environmental factors (Hu et al., 2001). Obesity and sedentary lifestyle are strongly linked with the apparition of the disease. As prevalence of obesity raises on a worldwide scale, prevalence of T2D also increases and there is now more than 370 million diagnosed diabetic patients in the world. The diagnosis is done if one of these tests is positive: 1) random plasma

glucose is superior or equal to 200mg/dl or, 2) Fasting plasma glucose is superior or equal to 126mg/dl or, 3) two hours plasma glucose is superior or equal to 200mg/dl during an Oral Glucose Tolerance Test (OGTT) or 4) the glycated haemoglobin (HbA1c) is superior or equal to 6.5%.

T2D is characterised by several metabolic defects, the major ones being β-cell secretory dysfunction and peripheral insulin resistance (Kahn et al., 2013). Peripheral insulin resistance is a pathophysiological condition in which peripheral tissues, such as muscle, liver and adipose tissue fail to respond to the normal action of the hormone insulin by normally taking up the blood glucose. (Meszaros, 2015 thesis). Insulin resistance is strongly linked with obesity and the increase of fat inside the organism. Insulin resistance depends on extrinsic mechanisms such as adipokines, elevated plasma free fatty acids (FFA) levels and pro-inflammatory cytokine but also intrinsic mechanisms provoked by abnormal intracellular lipid accumulation, oxidative stress, mitochondrial dysfunction and ER stress (Trayhurn, 2005). However insulin resistance cannot be seen as the sole factor for type 2 diabetes as most of the insulin resistant persons do not become diabetic. Obese patients only turn diabetic if their pancreatic β-cells fail to provide the needed insulin (Weir and Bonner-Weir, 2013).

Insulin resistance induces first a compensation phase characterised by an increase in pancreatic β-cell mass and function. The β-cell mass increase can be driven by proliferation of existing β-cells and/or neogenesis, the *de novo* creation of pancreatic β-cells (Levetan, 2010). Several hormones have been shown to triggers β-cell mass expansion such as GLP1, GIP, Insulin-like growth factor (IGF1) or insulin itself. Insulin resistance compensation is also achieved by increased insulin secreting capacity from the β-cells through intrinsic and extrinsic pathways which were already developed earlier, leading to hyperinsulinemia, the increased concentration of plasmatic insulin (Jetton et al., 2005). In opposition to insulin resistant prediabetic individuals, the β-cell mass in terminal diabetic patients was shown to be dramatically reduced (MACLEAN and OGILVIE, 1955) (Butler et al., 2002) because of global β-cell failure.

β-cell failure was thought to be mostly driven through β-cell loss and death (Halban et al., 2014). Although this could be the ultimate final results, a lot of different mechanisms can lead to β-cell loss. The classic view where apoptosis is the main driver of β-cell loss is more and more discussed and complemented by others concepts. It was reported that β-cell could undergo at the same time de-differentiation into α, δ or PP cells through the downregulation of the key identity maintaining transcription regulator Foxo1 (Talchai et al., 2012). Misregulation of key transcription factors due to oxidative stress was also shown to play a role (Guo et al., 2013).

Many physiological stressors impact on pancreatic β-cell function and survival under a TD2 diabetic environment. ER stress arises when overwhelming amount of insulin is processed to meet the metabolic demand, inducing the Unfolded Protein Response (UPR) thus leading to apoptosis. Metabolic and oxidative stress due to the excessive nutrients inputs also lead to β-cell glucotoxicity, lipotoxicity and glucolipotoxicity although β-cells are uniquely equipped for efficient oxidative metabolism. Mishandling of excessive cholesterol is commonly seen in T2D, with accumulation in β-cells, leading to impaired secretion (Kruit et al., 2011). In human, the strong accumulation of Islet amyloid polypeptide (IAPP) leads to the formation of the amyloid plaque and the proapoptotic IAPP oligomers formation (Montane et al., 2012) inducing the release of Interleukin-1β-to recruit macrophages and enhance local islet inflammation (Masters et al., 2010). Local islets inflammation is well established (Donath and Shoelson, 2011) and treatments with IL-1β-antagonist helps preserving the islets (Donath, 2013, 2014).

Aim of the project

Our previous work unveiled that β-cells in response to nutrient deprivation induce targeting of nascent insulin granules to lysosomes suppressing macroautophagy. This fundamentally new process could be, however, also enhanced in a situation of a chronic metabolic overload and T2D. This somehow parallels one of the hallmarks of T2D, which is constitutive induction of fasting-related processes, i.e. gluconeogenesis and lipolysis, in a situation of nutrient overload. While the latter phenomena are largely related to insulin resistance, we do not understand yet how nutrient deprivation and nutrient excess both can trigger lysosomal degradation of insulin granules in β-cells. This clearly asks for a better understanding of molecular and cellular mechanisms underlying the latter process. Because SINGD was shown to be a direct inhibitor of autophagy by activating at the lysosome mTORC1, we wanted to know whether a similar process could occur during diabetes. We already identified PKD as a major player controlling insulin granule turnover. Uncovering the mechanisms downstream of PKD leading to targeting of insulin granules with lysosomes will, however, be essential, and was the subject of my thesis.

Material and Methods

I. Materials

Reagents were obtained from the following sources: HRP-labeled anti-mouse and anti-rabbit secondary antibodies from IGBMC; primers, antibodies to phosphor-PKD, type V Collagenase solution, Bafilomycin A1, from Sigma Aldrich; antibodies to PKD total, mTOR, LAMP2 from Cell signaling technology; antibody to CD63 in mouse from Santa Cruz; antodibody to CD63 in rat from Biorad; antibody to LC3B (2G6) from nanotools; antibody to Lamp1 (Ly1C6) from Cayman chemical; antibody to p62 from Progen; antibody to Green Fluorescent Protein from Fischer Scientific; Mowiol from Calbiochem; cOmplete Protease inhibitor cocktail tablets from Roche; Rapamycin and CID755673 from Tocris Biosciences; 4',6-diamidino-2-phenylindole (DAPI), Image-iT® FX signal enhancer and Alex-488 -568 and -647 conjugated secondary antibodies from Life Technologies; Osmotic pumps from Alzet®.

II. Methods

A. Mouse maintenance and experimentation

BTBR *ob/+* mice were obtained from Charles River and were maintained by heterozygous breeding to generate +/+ and *ob/ob* littermates. Genotyping was performed with the oIMR1151 and oIMR1152 primers using the classical Taq polymerase conditions. The obtained PCR solutions were then digested using the HPyF3I restriction enzyme as the *ob* mutation inserts one cutting site. The bands were visualized on a 0.5% agarose gel containing 0.002% Ethidium bromide.

Primers	**Sequence (5'-3')**
oIMR1151	TGTCCAAGATGGACCAGACTC
oIMR1152	ACTGGTCTGAGGCAGGGAGCA

Mice were implanted with osmotic pumps according to the manufacturer protocol at 4 weeks of ages under anaesthesia induced by 3-4% Isoflurane inhalation and maintained with 1.5% Isoflurane. CID755676 was dissolved at 10mg/ml in 50% DMSO solution.

After 14h of fasting, blood samples were taken by a small incision at the tip of the tail. For Glucose Stimulated Insulin Secretion (GSIS) test, the mice were fasted and intraperitoneally injected with a glucose solution (2g/kg bodyweight). 100µl blood samples were repeatedly taken from the tail tip. Samples were immediately centrifuged and plasma was stored at -20°C until used. Insulin was measured in 25µl plasma using Insulin Ultrasensitive ELISA (ALPCO). Maintenance and animal experimentation were in accordance with the local ethical committee (Com'Eth) in compliance with the European legislation on care and use of laboratory animals.

B. Molecular cloning and knock-in cell line generation

The modified repair plasmid was generated by amplifying the rat CD63 C-terminal sequence with modified primers complementary for the DsRed sequence. The DsRed sequence was amplified from a DsRed containing plasmid with modified primers complementary for the CD63 C-terminal region. The PCR fragment obtained were isolated and purified using the PCR clean-up kit from Macherey-Nagel. The 3 PCR fragments were put together with a SmaI digested opened puc57 plasmid and treated with ExoIII nuclease which selectively remove the 3' end of double stranded DNA fragment and allow complementary annealing between the PCR fragments and the puc57 plasmid. The recombinant plasmid was transformed and amplified in STBL3 competent *E.coli* and verified by Sanger sequencing (GATC). The same strategy was used to generate the Phogrin-eGFP mutants (PTPRN2-eGFP).

Primers	**Sequence (5'-3')**
puc57-CD63 HR1 Fw	CGAATGCATCTAGATATGGGATCCTGACTGGGCCAGAGCAAGCCCTTTAAAT
CD63 HR1-DsRed Rv	GTCCTCGGTGTTGTCCATTACTTCGTAGCCACTCCGGATAC
CD63 HR1-DsRed Fw	GAGTGGCTACGAAGTAATGGACAACACCGAGGACGTCATCAAGG
DsRed-CD63 HR2 Rv	TCAGACACGCCCCCACCTCACTGGGAGCCGGAGTGGC
DsRed-CD63 HR2 Fw	CCACTCCGGCTCCAGTGAGGTGGGGGCGTGTCTGAGCTC
CD63 HR2-puc57 Rv	GCCTCTGCAGTCGACGGGCCCGGGCTTTACAGCAAGAGGCTGGTTTCGG
puc57-PTPRN2 HR1 Fw	CGAATGCATCTAGATATCGGATCCAGGCAGGGGCTGGTTCTGATTGCAC
PTPRN2 HR1-eGFP Rv	TGAACAGCTCCTCGCCCTTGCTCACCTGGGGAAGGGCCTTCAGGATGGCA
PTPRN2 HR1-eGFP Fw	TGCCATCCTGAAGGCCCTTCCCCAGGTGAGCAAGGGCGAGGAGCTGTTCA
eGFP-PTPRN2 HR2 Rv	TCCCGTCAGCTCCAGCTTCGGTGCCTACTTGTACAGCTCGTCCATGCCGA
eGFP-PTPRN2 HR2 Fw	TCGGCATGGACGAGCTGTACAAGTAGGCACCGAAGCTGGAGCTGACGGGA
PTPRN2 HR2-puc57 Rv	GCCTCTGCAGTCGACGGGCCCGGGCAAACTGGAGCATCCAGTGAGAATGT

The specific gRNA were designed with the help of the website crispr.mit.edu and purchased at Sigma Aldrich. They were clone inside the Cas9-containing pX330 plasmid according to the manufacturer protocols (Addgene). In red are the additional nucleotide for correct insertion after BbsI digestion.

gRNA	Sequence (5'-3')
CD63 KI gRNA 1 Fw	caccGGGCTACGAAGTAATGTAGGGTGG
CD63 KI gRNA 1 Rv	aaacCCACCCTACATTACTTCGTAGCCC
Phogrin KI gRNA 5 Fw	caccGTCCCCAGTAGGCACCGAAGC
Phogrin KI gRNA 5 Rv	aaacGCTTCGGTGCCTACTGGGGAC

For knock-in generation, plasmids were co-transfected at 20µg each. For single clone selection, cells were diluted at 70 cells /10ml concentration and spread over 96-well plates, with 100µl of solutions per well. Cells were screened by PCR using sequencing primers hybridizing outside the regions used to for homologous recombination to check for fluorescent tag sequence correct insertion. Primers were designed with additional sequence for insertion in the pUC57 plasmid (shown in orange) to amplify the sequence before sequencing. Correct insertion was then check at the DNA levels by Sanger sequencing (GATC) and at the protein levels by Immunofluorescence or Western Blot.

Primers	Sequence (5'-3')
Sequencing CD63-Dsred Fw	CGAATGCATCTAGATATCGGATCCTGTGGTCATCATTGCAGTGGGT
Sequencing CD63-DsRed Rv	TCTGCAGTCGACGGGCCCGGGGTACAAGGACAACATGCTCAACGAC
Sequencing Phogrin-GFP Fw	CGAATGCATCTAGATATCGGATCCTCAACATAAAGAGCAGAGGCCAAC
Sequencing Phogrin-GFP Rv	GCCTCTGCAGTCGACGGGCCCGGGCAGGTGGTAAGCCCAACGCCCAAA

C. Cell lines and transfections

INS1 cells were maintained in RPMI 1640 supplemented with 10% FCS tet system approved, 10mM Hepes, 1mM PyrNa, 2mM glutamine, 50µM β-mercaptoethanol, penicillin and streptomycin. Cells were transfected by using Amaxa Nucleofector (Lonza) according to the manufacturer's protocol with the T-027 program.

D. Isolation of pancreatic islets

Mice were killed by cervical dislocation. Islets were isolated by perifusion of 5ml of type V collagenase solution and picked manually under the binocular. Islets were kept in the same medium as INS1 cells.

E. Cell lysis

Cells were rinsed once with ice-cold PBS and lysed in ice-cold lysis buffer (50mM Tris (pH 7.5), 50mM NaCl, 0.5% Triton X-100, 0.5% NP40 substitute, 5mM EGTA, 5mM EDTA, 20mM NaF, 25mM beta-glycerophosphate, 1mM PMSF, 0.1mM NaVO3, 1x cOmplete protease inhibitor (Roche)). The soluble fractions of cell lysates were isolated by centrifugation at 14000xg for 10 minutes.

F. Western blot

Protein samples were separated by using SDS-PAGE or TRICINE-SDS-PAGE and transferred to PVDF membranes. Membranes were blocked at room temperature for 1 hour with 5% skimmed milk in TBST (0.05% Tween20). Primary antibody incubation was done overnight at 4°C. The membrane were washed 3 times with TBST and incubated with the secondary antibody for 1 hour and finally washed again 3 times with TBST. Proteins were visualized with Luminata Forte ECL (Millipore) on the AI600 camera (GE health).

G. qPCR analysis

Tissue or cells were homogenized in TRIzol reagent (Sigma). After phase separation by centrigugation, the aqueous phase was transferred into a new tube and RNA was precipitated by 75% ethanol. cDNA was synthesized with Oligo dT primers using SuperScript III forst-strand cDNA synthesis kit (Invitrogen) according to manufacturer's protocol. Quantitative real-time PCR was performed using SYBR Green (Roche) on a LightCycler 480 (Roche). The expression valies were individually normalized to housekeeping genes HPRT and GAPDH. Primers used are indicated in the following table.

primers	Sequence (5'-3')
HPRT mouse fw	AGTCCCAGCGTCGTGATTAG
HPRT mouse rv	TTTCCAAATCCTCGGCATAATGA
GAPDH mouse fw	TTGGCCGTATTGGGCGCCTG
GAPDH mouse rv	CACCCTTCAAGTGGGCCCCG
PrKD1 mouse fw	CGTGGTTAACCCATCAAGTT
PrKD1 mouse rv	AATTCCAAACTGTCCGGAAC
PrKD2 mouse fw	GCAACTAGCCTGTTCTATCGTG
PrKD2 mouse rv	AGAGCAGGATCTTGTCGTACA
PrKD3 mouse fw	CAGTGGAAGACTTCCAGATCC
PrKD3 mouse rv	GAATCTTGAAGGCACATCGTTTATG
CD63 mouse fw	GAAGCAGGCCATTACCCATGA
CD63 mouse rv	TGACTTCACCTGGTCTCTAAACA

H. Immunofluorescence

INS1 cells were plated on 9-15mm glass coverslips (Menzel-Glaser) in 24-well tissue culture plates and allowed to grow for 24 hours. In the end of experiment the cells were washed once with PBS and fixed for 20 min with 4% paraformaldehyde (PFA) in PBS at room temperature. The coverslip were rinsed 3 times with PBS and permeabilized with 0.1% Triton X-100 in PBS for 5 minutes. After rinsing 3 times with PBS, the coverslips were blocked by Image-iT® Fx Signal enhancer for 30min, rinsed once with PBS and incubated for 30min in blocking buffer (3% BSA in PBS). Coverslips were subsequently incubated with primary antibodies in blocking buffer for 1 hour at room temperature, rinsed 3 times in PBS and incubated with the secondary antibodies, diluted in blocking buffer, for 40 minutes at room temperature in the dark. After incubation coverslips were rinsed 3 times with PBS (with DAPI added in the second washing step, when present) and mounted on glass slides using Vectashield or Mowiol and imaged with a 100X or 63X objective using fluorescence microscope of confocal Leica spinning Disk Andor/Yokogawa or Nikon Ti PFS.

I. Histochemistery

Pancreata were fixed by intracardiac perfusion with PDA 4% in PBS. Tissues were post-fixed overnight at 4°C in the same solution, cryoprotected in 30% sucrose in PBS solution, embedded in Cryomatrix (Thermo scientific) and kept at -80°C. Pancreas sections were cut with a cryostat

(CM3050, Leica) and mounted on Superfrost Ultra Plus slides (Menzel-Glaser). 10µm cryosections were incubated for 2 hours at room temperature in the blocking solution (PBS/5% Normal Goat serum /0.3% Triton X-100), then left overnight at 4°C, in a wet chamber, with …. After 3 washes in PBS, the sections were blocked for 15min at room temperature in the blocking solution and incubated for 2 hours at room temperature, in wet chamber, with …. And … diluted in blocking solution. After 3 washes in PBS, 1 wash in milliQ water, the slides were dried and mounted in Mowiol (Calbiochem) containing DAPI (0.5µM). Images were taken using confocal microscope Leca Spinning Disk Andor/Yokogawa.

J. Colocalisation analysis

To assess colocalisation, we used the automatic threshold Person's analysis to obtain unbiased results (Figure 8) with the Fiji® plugin Colocalisation thresholds. The plugin generated the colocalised pixel maps, a scatter plot as well as the Pearson's correlation coefficient.

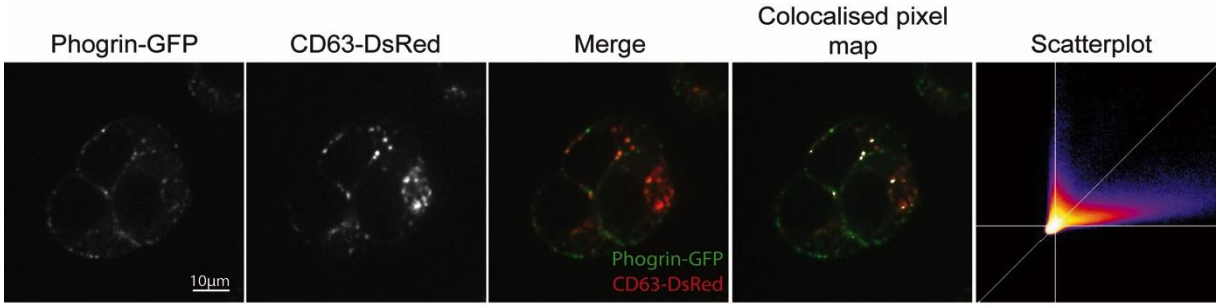

Figure 8. Colocalisation analysis scheme using the Colocalisation Threshold plugin from Fiji.

K. Transmission electron microscopy (TEM)

For TEM, cells and primary islets were first fixed in 0.05% malachite green, 2.5% glutaraldehyde, 0.1 M sodium cacodylate buffer, post-fixed in 0.8% K3Fe(CN)6, 1.0% OsO K3Fe(CN)6 and stained with 1% tannic acid and 0.5% uranyl acetate. The samples were then dehydrated in graded ethanol solutions and embedded in Epon (Ladd Research Industries). Ultrathin sections (50-60nm) were examined under a Phillips CM12 80kV electron microscope equipped with an ORIUS SC1000 CCD camera.

Quantitative analysis of autophagic compartment, GCLs and insulin granules of INS1 cells and primary islets have been assessed by TEM as described (Yla-Anttila, Vihinen et al 2009. Briefly, the areas of cytoplasm and Golgi were evaluated by stereological approach using x5600 magnification with ImageJ-based open source Fiji software package. The numbers of

compartments were quantified using x15000 magnification. Data from 3 independent experiment were expressed as mean +- SEM. The numbers of granule containing lysosomes (GCLs) in Golgi area were counted for 30 cells from 3 independent experiments using x19500 magnification. The data were expressed as mea +- SEM. All quantitative analyses relied on systematic uniform random sampling.

L. α-cells isolation

Rat islets were isolated as for the mice. Islets were dispersed using a tripsine treatment. The solution containing the mixed cell population was send to FACS sorting where α-cells were separated from β-cells.

M. Statistical analysis

The statistical significance of the differences between two groups was investigated by unpaired t test. The statistical analysis was performed using GraphPad Prism software (GraphPad Software Inc.).

Results

I. Targeting of insulin granules to CD63-positive compartments is increased in diabetic β-cells

A. Pancreatic β-cells from diabetic BTBR *ob/ob* mice contain numerous Granule-Containing Lysosomes (GCLs)

SINGD is characterized by lysosomal degradation of insulin granules, local activation of mTOR and inhibition of protein kinase D1 (PKD1). To address the importance of a similar process happening during diabetes, we decided to assess these features in different diabetic models. I focused on the well-established *ob/ob* leptin-deficient mice in the BTBR genetic background (Clee et al., 2005)(O'Brien et al., 2014)(Xu et al., 2012). The *ob/ob* mice are homozygous for a loss-of-function mutation on the *leptin* gene, which leads to a hyperphagic phenotype accompanied by rapid weight gain and morbid obesity. The BTBR strain is characterized by marked insulin resistance (Ranheim et al., 1997). The combination of the *ob* mutation and the BTBR genetic background results in severe obesity (Figure 9A) and full-blown diabetes (Figure 9B) in BTBR *ob/ob* mice already in less than 8 weeks of age.as previously described (Clee et al., 2005).

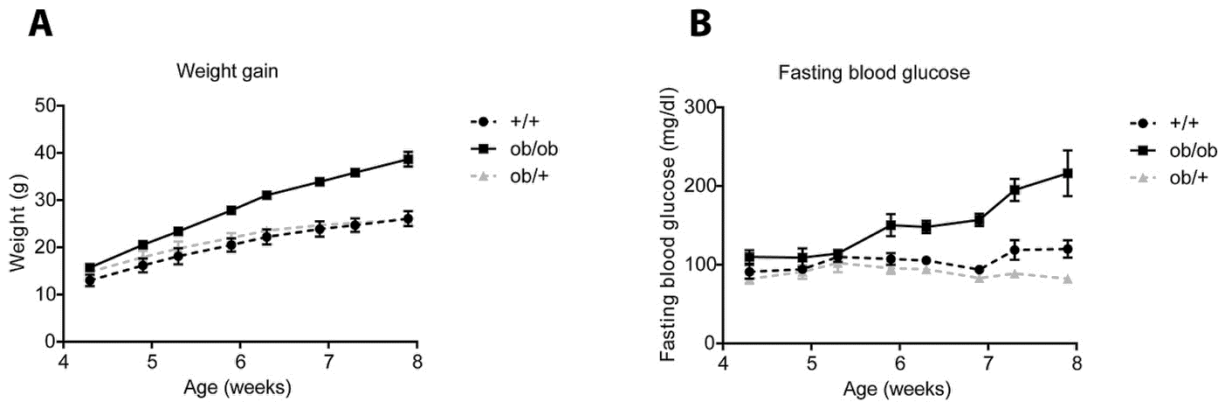

Figure 9. BTBR *ob/ob* mice become severely obese and diabetic 8 weeks after birth. (**A)** Time-course of the body weight of BTBR +/+ controls mice, homozygous BTBR *ob/ob* mice, or heterozygous BTBR *ob/*+ mice (n=5/group). **(B)** Time-course of fasting blood glucose levels of BTBR +/+ controls mice, homozygous BTBR *ob/ob* mice, or heterozygous BTBR *ob/*+ mice (N=5/group).

Using Electronic Microscopy (EM) analysis of isolated pancreatic islets, we found that the number of insulin granules was strikingly reduced in diabetic mice compared to controls (Figure 10A, left panels). Importantly, the number of insulin granule containing lysosomes (GCLs) was increased by at least 2-fold in pancreatic β-cells from diabetic mice as compared to β-cells from age-matched healthy controls (Figure 10A right panel, and B). The paradigm in the field is that insulin granule loss under diabetic conditions in pancreatic β-cells is mostly due to their

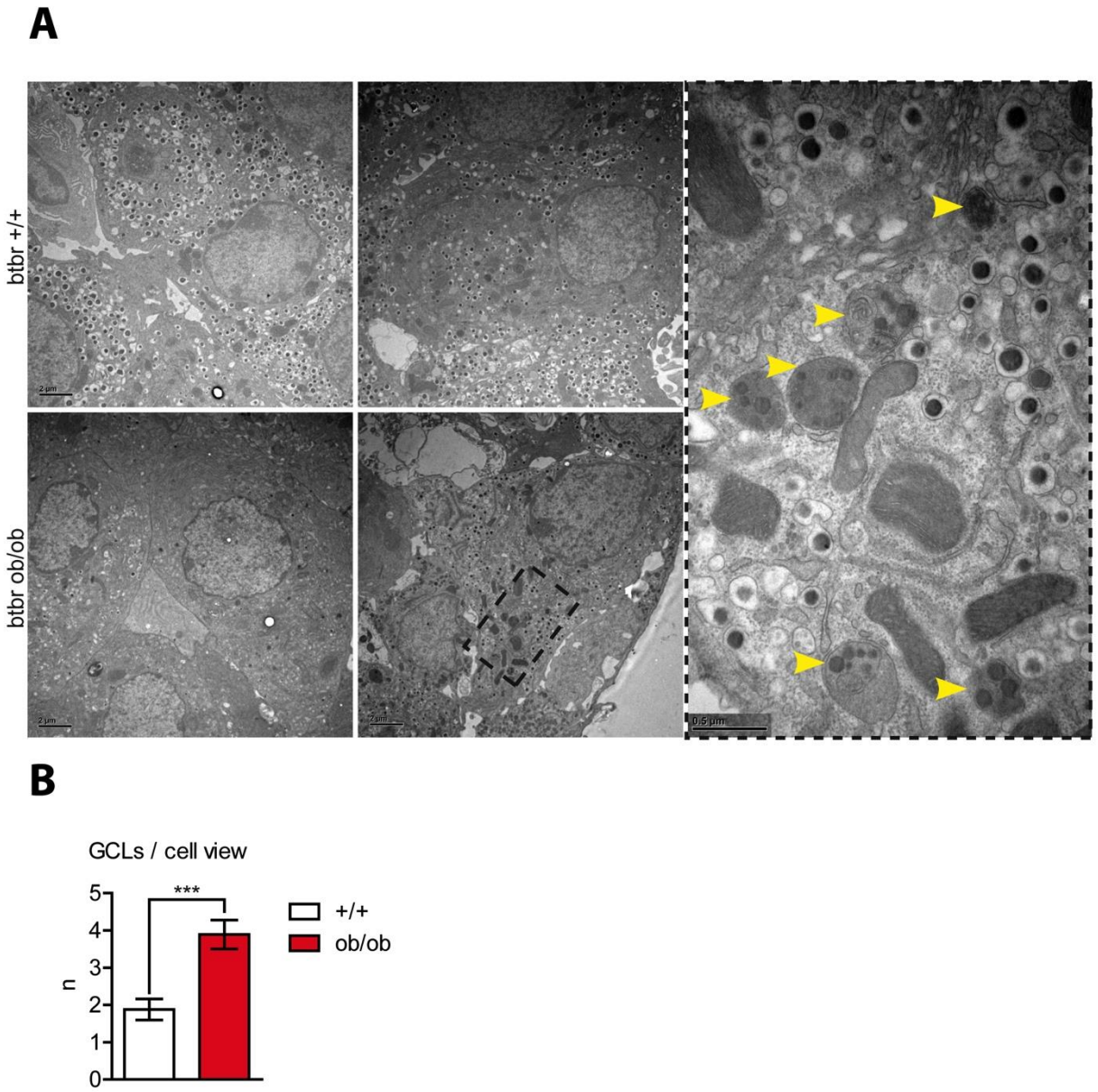

Figure 10. Increased numbers of GCLs in β-cells of diabetic mice. (A) Electron microscopy images of control (BTBR +/+) and diabetic (BTBR *ob/ob*) β-cells from isolated pancreatic islets. The dashed-lined rectangle is a close-up of the region of interest. The yellow arrow heads show GCLs. **(B)** Quantification of GCLs per cell view. $N_{+/+}$ = 25 cells and $N_{ob/ob}$ = 36 cells counted in 3 different mice for each group.

enhanced secretion out of the cells due to chronically elevated glycaemia. The fact that we found higher GCL number in diabetic islets hints at the possibility that increased lysosomal degradation of insulin granules may contribute to an overall loss of insulin.

To characterize better changes in the lysosomal compartment, we performed an immunofluorescence analysis (IF) of the four main lysosomal markers: LAMP1, LAMP2, the Cluster of Differentiation antigen protein 63 (CD63, also known as LAMP3 or LIMP1) and the Lysosome Membrane Protein 2 (LIMP2) co-staining β-cells in islets from these mice with insulin.

LAMP1 and 2 are part of the lysosomal-associated membrane glycoprotein family and represent together 50% of the lysosomal membrane proteins. They may have overlapping functions as the single knock-out mice do not display severe phenotypes, whereas the double knock-out mice are embryonic lethal (Eskelinen et al 2004). LAMP1 and 2 are extensively used as lysosomal markers including in studies on autophagy. Our IFs revealed that LAMP1 was unchanged, while LAMP2 was rather decreased in diabetic β-cells as compared to non-diabetic cells (Figure 11).

LIMP2 protein is encoded by the *SCARB2* gene and was shown to be implicated in the mannose-6-phosphate-independent transport of glucocerebrosidase to lysosomes (Blanz et al., 2015)(Reczek et al., 2007). Glucocerebrosidase is the enzyme responsible for lysosomal degradation of glucosylceramide. Defects in its degradation leads to Gaucher disease (Jović et al., 2012). In our screen, we observed restricted expression of LIMP2 in insulin-negative cells. Interestingly, the expression pattern is reminiscent of the one observed in IF analysis of glucagon, potentially indicating that LIMP2 is highly abundant in α cells. Additional data related to this finding are provided at the end of the result section.

A. Dramatic changes in CD63 expression and localization in diabetic β-cells

CD63 is part of the tetraspanin family and can form tetraspanin-enriched microdomains (TEM) on lipid membranes (Pols and Klumperman, 2009). It is highly abundant in lysosomes and late endosomes predominantly localizing inside the lysosomal lumen on intraluminal vesicles (ILVs) as well as exosomes. IF revealed that the CD63 signal was markedly enhanced in diabetic pancreatic β-cells in islets of BTBR *ob/ob* mice as compared to islets of non-diabetic

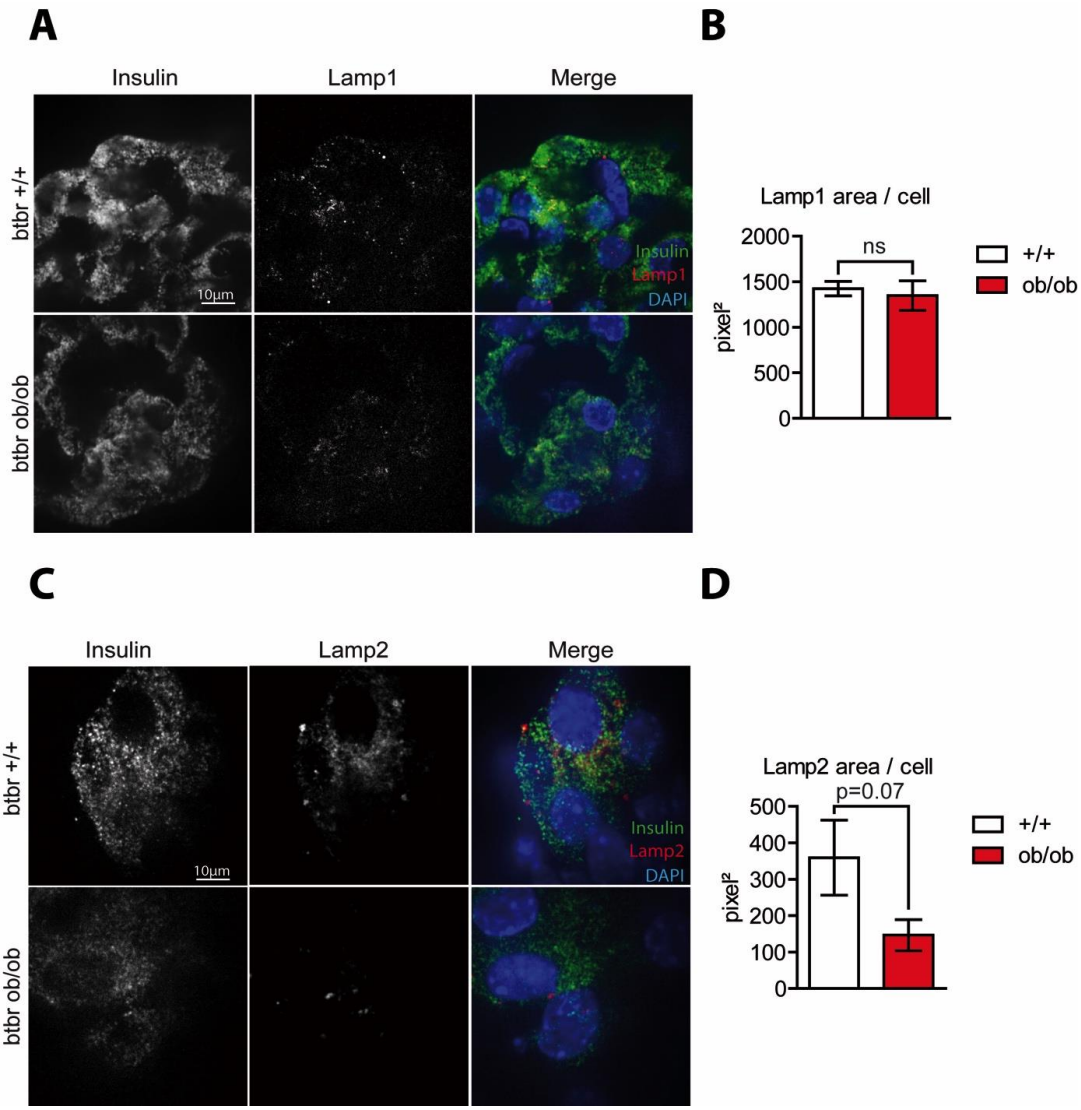

Figure 11. Expression of LAMP1 is unchanged, while LAMP2 expression is slightly decreased in β-cells of diabetic islets . (A) IF staining of β-cells in islets of pancreata from control (BTBR +/+) or diabetic (BTBR ob/ob) mice using antibody against insulin (green) and against LAMP1 (red). **(B)** Quantification of LAMP1 signal intensity per cell. The area was measured by quantification of pixel² over a fixed signal intensity threshold. **(C)** IF staining of β-cells in islets of pancreata from control (BTBR +/+) or diabetic (BTBR ob/ob) mice using antibody against insulin (green) and against LAMP2 (red). **(D)** Quantification of LAMP2 signal intensity per cell. The area was measured by quantification of pixel² over a fixed signal intensity threshold. Corresponding scale bars are indicated. $N_{+/+}$=17; $N_{ob/ob}$=18; 3 mice per group.

mice (Figure 12). CD63 expression in total islets of diabetic mice was also enhanced at the mRNA level as determined by quantitative RT-PCR (Figure 13A). Furthermore, western blotting revealed enhanced protein levels at 25kDa corresponding to the expected size of unmodified CD63 in line with IF experiments (Figure 13B). However, a band migrating at 30kDa was dramatically decreased. Even though we do not yet understand the nature of this

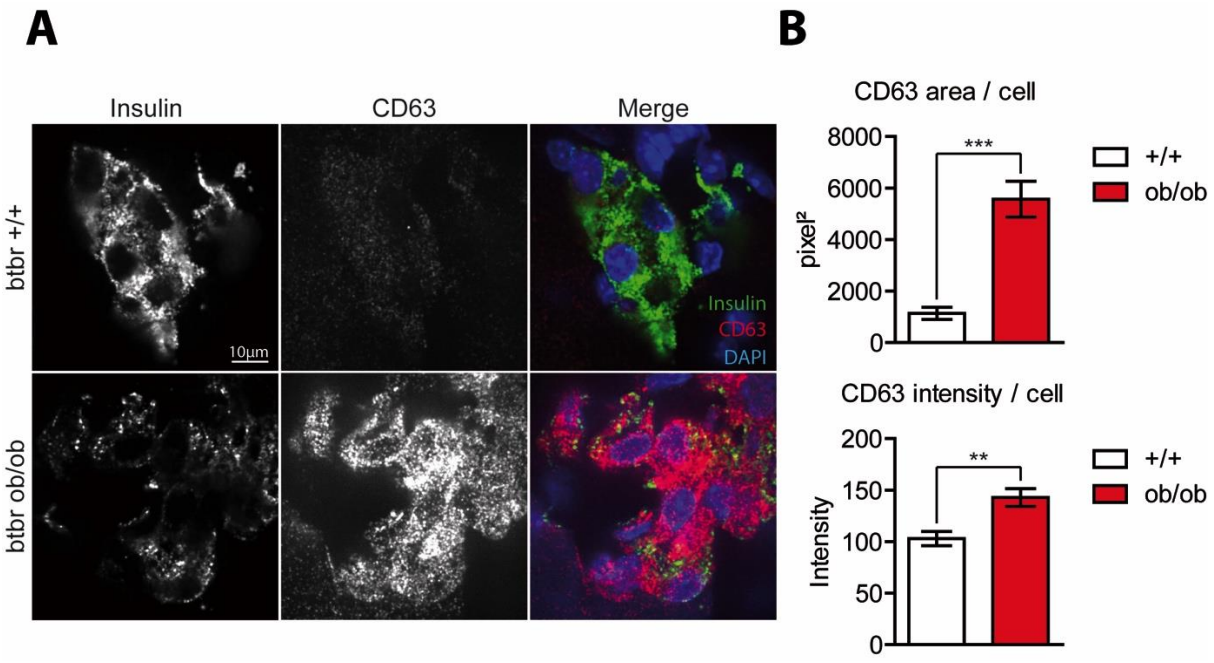

Figure 12. CD63 staining is strongly enhanced in diabetic β-cells. (A) IF staining of β-cells in islets of pancreata from control (BTBR +/+) or diabetic (BTBR ob/ob) mice using antibody against insulin (green) and against CD63 (red). **(B)** Quantification of the CD63 signal per cell. The area was measured by quantification of pixel² over a fixed signal intensity threshold. Signal intensities per cell is also shown. Corresponding scale bars are indicated. $N_{+/+}$=17; $N_{ob/ob}$=18; 3 mice per group. ***P<0.01; ***P<0.001*.

band, this may suggest that a posttranslational modification of CD63 is altered and may account for the overall higher CD63 levels. Further experiments including CD63 knockout samples need to be performed in the near future to shed light onto this interesting observations.

To assess localization of CD63 in relation to insulin granules, we next used the INS1 β-cell line derived from rat insulinoma. We challenged these cells *in vitro* with a high glucose/high palmitate cocktail, a widely accepted model to mimic glucolipotoxicity as a means to trigger β-

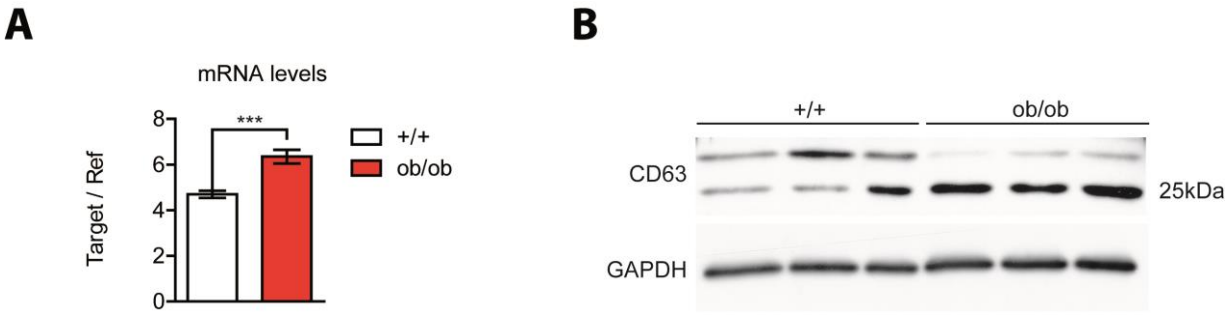

Figure 13. mRNA and protein levels of CD63 are enhanced in a diabetic context. (A) Quantitative RT-PCR using mRNA isolated from pancreatic islets of control (btbr +/+) and diabetic mice (btbr ob/ob). $N_{+/+}$=5; $N_{ob/ob}$=7; ****P<0.001* **(B)** Immunoblot of CD63 using lysates from isolated pancreatic islets of control (btbr +/+) or diabetic mice (btbr ob/ob).

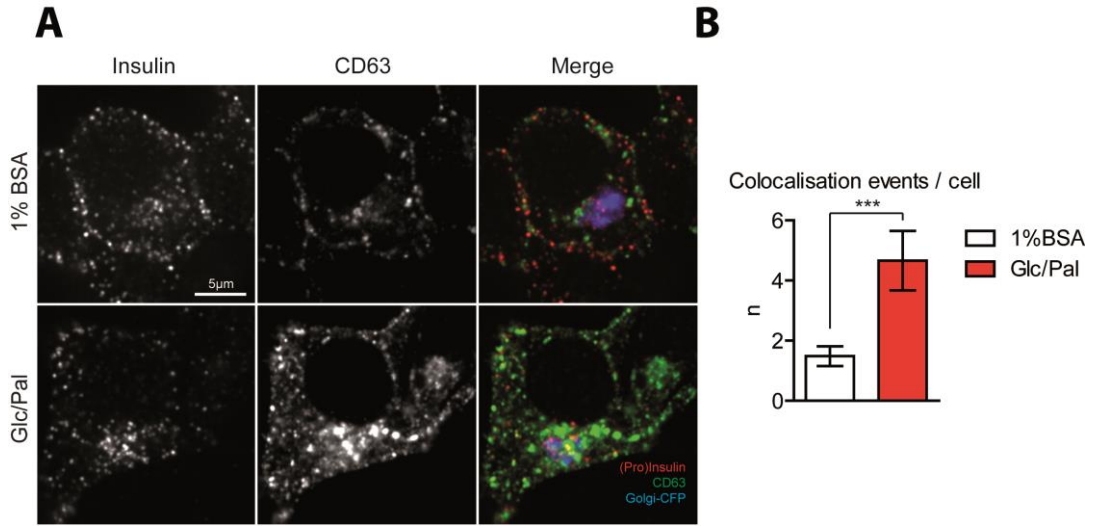

Figure 14. Increase in co-localisation between CD63 and insulin upon glucolipotoxic stress. (A) IF of INS1 cells under control (1% BSA) or diabetic (Glc/Pal) conditions using antibodies against insulin (green) and CD63 (red). The Golgi-CFP probe was used to visualize the Golgi apparatus. Corresponding scale bars are indicated. **(B)** Quantification of co-localisation between insulin and CD63-positive signals. Corresponding scale bars are indicated. $N_{1\%BSA}=11$;$N_{Glc/Pal}=10$;$***P<0.001$

cell failure in diabetes. To this end, we cultured INS1 cells in high glucose (30mM) and high palmitate (0.4mM) as previously described (Gjoni et al., 2014)(Oh et al., 2013). In line with observations in diabetic islets from mice, CD63 levels were enhanced upon glucolipotoxicity treatment, as revealed by the IF analysis (Figure 13A). CD63 strongly co-localized with insulin in the vicinity of the Golgi-apparatus upon glucolipotoxicity treatment as compared to control-treated cells, potentially indicating that insulin granules are targeted to CD63 positive compartments (Figures 14). To better understand the dynamics of co-localisation between CD63-positive structures and insulin granules, we decided to generate double knock-in INS1 cells tagging endogenously CD63 and the granule marker Phogrin with dsRED and GFP, respectively.

B. Generation of a double knock-in INS1 cell line expressing CD63-DsRed and Phogrin-eGFP

In a first step, I aimed at a single knock-in cell line tagging CD63 with DsRed. To introduce the DsRed fluorescent tag into the corresponding endogenous *CD63* locus, we used the CRISPR/Cas9 technology. DsRed was introduced into the C-term of the last exon of CD63 via the generation of a repair plasmid containing the DsRed sequence flanked by two homologous regions of approximately 1000bp 5' and 3' of the CD63 stop codon. The stop codon locus was

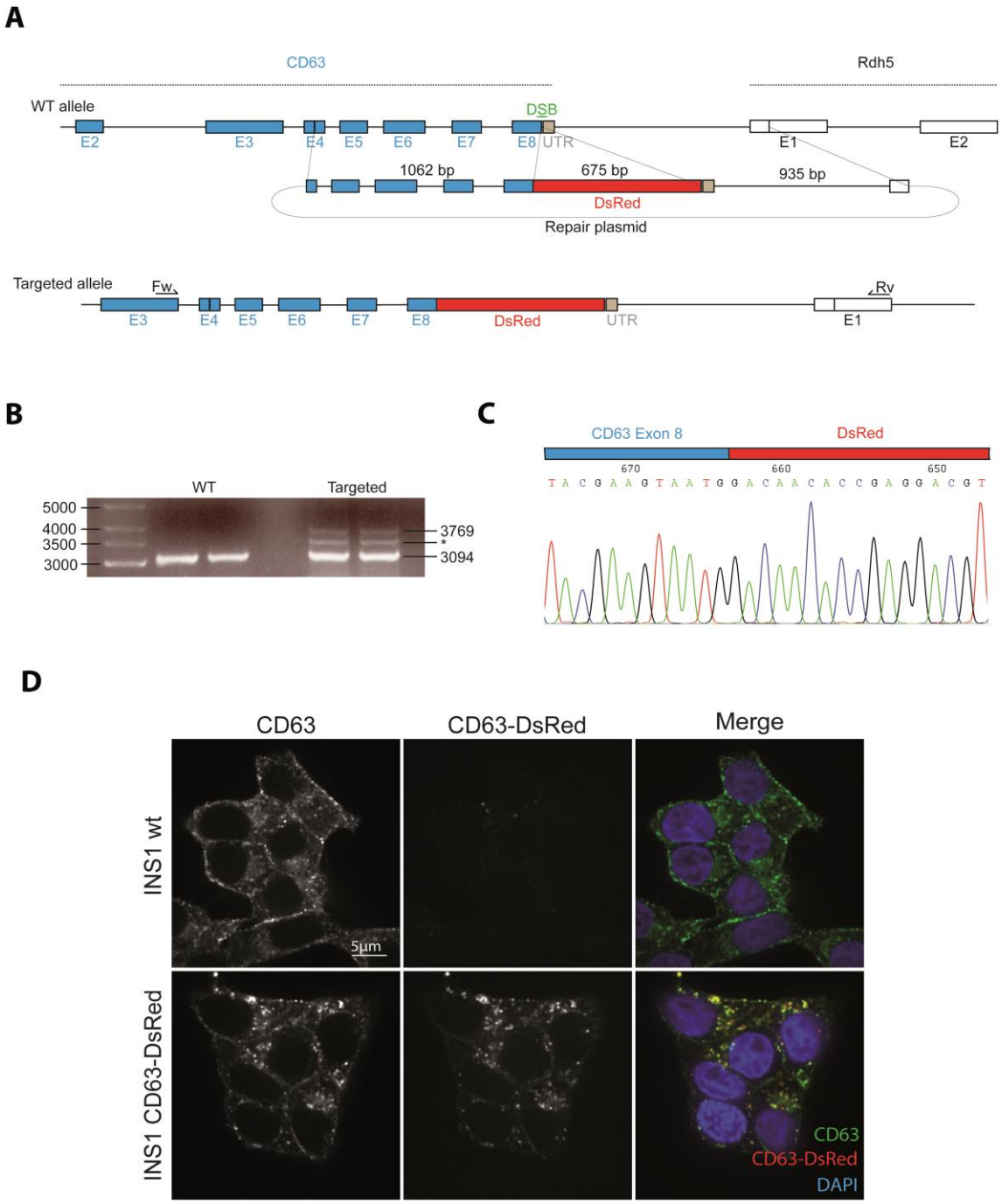

Figure 15. Generation of CD63-DsRed single knock-in INS1 cells. (A) Strategy to insert DsRed after the last CD63 exon. Details are described in the main text. Indicated Forward and Reverse genotyping primers outside the Homologous regions are designated as Fw and Rv, respectively. DSB, Double-stranded break. E, exon. UTR, Untranslated Region. **(B)** Genotyping PCR of DNA isolated from one single clone using the Fw and Rv primers. The wild-type band is expected at 3094bp and the targeted band at 3769bp. Existence of both bands indicate heterozygous insertion of DsRed. *, unspecific band. **(C)** Sanger sequencing of DNA isolated from one single selected clone for verification of the correct insertion of the DsRed sequence. **(D)** IF of CD63-DsRed single knock-in INS1 cells and wild type (wt) INS1 cells using an antibody against endogenous CD63. DAPI is used to stain nuclei. Corresponding scale bars are indicated.

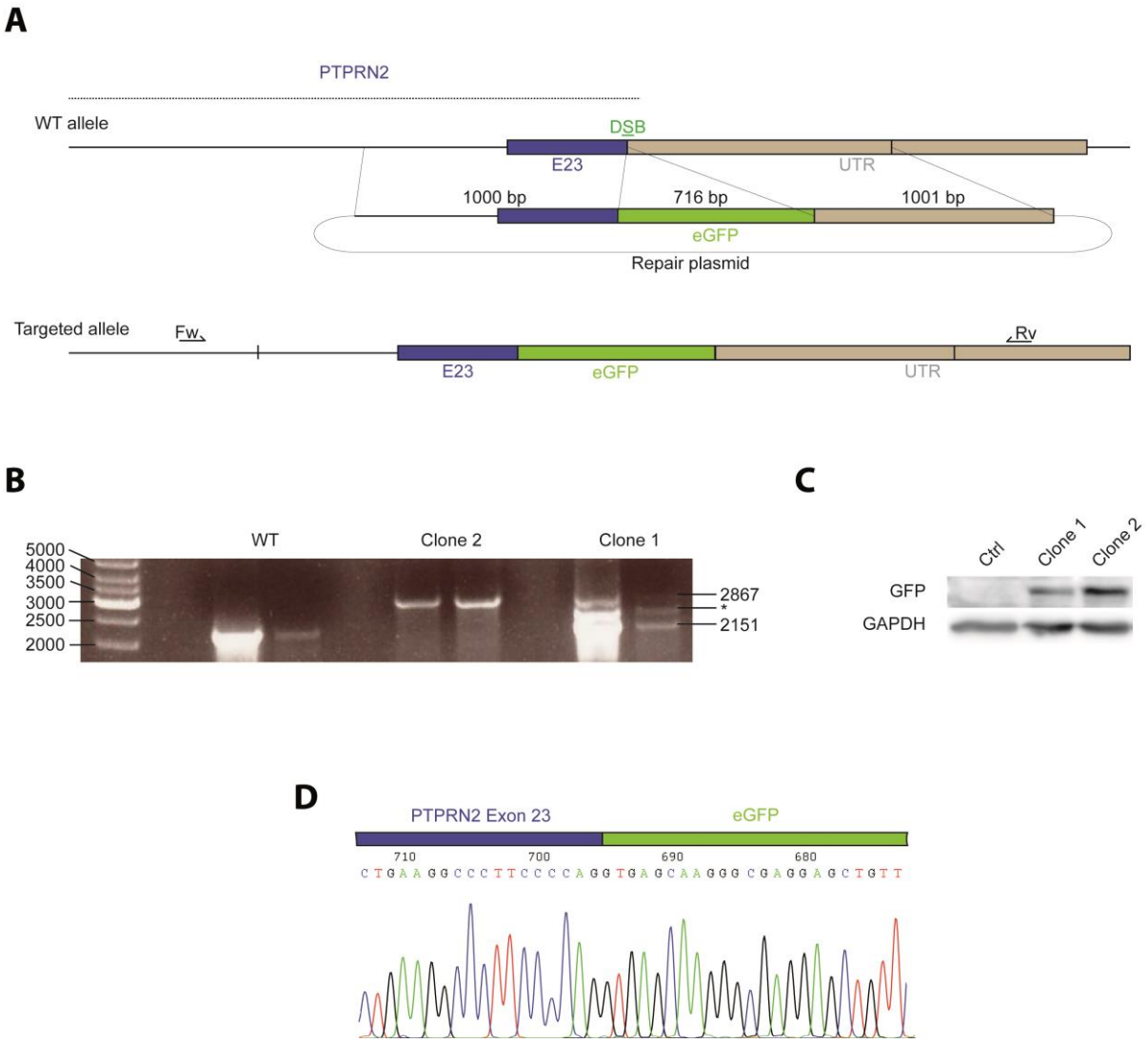

Figure 16. Generation of CD63-DsRed/Phogrin-eGFP double knock-in INS1 cells. (A) Strategy to insert eGFP after the last exon of Phogrin by Homology Direct Repair. Homology regions and their sizes are indicated. Indicated Forward and Reverse genotyping primers outside the Homologous regions are designated as Fw and Rv, respectively. DSB, Double-stranded break. E, exon. UTR, Untranslated Region. **(B)** Genotyping PCR of DNA isolated from two different clones using the Fw and Rv primers. The wild-type band is expected at 2151bp and the targeted band at 2867bp. PCR with DNA derived from clone 1 showed heterozygous insertion of eGFP, while it showed homozygous insertion of eGFP for clone 2. *, unspecific band. **(C)** Immunoblot with lysates of two different clones using an antibody against GFP. GFP signals appeared at the expected size of GFP-Phogrin at 100 kDa. GAPDH is used as a loading control **(D)** Sanger sequencing of DNA isolated from one clone for verification of the correct insertion of the DsRed sequence.

replaced with the repair plasmid sequence through Homology-Direct Repair (HDR) after the creation of double-strand breaks on the stop codon induced by targeted Cas9 (Figure 15A). In parallel, we generated the plasmid containing both the Cas9 and the gRNA targeting the end of the CD63 sequence as a tool to induce the double-strand breaks (DSBs). The two plasmids were

co-transfected into INS1 cells by electroporation and single-clone colonies were selected. We checked correct insertions of the fluorescent tag sequence by PCR using primers hybridizing outside of the homology regions (Figure 14A). The PCR confirmed correct insertion of DsRed as evidenced by the occurrence of an upshifted band with the expected size (Figure 15B). I also verified correct insertion using Sanger sequencing (Figure 15C). Finally, I verified proper subcellular localisation by IF using an antibody against endogenous CD63. Indeed, I could demonstrate that DsRed signals perfectly merged with the CD63 antibody signal in single knock-in cells. In addition, no DsRed signal could be detected in control wild type (wt) cells (Figure 15D). The single knock-in CD63-DsRed cell line was used to generate the double knock-in INS1 cell line. I inserted the eGFP sequence behind the exon 23 of Phogrin encoded by the *PTPRN2* gene from which we removed the stop-codon (Figure 16). In parallel, I also generated the single knock-in Phogrin-GFP cell line (data not shown).

C. Insulin granules are targeted to CD63 compartments in double knock-in INS1 cells in response to glucolipotoxicity stress

Using the newly generated double knock-in INS1 β-cell line, I was able to demonstrate increase co-localisation of CD63 with Phogrin in response to a glucolipotoxicity challenge as compared to control conditions. Unbiased quantification was done using person's correlation coefficients based on an automatic signal intensity threshold analysis (Figures 17A and 17B). These results thus confirm that insulin granules are targeted to CD63-positive compartments. Another observation was the presence of CD63-positive tubules that could not be previously visualized with fixed samples under IF. Interestingly, these CD63-positive tubules seemed to be increased in response to a glucolipotoxicity treatment. However, this feature still needs to be further quantified and analysed in the near future. These cells will also be used to further characterize that nature of targeting of insulin granules to CD63-positive compartments.

Altogether, we observed increased levels of CD63 in diabetic murine islets as compared to normal islets. Furthermore, diabetic conditions in vitro enhanced co-localization of CD63 with the granule marker phogrin potentially indicating that targeting of insulin granules to the lysosomal compartment and their degradation is enhanced in diabetes. Hence, this mechanism may account for insulin loss in the course of β-cell failure. In our previous study, we found that enhanced lysosomal degradation of insulin granules in response to nutrient deprivation

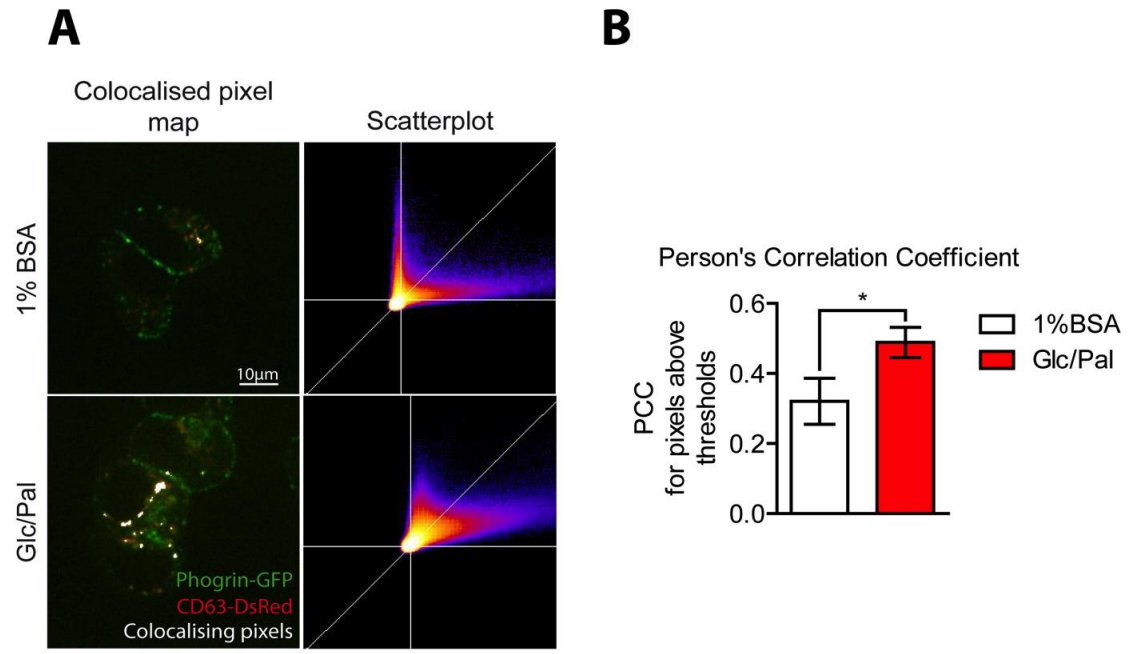

Figure 17. Increase in colocalisation between CD63-Dsred and Phogrin-GFP upon glucolipotoxic stress. (A) Colocalised pixel map of CD63-DsRed / Phogrin-GFP INS1 under control (1% BSA) or diabetic (Glc/Pal) conditions. White pixels indicates colocalisation events. **(B)** Quantification of the colocalisation events between CD63-DsRed and Phogrin-GFP upon control of diabetic condition using Pearson's correlation coefficient for pixels above threshold automatically set by the plugin. Corresponding scale bars are indicated. $N_{1\%BSA}=12$; $N_{Glc/Pal}=17$ from 2 independent experiments. *$P<0.05$.

suppressed autophagy in an mTOR-dependent manner. We thus wondered whether enhanced targeting of insulin granules to lysosomes in diabetes is accompanied with a decrease in autophagy. In fact, decreased autophagy has been shown to contribute to β-cell failure. I therefore next decided to address autophagy in a diabetic context.

D. Diabetic conditions inhibit autophagic flux and autophagosome formation

Autophagy plays a protective housekeeping 3333333333… in cells and its dysfunction or inhibition during metabolic challenges is rather deleterious (Lee, 2014). To evaluate autophagy in our diabetic models, I assessed the autophagic flux by measuring the level of p62 protein in isolated islets isolated from diabetic BTBR ob/ob and corresponding control mice. p62 is an adaptor protein, which binds to polyubiquitinated proteins as well as LC3-II, thus mediating their recruitment to the autophagophore (Figure 5). The fusion between the autophagosome and the lysosome, which leads to the autolysosome formation, induces p62 degradation. Therefore

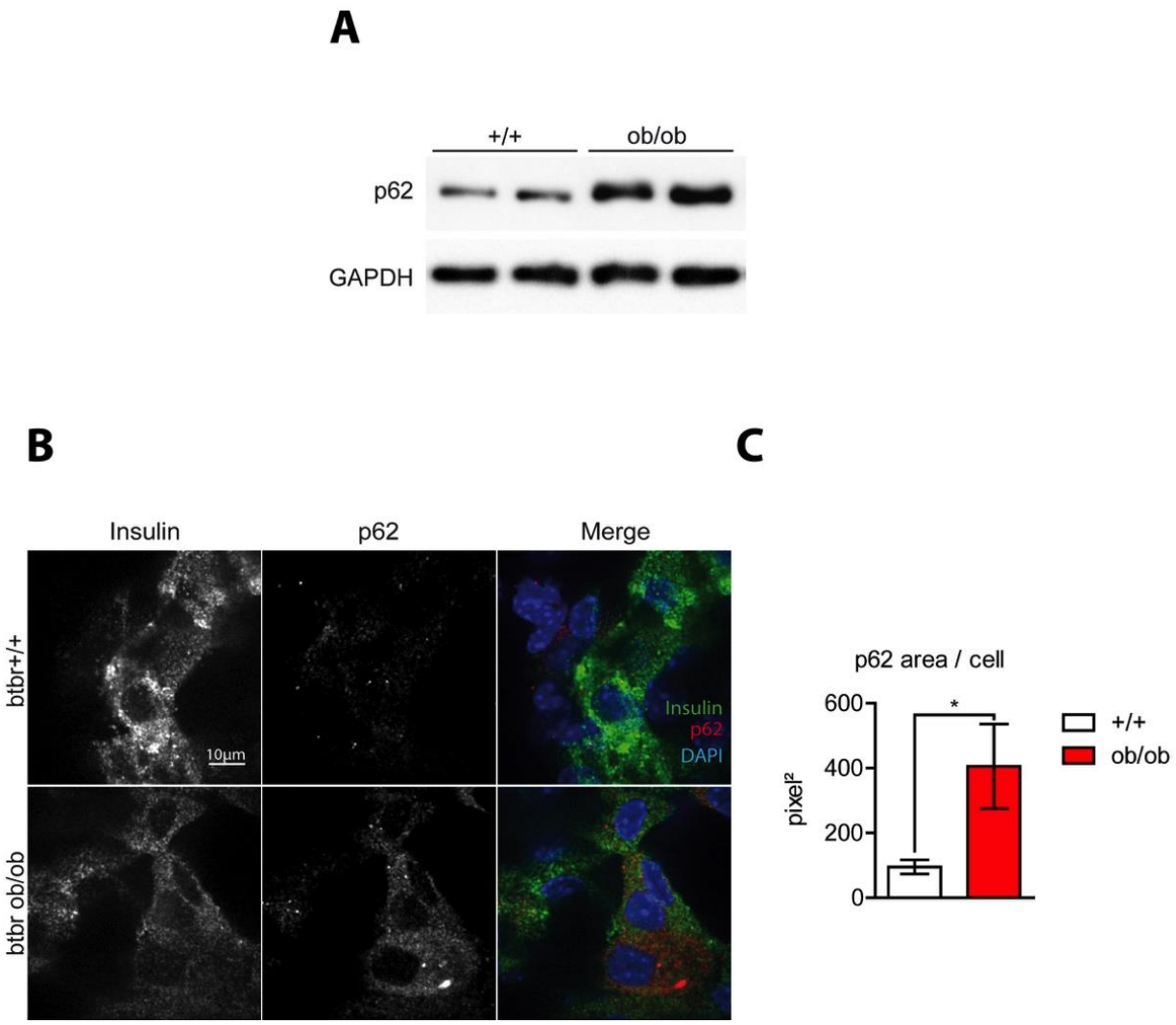

Figure 18. Autophagic flux is decreased in diabetic β-cells. (A) Immunoblot with lysates from isolated islets from control (+/+) or diabetic (ob/ob) mice using an antibody against p62. GAPDH is used as a loading control. **(B)** IF of β-cells in islets of pancreata from control (BTBR +/+) or diabetic (BTBR ob/ob) mice using antibodies against insulin (green) and against p62 (red). DAPI is used to stain nuclei. Corresponding scale bars are indicated.**(C)** Quantification of p62 signals observed by IF. $N_{+/+}$=15 $N_{ob/ob}$=15 from 3 different mice in each group. The area was measured by quantification of pixel² over a fixed signal intensity threshold. *$P<0.05$.

determination of p62 levels provide valuable information on the autophagic flux. Western blotting revealed enhanced p62 levels in islets isolated from diabetic mice in comparison to control islets. (Figure 18A). IF showed the presence of p62 aggregates in diabetic islets in line with enhanced p62 levels seen in Western blots (Figure 18B and 18C). To determine whether p62 accumulation was caused by an increased autophagosome formation or decreased autophagosome degradation, I performed subsequent experiments in INS1 cells. Western blot analysis with lysates from INS1 cells confirmed enhanced p62 levels in cells under glucolipotoxicity stress in comparison to non-treated cells (Figure 19).

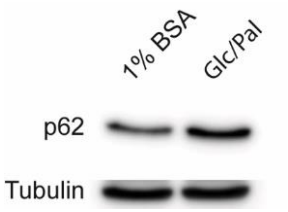

Figure 19. Autophagic flux is decreased in INS1 cells under glucolipotoxic conditions. Immunoblot with lysates from INS1 cells treated either with 1% BSA or subjected to a glucolipotoxicity challenge (Glc/Pal) using an antibody against p62. Tubulin was used as a loading control.

To monitor autophagosome formation, we used a knock-in GFP-LC3B INS1 cell line, which was recently generated by our laboratory (Goginashvili et al., 2015). This cell line allows for live visualisation of endogenous LC3B. In this cell line, autophagosome formation is detected by quantifiable green fluorescent puncta. By counting the number of LC3 positive puncta, we found that the number of autophagosome per cell was decreased in response to prolonged glucolipotoxicity in comparison to control treatment (Figure 20).

Upon its insertion in autophagosome membranes, LC3B is lipidated with PE changing its electrophoretic migration rate in an SDS page. Lipidated LC3B (LC3B II) is expected to run faster than the corresponding non-modified form of LC3B (LC3B I). Immunoblot analysis against LC3 using lysates from INS1 cells revealed that the LC3B-II levels were decreased in response to glucolipotoxicity in comparison to control treatment (Figure 21). In addition, blocking of the fusion between lysosomes and autophagosomes using the autophagy and lysosomal inhibitor Bafilomycin A1 (BafA1) also showed a decrease in LC3B-II levels upon

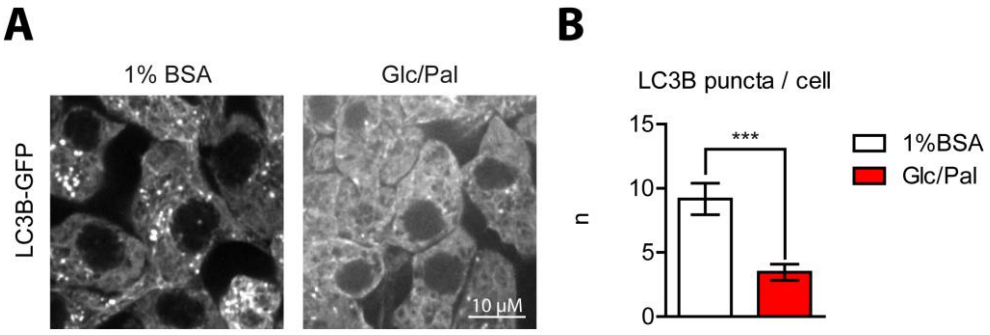

Figure 20 : LC3B-GFP dots decrease under glucolipotoxic conditions. (A) Representative pictures of LC3B-GFP expressing INS1 cells subjected to control (1%BSA) or glucolipotoxic conditions (Glc/Pal) for 40h. Corresponding scale bars are indicated. **(B)** Quantification of the number n of puncta per cell. Number N of cells is $N_{1\%BSA}$=22; $N_{Glc/Pal}$=24 from 2 independent experiments. ****P<0.001*.

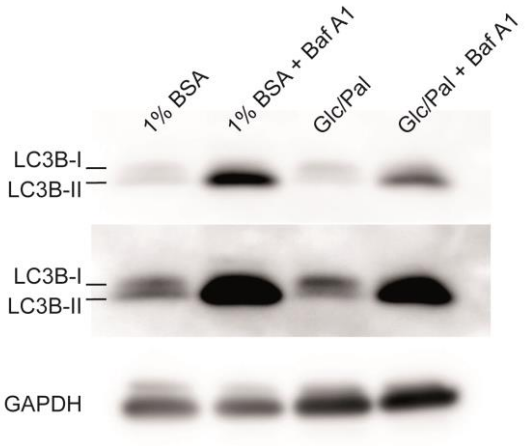

Figure 21 : Glucolipotoxic treatment decreases the levels of LC3B II. Western blot of lysates from INS1 cells treated with 1% bovine serum albumin (BSA) or glucose/palmitate (Glc/Pal) in the presence and absence of bafilomycin A1 (BafA1) using an antibody against LC3B. GAPDH was used as a loading control.

glucolipotoxicoty in comparison to control treatment. Thus, enhanced targeting of insulin granules to lysosomes is associated with decreased autophagy flux, both of which may contribute to β-cell failure. Thus, in our study, formation of GCLs coincides with an overall reduction in autophagy, suggesting that autophagy is not the primary pathway for SGs degradation in diabetes.

E. Inhibition of lysosomal degradation and autophagy by BafA1 enhances co-localization of CD63 and phogrin

To better characterize lysosomal granule degradation versus autophagy, we treated double knock-in INS1 cels with Bafilomycin A1 using co-localization of CD63 and phogrin as a readout. As mentioned in the previous section, Bafilomycin A1 inhibits the fusion between lysosomes and autophagosomes. In addition, it acts on the vacuolar H^+-pump (vATPase), preventing lysosomal acidification, thereby inhibiting degradation of targeted components. Treatment for 4h with Bafilomycin A1 led to a striking co-localisation of CD63 and phogrin as compared to control conditions (Figure 22). This result allows us to conclude that a massive amount of insulin granules are targeted to and degraded in CD63 positive compartments independent of autophagy. Lysosomes are nutrient sensing hubs of the cells. Insulin degradation in the lysosomes should release nutrients that should recruit mTORC1. We thus assessed whether mTOR recruitment to CD63-positive compartments was enhanced in response to a glucolipotoxic stress.

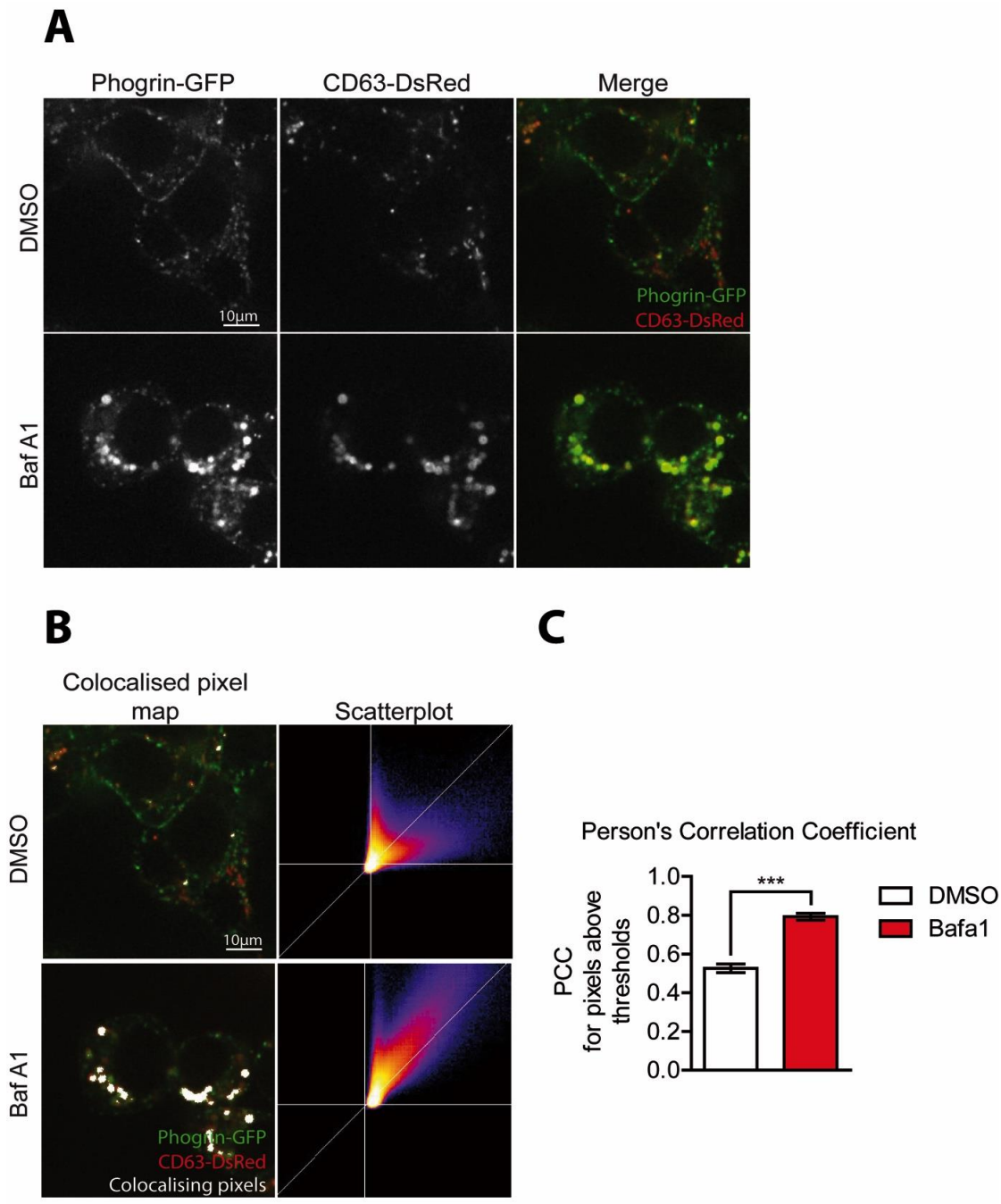

Figure 22. Bafilomycin A1 treatment enhanced formation of CD63 and phogrin double positive structures. (A) Representative image showing double knock-in INS1 cell line in response to control (DMSO) or Baf A1 (15nM for 4h) treatment. Corresponding scale bars are indicated. **(B)** Colocalised pixel map of double knock-in INS1 cell line under control (DMSO) or Baf A1 (15nM for 4h). White pixels indicates colocalisation events. **(C)** Quantification of the colocalisation events between CD63-DsRed and Phogrin-GFP upon control (DMSO) or Baf A1 using Pearson's correlation coefficient for pixels above threshold automatically set by the plugin. N_{DMSO}=12; N_{BafA1}=12. ****P<0.001*.

F. mTOR is recruited to CD63-positive compartments during glucolipotoxicity challenge

Upon a glucolipotoxicity challenge, I observed markedly enhanced recruitment of mTOR to CD63 positive compartments close to the Golgi (Figure 23). Recruitment of mTOR to CD63 positive compartments leads to its local activation. Hence, enhanced lysosomal activity in response to glucolipotoxicity might be responsible for local mTOR activity that may contribute to inhibition of autophagy. The activity status of mTOR will be assessed in the future analysing phosphorylation of known substrates including ULK1. These results in INS1 cells are also in line with observations in diabetic islets.

Altogether these data indicate that targeting of insulin granules to the CD63-positive compartment is enhanced during metabolic stress. To determine the importance of CD63 in insulin granule homeostasis, we silenced CD63 in INS1 cells and assessed insulin levels upon a metabolic challenge.

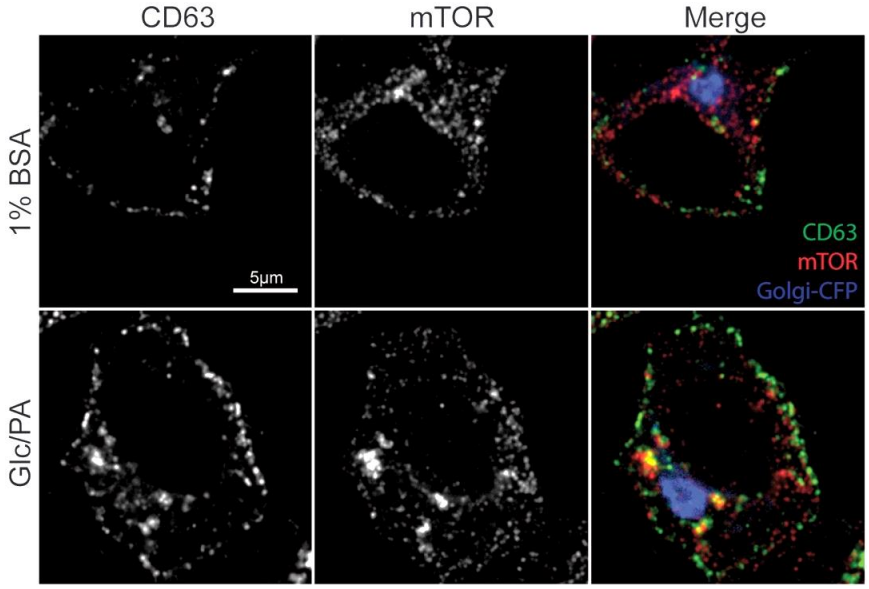

Figure 23. mTOR is recruited to CD63-positive structures upon glucolipotoxic conditions. IF of INS1 cells under control (1% BSA) or diabetic (Glc/Pal) conditions using antibodies against mTOR and CD63. The Golgi-CFP probe was used to visualize the Golgi apparatus. Corresponding scale bars are indicated.

G. Knock-down of CD63 restores insulin granules in response to a glucolipotoxic stress

Effective silencing of CD63 using siRNA pools was assessed by IF on INS1 cells using an antibody against CD63 (Figure 24A). Western blot analysis using lysates from INS1 cells subjected to a 1% BSA control condition did not reveal major differences in total insulin and pro-insulin levels upon knock-down of CD63. However, under glucolipotoxic conditions, knock-down of CD63 restored pro-insulin levels in comparison to non-silencing siRNA (Figure 24B). In addition, IF analysis on INS1 cells with an antibody against insulin showed that CD63 silencing during a glucolipotoxicity stress restored plasma membrane localisation of insulin granules in comparison to non-silenced cells under glucolipotoxic treatment. Overall these results indicate that CD63 contributes to insulin granule degradation.

II. PKD inhibition contributes to β-cell failure in diabetes

Our laboratory showed that SINGD is dependent on PKD activity. Inhibition of PKD upon fasting promotes targeting of nascent insulin granules to lysosomes for their degradation. I thus wondered whether PKD expression is affected in diabetes and whether a drop in its activity contributes to insulin loss and beta cell failure through targeting of insulin granules to the lysosome.

A. PKD1 expression is reduced upon onset of diabetes

Western blot analysis using lysates from isolated islets of control or diabetic mice revealed a clear decrease in total PKD levels in diabetic compared to control mice (Figure 25A). Furthermore quantitative RT-PCR analysis of the mRNA of the three PKD family members, PKD1, PKD2 and PKD3 showed that PKD1 was clearly more abundant in pancreatic islets in comparison to PKD2 and PKD3. Importantly, in islets of diabetic mice, PKD1 mRNA levels decreased two times as compared to levels in islets of non-diabetic mice (Figure 25B).

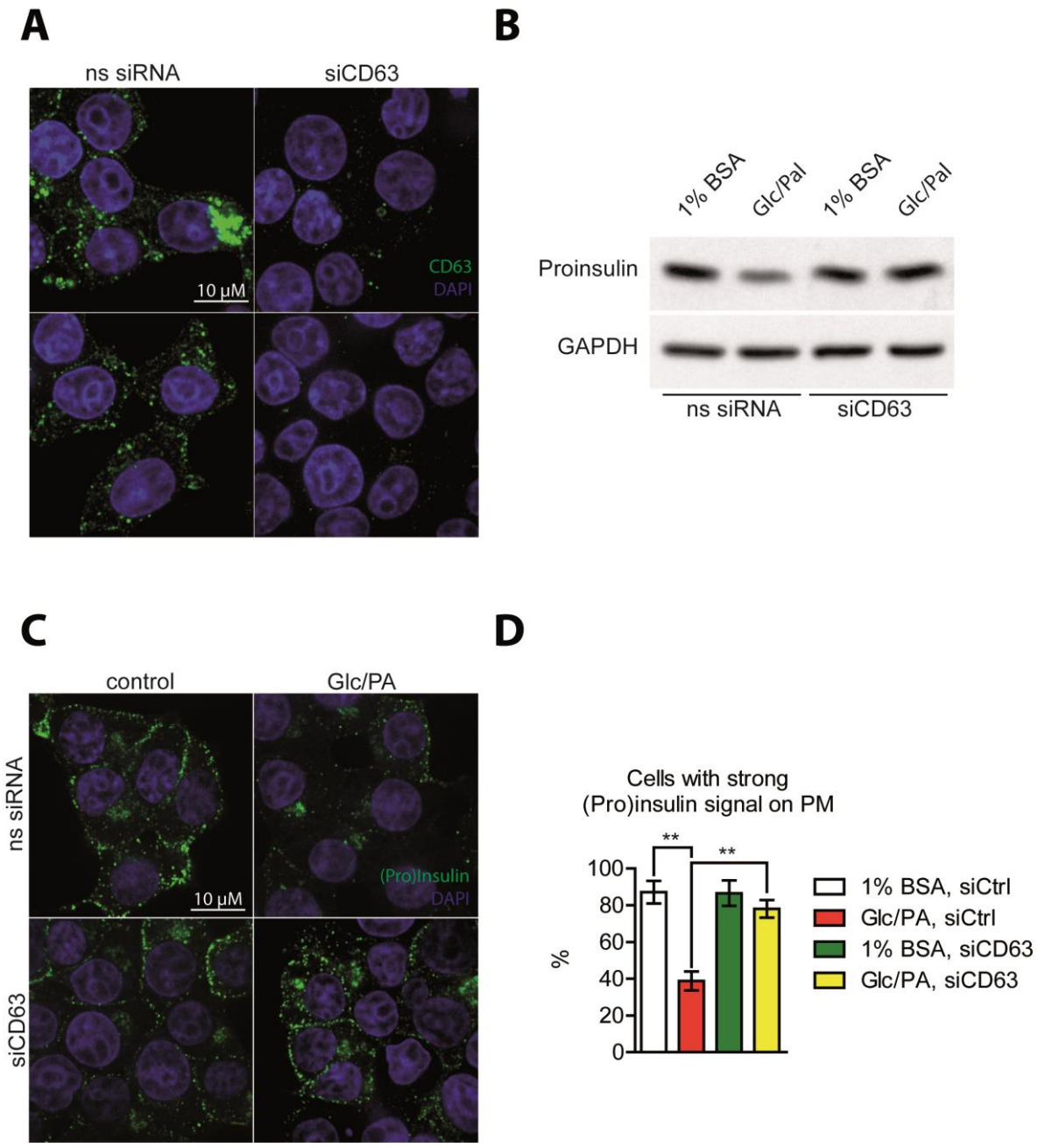

Figure 24. CD63 knock-down leads to restoration of insulin content under glucolipotoxic conditions. (A) IF of INS1 cells treated with non-silencing siRNA (ns siRNA) or siCD63 using an antibody against CD63. DAPI was used to visualise the nuclei. The corresponding scale bars are indicated. **(B)** Western blot of lysates from INS1 cells treated with 1% BSA or Glc/Pal in the presence of non-silencing siRNA or siCD63 using an antibody against (pro)insulin. GAPDH was used as a loading control. **(C)** IF of INS1 cells treated with 1% BSA or Glc/Pal in the presence of non-silencing siRNA or siCD63 using an antibody against (pro)insulin. **(D)** Quantification of (pro)insulin signals at the plasma membrane under control (1% BSA) or diabetic (Glc/Pal) conditions in presence of non-silencing siRNA or siCD63. $N_{1\%BSA,\ sictrl}=63$;$N_{Glc/Pal,\ sictrl}=62$; $N_{1\%BSA,\ siCD63}=86$; $N_{Glc/Pal,\ siCD63}=71$; $^{**}P<0.01$.

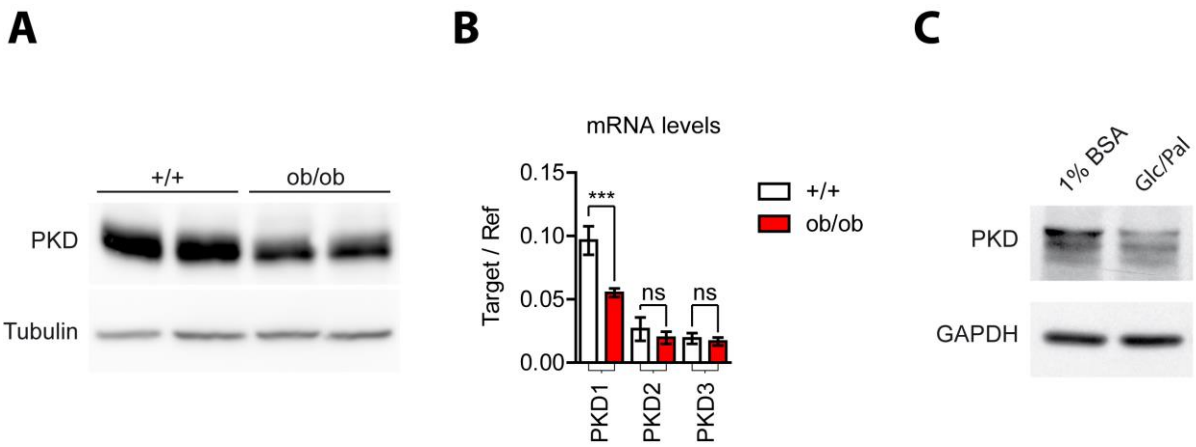

Figure 25. PKD1 levels are decreased in diabetic islets and INS1 cells. (A) Representative western blot of lysates from isolated islets of healthy control mice (BTBR +/+) or diabetic mice (BTBR *ob/ob*) using an antibody against PKD. Tubulin was used as a loading control. **(B)** Quantitative RT-PCR using mRNA isolated from pancreatic islets of control (BTBR +/+) and diabetic mice (BTBR *ob/ob*) using primer pairs amplifying cDNA of PKD1, 2 and 3. $N_{+/+}$=6; $N_{ob/ob}$=6; ****P<0.001* **(C)** Representative western blot of lysates from INS1 cells under control (1%BSA) or glucolipotoxic conditions (Glc/Pal) using an antibody against PKD. GAPDH was used as a loading control.

Western blot analysis with lysates of INS1 cells under glucolipotoxic or control conditions also revealed a decrease in the level of PKD upon glucolipotoxicity (Figure 25C). As glucolipotoxicity stress increased co-localisation between CD63-positive compartments and insulin granules, and at the same time decreases PKD1 levels, we wondered whether PKD1 activity was involved in targeting of insulin granules to the CD63-positive compartments.

B. PKD1 inhibition increases co-localisation of CD63-positive compartments and insulin granules

We assessed the role of PKD1 activity using the PKD inhibitor CID755673 (CID) (Sharlow et al., 2008). My host laboratory showed that treatment of INS1 cells with CID led to insulin loss through increased lysosomal degradation (Goginashvili et al., 2015). We confirmed insulin loss upon CID treatment on murine and human islets by western blot analysis. I next wanted to test if PKD inhibition led to enhanced targeting of insulin granules to CD63-positive compartments. To this end, I used the double knock-in INS1 cells and treated them with CID or under DMSO control conditions. In comparison to DMSO, an increase in co-localisation was observed in response to CID treatment (Fig. This result was also confirmed by IF using antibodies against CD63 and insulin in wild-type INS1 cells. As for the glucolipotoxicity treatment, we could not

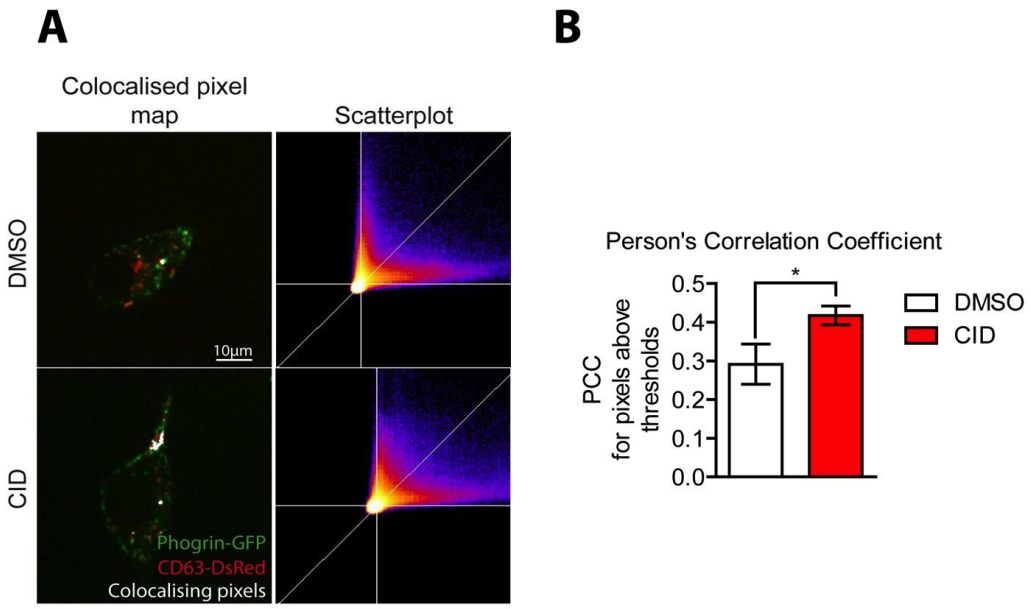

Figure 26. PKD inhibition led to increased co-localisation between CD63-DsRed and Phogrin-GFP. (A) Co-localised pixel map of CD63-DsRed / Phogrin-GFP INS1 under control (DMSO) or CID755673 (30µM for 12h) conditions. The white pixels indicate co-localisation events. Corresponding scale bars are indicated. **(B)** Quantification of the co-localisation events between CD63-DsRed and Phogrin-GFP upon control (DMSO) or CID755673 using Pearson's correlation coefficients for pixels above a threshold that was set automatically by the software plugin. N_{DMSO}=6; N_{CID}=8; *$P<0.05$.

capture many fusion events between CD63 positive compartments and Phogrin granules. Instead, it appears that the colocalising structures were already formed earlier during their biogenesis during their formation at the TGN.

C. CD63 knock-down partially rescues insulin content in PKD1 depleted INS1 cells

Acute and constitutive knock-down of PKD1 led to insulin loss (Goginashvili et al., 2015). To determine if CD63 was required in PKD-dependent lysosomal insulin granule degradation, we decided to knock-down CD63 using siRNA in INS1 cells stably lacking PKD1 (shPKD1-INS1). Western blot analysis of shPKD1-INS1 cells treated with siCD63 using a (pro)insulin antibody revealed an increase in insulin levels in comparison to ns siRNA controls (Figure 27A). IF of these cells confirmed a restoration of insulin levels and recovery of plasma membrane localisation of insulin granules in response to siCD63 in comparison to ns siRNA (Figure 28B).

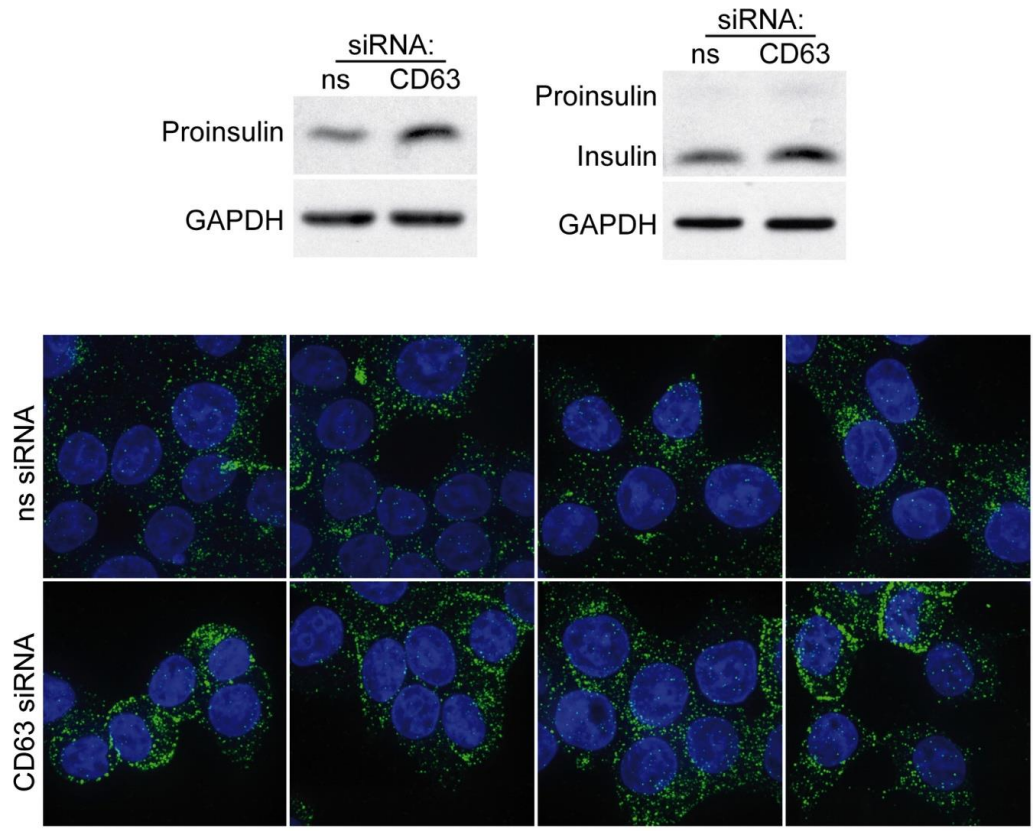

Figure 27. Knock-down of CD63 restores abundance and localisation of insulin granules in PKD1-depleted cells. (A) Western blot of lysates of shPKD1-INS1 cells in presence of non-silencing siRNA and siCD63 using an antibody against (pro)insulin. GAPDH was used as a loading control **(B)** IF of shPKD1-INS1 cells treated with control non-silencing siRNA (ns siRNA) or siCD63 using an antibody against (pro)insulin**.** DAPI is used to visualise nuclei.

These results indicate that CD63 acts downstream of PKD1 in the lysosomal insulin granule degradation pathway.

D. PKD inhibition *in vivo* leads to faster onset of diabetes in our murine model

I next wanted to assess the impact of PKD1 inhibition *in vivo* in a diabetic context. To this end, I implanted osmotic Alzet® pumps containing CID or the solvent control and monitored glycaemia in mice over 2 weeks of treatment. CID treatment dramatically accelerated diabetes as shown by increased fasting blood glucose levels (> 150 mg/dl) as compared to control-treated mice (Figure 29B). This was accompanied by a severe weight loss that is a cardinal sign of full-blown diabetes (Figure 28A). To further characterize β-cell function, I performed an *in vivo* Glucose-Stimulated Insulin Secretion test (GSIS) and observed significantly lower blood

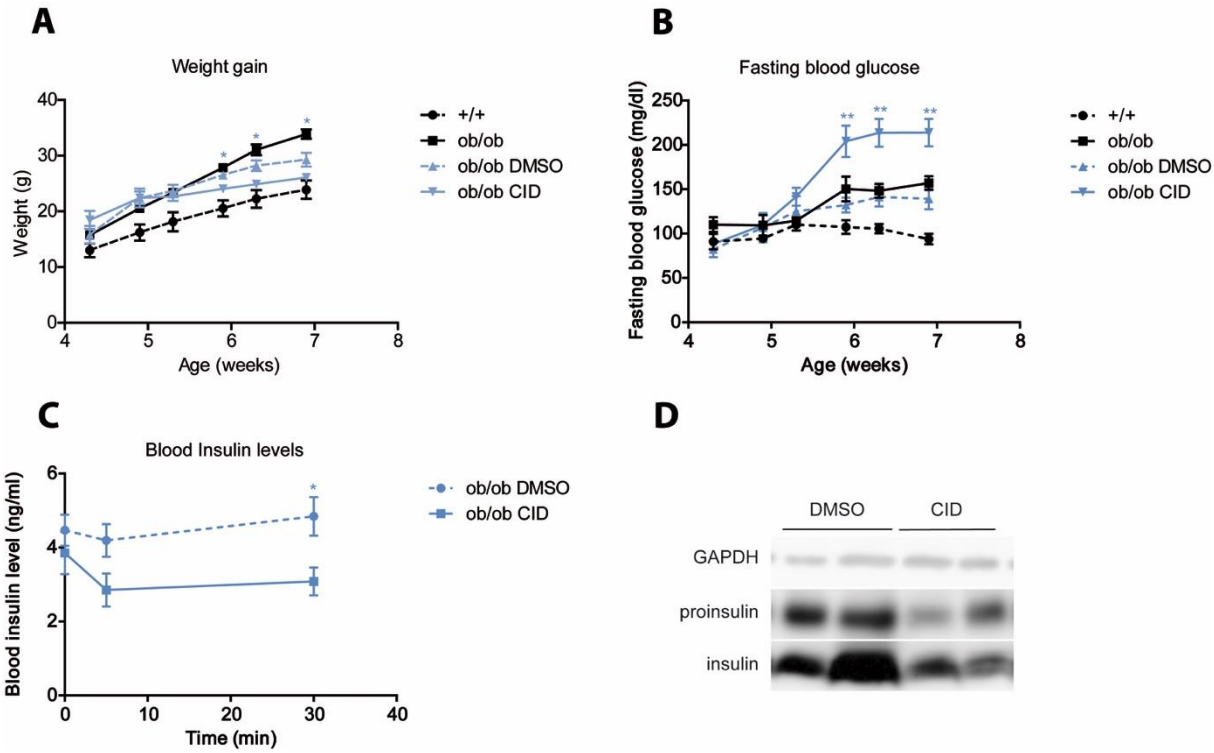

Figure 28. *In vivo* inhibition of PKD led to acceleration of diabetes. (**A)** Time-course of body weights of BTBR ob/ob mice treated with the control solvent (DMSO) or with CID755673 (CID) in comparison to mice that were not implanted pumps (+/+ and ob/ob) **(B)** Time-course of fasting blood glucose levels of BTBR ob/ob treated with the control solvent (DMSO) or with CID755673 (CID) in comparison to non-implanted mice (+/+ and ob/ob) $N_{DMSO}=5$; $N_{CID}=5$; *$P<0.05$; **$P<0.01$ **(C)** GSIS of BTBR ob/ob treated with the control solvent (DMSO) or with CID755673 (CID). $N_{DMSO}=3$; $N_{CID}=3$ *$P<0.05$. **(D)** Immunoblot against (pro)insulin of isolated islets from DMSO- or CID-treated mice. GAPDH was used as a loading control.

insulin levels in CID-treated as compared to control-treated mice (Figure 28C). Immunoblot analysis with lysates from isolated islets using an antibody against insulin revealed decreased total insulin levels in CID-treated in comparison to control-treated mice (Figure 28D). To understand the cause of insulin loss, I next performed quantitative EM analysis with isolated islets from control and CID-treated mice. A marked increase in GCLs was observed upon PKD inhibition indicating that insulin loss in β-cells most likely is the consequence of increased lysosomal degradation (Figure 29). Overall, I found that PKD1 levels were decreased upon onset of diabetes in mice and glucolipotoxicity-stressed INS1 cells. PKD inhibition leads to increased targeting of insulin granules to CD63-positive compartments in INS1 cells. PKD inhibition *in vivo* results in acceleration of diabetes most likely as a consequence of premature lysosomal insulin granule degradation as the numbers of GCLs was dramatically increased. These data are in line with our hypothesis. In the future, I will have to explore whether systemic pharmacological inhibition of PKD will entail additional metabolic effects in mice. For

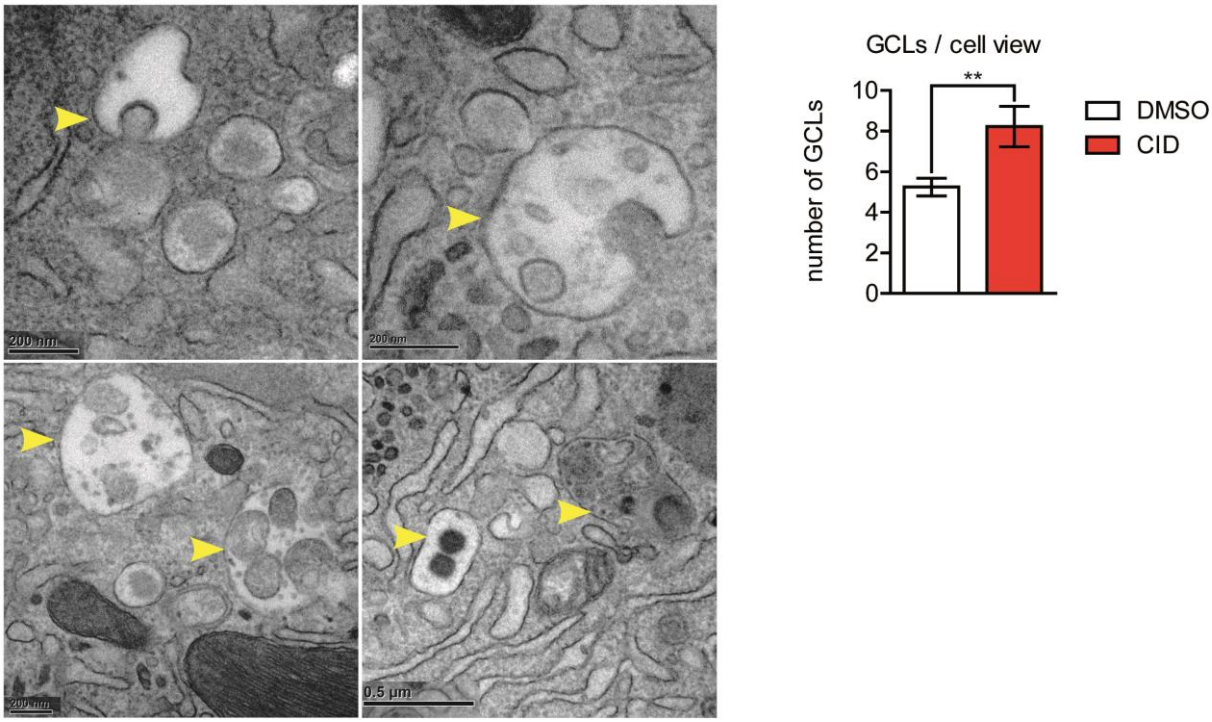

Figure 29. Inhibition of PKD *in vivo* led to increased GCL formation. (A) Electron microscopy pictures of β-cells of BTBR *ob/ob* mice treated with CID755673. The yellow arrow heads show GCLs. **(B)** Quantification of GCLs per cell view. N_{DMSO}=25 cells and N_{CID}=27 cells coming from 3 different mice for each group. ***P<0.01*.

example, it will be important to understand whether PKD inhibition affects insulin sensitivity. In addition, we will use conditional PKD1 knockout mice to complement pharmacological data with genetic evidence in vivo for PKD1 to be important in these processes. PKD1 activation in pancreatic β-cells was shown to be beneficial in obesity and streptozotocin-induced diabetes (Sumara et al., 2009).

III. PKD1 activation leads to restoration of the insulin content and improved glucose homeostasis in mice.

PKD1 activation in p38δ knock-out mice resulted in decreased lysosomal insulin granule degradation upon starvation (Goginashvili et al., 2015). We thus wondered whether pharmacological inhibition of p38δ leading to increased PKD1 activation is beneficial in a diabetic context. As deletion of p38δ led to chronic PKD1 activation, the design of specific inhibitors against p38δ appears to be necessary. Moreover, p38δ expression is restricted to few

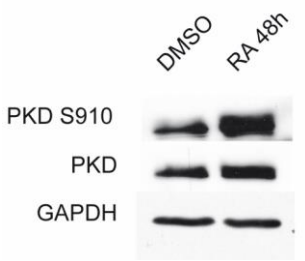

Figure 30. RA treatment activates PKD1 in human islets. Western blot using lysates from isolated human islets treated with DMSO or RA for 48h using antibodies against phospho-PKD (PKD S910) and total PKD (PKD). GAPDH was used as a loading control.

tissues (including pancreas) as compared to its closely related kinase p38α that is ubiquitously expressed in all tissues. This makes p38δ as an interesting and potential pharmacological target. Through a recent collaboration with an industrial partner, we have generated a compound (herein referred to as RA) with high potential to specifically inhibit p38δ and no other members of the p38 kinase family as well as 260 other kinases. A substantial part of pre-analysis has already been performed including cytotoxicity and cell permeability assays (ADME-T: Caco2 permeability, Met lability, CIB3A4 MBI, hERG inhibition). Finally, the compound fulfils the criteria for a prospective lead chemistry based on structure-activity relationship (SAR), drug design and X-ray data. Hence, we are currently at the stage to address the effects of specific pharmacological inhibition of p38δ and lysosomal insulin granule degradation in the context of diabetes.

A. p38δ inhibition activates PKD

Upon its activation, autophosphorylation of PKD occurs at serine 910 (human PKD) (Fu and Rubin, 2011). To test whether PKD gets activated upon p38δ inhibition, I used an antibody against phosphorylated Serine 910 (PKD S910). Western blot analysis using lysates from isolated human islets treated with DMSO (solvent control) or RA for 48h revealed an increase of autophosphorylated PKD upon p38δ inhibition (Figure 30).

B. PKD activation *in vivo* delays onset of diabetes

To test the effects of RA *in vivo* in mice, we decided to conduct similar experiments as described above in the context of *in vivo* PKD inhibition. I implanted osmotic Alzet® pumps containing the RA compound into BTBR *ob/ob* mice and monitored glycaemia in the course of 2 weeks of treatment (Figure 31). I observed a marked delay in the raise of fasting blood glucose in RA-

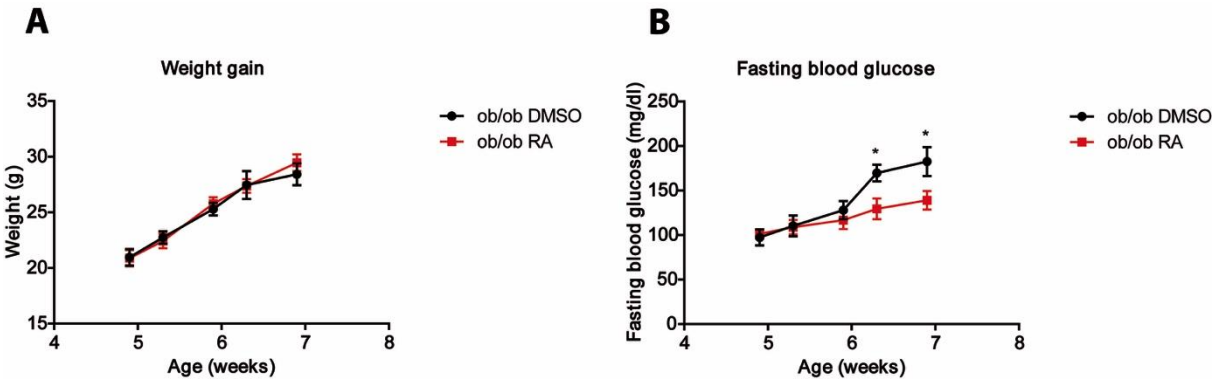

Figure 31. Inhibition of p38δ *in vivo* delayed diabetes development in BTBR ob/ob mice. (**A)** Time-course of body weights of BTBR *ob/ob* treated with the solvent (DMSO) or with RA. **(B)** Time-course of fasting blood glucose levels of BTBR *ob/ob* mice treated with the solvent (DMSO) or RA. N_{DMSO}=5; N_{RA}=7; **P* < 0.05 (*t* test).

treated as compared to control-treated mice. RA treatment did not affect the body weight and had no obvious toxic side effects.

C. PKD activation increases insulin granules levels in normal and diabetic human islets

Importantly, further experiments are necessary to confirm that beneficial effects related to p38δ inhibition are indeed caused by inversing lysosomal insulin granule degradation in the β-cell. To this end, I measured insulin secretion in response to glucose stimulation upon RA treatment of non-diabetic human islets using an ELISA for insulin (Figure 32A). RA did not affect glucose-stimulated insulin secretion. However, total insulin levels in lysates of islets treated for 48 hours with RA were increased in comparison to control-treated islets. This result was confirmed by western blot analysis using an antibody against insulin (Figure 32B). Importantly, RA treatment led to a decrease in p62 levels, suggesting that the autophagy flux could be enhanced. The question remained whether such effects can be obtained in islets of patients suffering from T2D. Indeed, the insulin content increased upon RA treatment in diabetic islets in comparison to control-treated diabetic islets.

Collectively, my results suggest an involvement of lysosomal degradation of insulin granules-autophagy in β-cell failure in T2D and provide compelling evidence for beneficial outcomes upon targeting of this process in diabetic β-cells, thus presenting a potential therapeutic strategy for treatment of T2D.

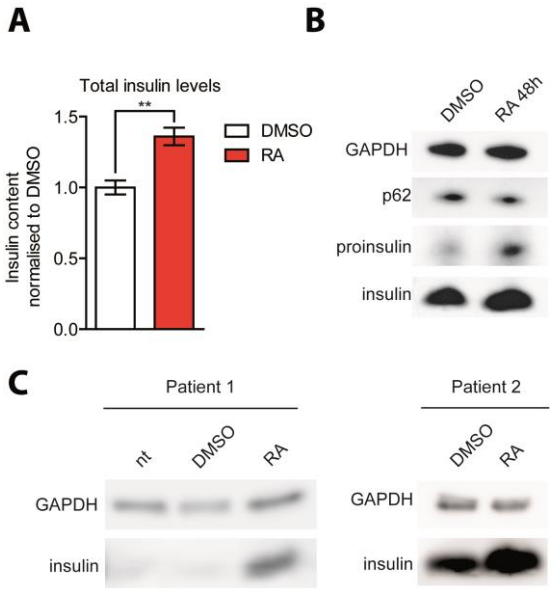

Figure 32. RA treatment increases insulin content in human islets from non-diabetic as well as diabetic donors. (**A)** ELISA using supernatants and lysates of isolated human islets treated with RA or DMSO for 48h (N=3). ***P<0.01* **(B)** Western blot using lysates of isolated human islets treated with RA or DMSO for 48h using antibodies against (pro)insulin and p62. GAPDH was used as a loading control. **(C)** Western blot of lysates from isolated human islets of two diabetic donors (patient 1 and 2) using an antibody against (pro)insulin. Proinsulin was not detectable in lysates of diabetic islets. GAPDH was used as a loading control. Islets were either left untreated (nt) or treated with RA or DMSO.

IV. LIMP2 is highly expressed in alpha-cells.

While levels of LAMP1 and 2 were largely unchanged, CD63 levels were dramatically enhanced in β-cells of diabetic mice. Interestingly, LIMP2 expression was restricted to insulin-negative cells in the periphery of the islet (Figure 34). In murine islets, α cells expressing glucagon are also located in the periphery of the islets. Indeed, LIMP2 and glucagon IF revealed

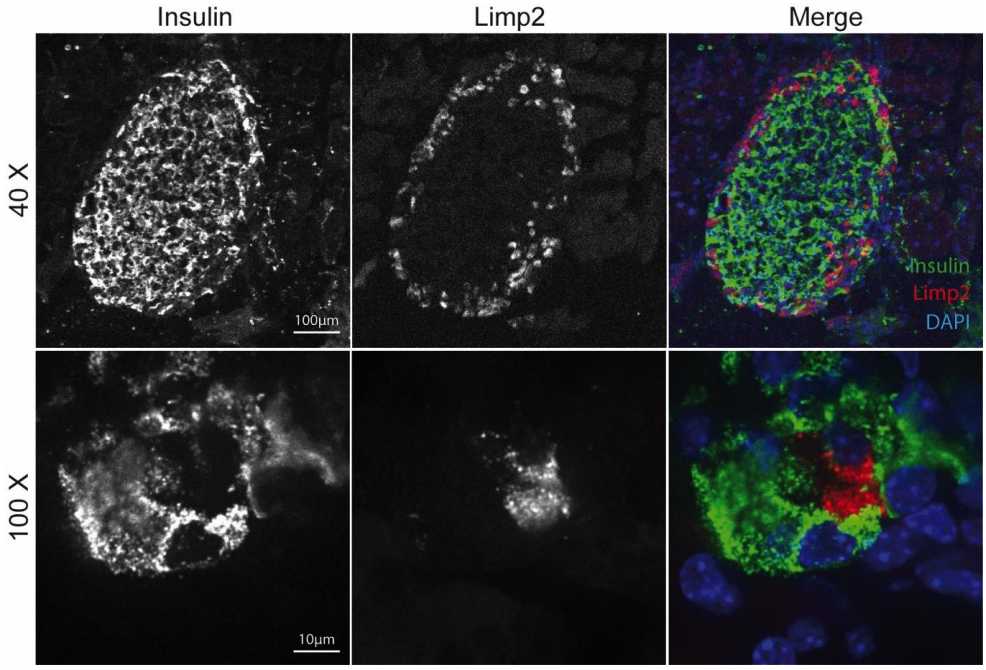

Figure 34. LIMP2 is highly expressed in insulin-negative cells in the periphery of murine islets. IF of islets of pancreata from BTBR +/+ mice using antibodies against insulin (green) and against LIMP2 (red). DAPI is used to visualise nuclei. Magnifications 40X or 100X are shown. Corresponding scale bars are indicated.

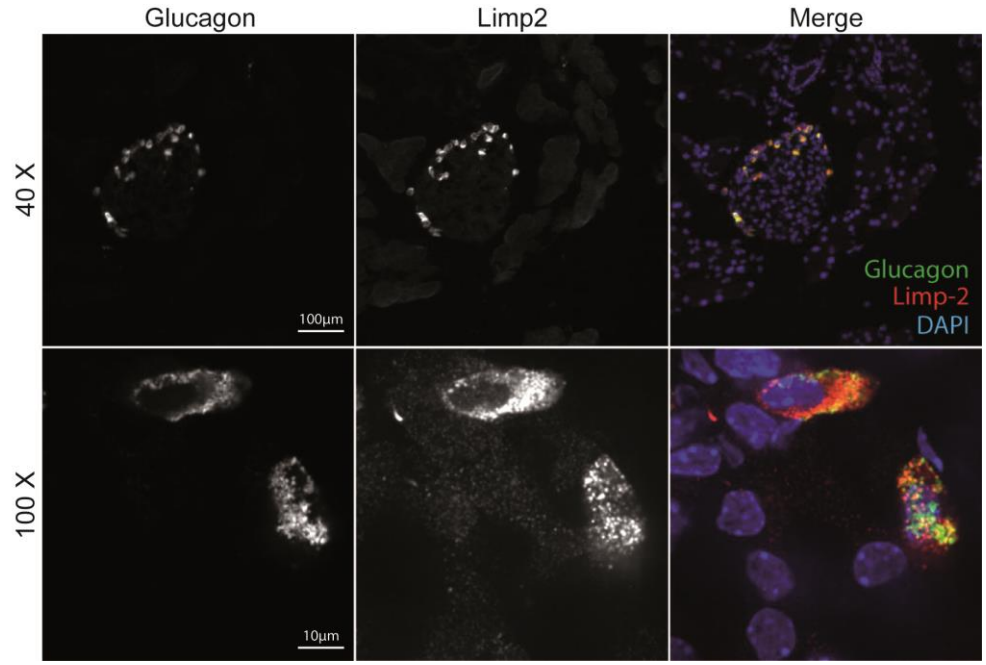

Figure 33. LIMP2 is higly expressed in α-cells. IF of islets of pancreata from BTBR +/+) mice using antibodies against glucagon (green) and against LIMP2 (red). DAPI is used to visualize nuclei. Magnification 40X or 100X are shown. Corresponding scale bars are indicated.

predominant expression of LIMP2 in α cells (Figure 34). To verify specificity of the antibody against LIMP2, I confirmed expression and localization of LIMP2 using another antibody. Indeed, my observations could be confirmed (data not shown). In order to improve resolution of LIMP2 localization, I next performed IF experiments in dispersed α cells derived from rat pancreatic islets. After isolation and dispersion of the rat islets, α cells were separated from β-cells by FACS. In fact, IF demonstrated that LIMP2 co-localized with gucagon potentially indicating that LIMP2 resides on glucagon granules (Figure 35). In the future, the function of LIMP2 in a cells and potentially in glucagon granule biogenesis will be addressed.

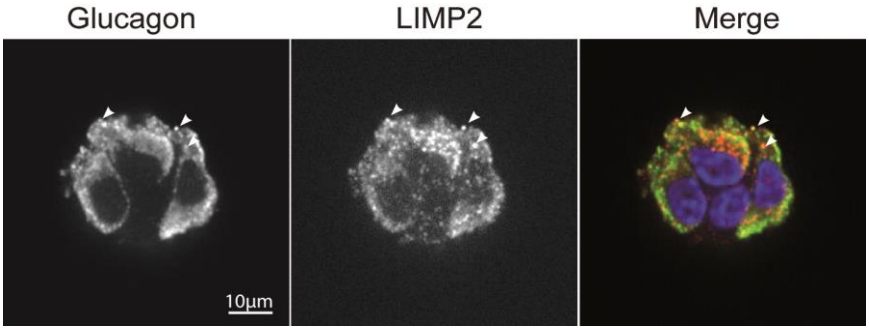

Figure 35 : LIMP2 co-localises with glucagon in glucagon granules. IF of α-cells from dispersed and sorted from isolated rat islets using antibodies against glucagon (green) and against LIMP2 (red). DAPI is used to visualise nuclei. Co-localisation (yellow) is indicated by white arrow heads. The corresponding scale bar is indicated.

Discussion

My data suggest that lysosomal degradation of insulin granules is enhanced in diabetic β-cells leading to suppression of autophagy as well as insulin loss. Thus, this mechanism may confer transition of compensated to decompensated β-cell function.

The diabetic BTBR *ob/ob* mice display markedly reduced pancreatic insulin levels, which was suggested to be caused by a decrease in total β-cells mass due to apoptosis, dedifferentiation or hypoplasia (Clee et al., 2005). We suggest that in addition to a drop in β-cell mass, remaining β-cells contain less insulin granules as compared to non-diabetic β-cells (Figure 10A left panels). However, defects in insulin synthesis and insulin granule biogenesis has been shown to be also altered in diabetic patients (Kahn et al., 2009). Deletion of genes involved in insulin vesicle formation in pancreatic β-cells such as for example SORCS1 led to decreased insulin granule replenishment after secretagogue treatment (Kebede et al., 2014). In this latter study, defects in insulin granule replenishment induced by a glucolipotoxic challenge resulted in insulin loss and diabetes. In addition to the diminution of insulin granules per β-cell in diabetic mice, we also observed increased numbers of GCLs in comparison to controls. This finding suggests that in addition to the decrease of β-cells mass and insulin granule biogenesis, insulin loss could also be attributed to enhanced lysosomal insulin granule degradation during diabetes.

To get a first idea about mechanisms underlying lysosomal degradation of insulin granules, we first decided to look at the expression of canonical lysosomal proteins. Expression of LAMP1/2 was not affected in diabetic as compared to control islets (Figure 11). However, CD63 levels were markedly increased in diabetic as compared to non-diabetic β-cells (Figure 12). CD63 is a transmembrane protein, from the tetraspanin family which localises to a minor extend on the limiting membrane of lysosomes and late endosomes but mainly on intra luminal vesicles (ILVs) and exosomes in the multivesicular bodies (Pols and Klumperman, 2009). It has been shown to form tetraspanin-enriched microdomains (TEM) with others tetraspanins which can serve as a molecular platform for recruitment of other proteins. (Levy and Shoham, 2005). CD63 contains four transmembrane domains, forming the characteristic two intraluminal loops of the tetraspanin family. It is extensively modified at the posttranslational level mainly by gycosylation and palmitoylation (Pols and Klumperman, 2009). It is targeted to the lysosome thanks to its GYEVM sequence present in its C-terminus (Pols and Klumperman, 2009). While CD63 is trafficking from the TGN to the plasma membrane, a large fraction is transported directly to the endosomal/lysosomal compartment in an AP-3 dependent manner (Banting et

al., 2002). CD63 has been shown to interact with the synaptotagmin VII (Syt7) protein in macrophages and to be responsible for its transport to the lysosomal compartment upon Syt7-palmitoylation (Flannery et al., 2010). Syt7 also resides on insulin granule membranes, where it confers Ca2+ sensitivity to membrane fusion events (Flannery et al., 2010). Total CD63 knock-out mice have been generated and display a mild kidney failure phenotype, which develops in aged mice (Schröder et al 2009). Even though this suggests that CD63 function *in vivo* is rather redundant, it is not exluded that a function for lysosomes may become apparent once mice will be metabolically challenged. This will be my immediate future task for my project to be completed.

To better assess insulin granules and CD63 localisation upon metabolic stress, I used INS1 cells subjecting them to a glucolipotoxicity challenge in comparison to control conditions. In line with experiments in diabetic mice, I observed an increase in CD63 levels. In addition, this observation was coupled with an increase in co-localisation of insulin granules with CD63-positive compartments (Figure 14). In order to better understand co-localisation events and its dynamics, I generated a double knock-in INS1 cell line fusing CD63 with DsRed and Phogrin with GFP to study these markers at the endogenous level. Using these cells, I confirmed an increase in co-localisation between CD63-DsRed and Phogrin-GFP upon a glucolipotoxic stress. Preliminary observations revealed that co-localization occurred already at the level of the TGN. This favours a model in which nascent insulin granules containing lysosomal signals are sorted out from the TGN to the endosomal/lysosomal compartment. More extensive live-cell imaging in the presence of specific organelle markes will be required to have a more conclusive basis for our preferred model. I also observed an increase in formation of CD63-positive tubules in response to a glucolipotoxic stress. Tubules can form in response to several processes, for example during autophagosome-lysosome fusion in the late stage of autophagy. This process is also known under the term Autophagic Lysosome Retrieval (ALR), the function of which is to reform lysosomes from autolysosomes. Interestingly, this tubulation process is controlled by mTORC1. Tubules can also be generated during partial lysosome-endosome fusion (kiss-and-run) to exchange cargo (Luzio et al., 2007). Tubules can also be derived from the tubular sorting endosome, which has been described by the Klumperman lab (Peden et al., 2004). Finally, tubules can be formed during early onset of endocytosis. By using the late endosomal marker Rab7a-GFP (Thermofisher) (data not shown), we determined that CD63-DsRed signals mainly come from late endosomes and lysosomes, so tubules are probably

generated by lysosomes and late endosomes and not early endosomes. Further studies and quantification are needed to determine the nature of these tubules appearing in response to metabolic challenges.

To assess the importance of lysosomal degradation of insulin granules, we used the lysosomal inhibitor BafA1, which binds the v0 subunit of the v-ATPase, interfering with the proton transport inside the lysosomal lumen (Cotter et al., 2015). BafA1 is also used as an autophagy inhibitor as it prevents the fusion between autophagosomes and lysosomes (Klionsky et al., 2016). In response to BafA1 treatment, I observed the formation of massive co-localising between CD63 and Phogrin, indicating an increase of insulin granule inside late endosomes/lysosomes. Because BafA1 inhibits the fusion between autophagosomes and lysosomes, this finding suggests that insulin granules are targeted to the lysosome independently of autophagy. This observation was already independently made by another laboratory (Sobota et al., 2009). According to their study, they speculate that this phenotype was caused by defective sorting at the Golgi (fully in line with our preferred model) leading to the targeting of nascent insulin granules to the lysosomes upon BafA1 treatment. In their hand, the use of cyclohexamide, a protein synthesis inhibitor, could reverse co-localization. They determined that structures with co-localizing signals, did not share all the characteristics of autophagosomes, confirming our hypothesis that autophagy is not the main driver of insulin loss during a metabolic stress. They also claim that the co-localising vesicle formation is mainly dependent of the v-ATPase inhibition and is independent of the loss of lysosomal acidic pH as they lost the effect by using only lysosomal lumen alkalizers such NH4Cl and methylamine. In the near future, I therefore also want to test other lysosomal inhibitors such as Pepstatin A coupled with E64d or Chloroquine and assess the co-localisation between CD63-DsRed and Phogrin-GFP.

To further exclude the role of autophagy in targeting of insulin granules to the CD63-positive compartments in response to glucolipotoxicity, I also monitored the levels of the adaptor protein p62. Western blot analysis revealed accumulation of p62 in response to glucolipotoxicty indicating the decrease of autophagic flux. Furthermore, the reduction in the conversion of LC3B-I into LC3B-II indicated a decrease in autophagosome formation after 40h of glucolipotoxic treatment. This result was confirmed by the drop in the number of LC3-GFP dots per cell upon glucolipotoxic stress. Overall, my results clearly indicate that autophagy is

shut down upon glucolipotoxicty. This contradicts other published results from Marchetti et al. which found that autophagy was induced upon palmitate treatment, however this result need to be carefully interpreted as they did not assess lysosomal activity in this study. However, the dominant shared view in the field is that autophagosome formation is increased upon lipotoxicity because of impaired lysosomal activity due to weak lysosomal acidification (Las et al., 2011)(Mir et al., 2014) (Trudeau et al., 2016). The difference with my results can be explained by longer duration of the treatment I applied in my experiments. Indeed, looking in details to Mir et al. data, the LC3-II signals appears to decrease over a longer incubation time (24h) in their hands. Moreover, my analysis was also inducing glucotoxic stress in addition to lipotoxicity. Altogether, targeting of insulin granules targeting to CD63-positive compartments cannot be explained by increased autophagy as the autophagic flux and the number of autophagosomes are both decreased. Observations in the INS1 cell model fit with the decrease in autophagic flux observed in isolated islets from diabetic mice. An additional experiment planned in the near future is the assessment of LC3B I and LC3B II levels with lysates from isolated islets from diabetic mice in comparison to islets from healthy sex/age-matched mice.

According to our model, targeting of insulin granules to the CD63-positive compartments should lead to insulin degradation and *de novo* formation of nutrients. Nutrients should be sensed by recruitment of the mTORC1 to the endosome/lysosome membrane. Indeed we observed the recruitment of mTORC1 to CD63-positive compartments upon glucolipotoxic conditions, which was not observed under control conditions suggesting that insulin is degraded in the CD63-positive compartment under glucolipotoxic conditions. This hypothesis was further confirmed in experiments, for which I used silencing of CD63 in INS1 cells subjected to a glucolipotoxic treatment. With this approach, I showed that CD63 knockdown resulted in restoration of insulin levels. This last result also suggests an important role of CD63 in the targeting of insulin granule to lysosomes/endosomes, which I will have to confirm in other genetically manipulated systems including knockout cells and mice.

Targeting of the insulin granules to endosomes/lysosomes can occur in different ways. One option is,, the direct fusion of already formed insulin granules with lysosomes in the cytoplasm. This would require new molecular players, which could be similar to those involved in the endosome-lysosome fusion process such as the SNARE proteins VAMP7, VAMP8 and Vti1B (Figure 36, model 2). Our preferred model as outlined above, is the targeting of the insulin granules to the lysosomes directly through sorting mechansims at the TGN (Figure 36, model 1). CD63 was shown to be transported from the TGN to the lysosomes in an AP-3-dependent

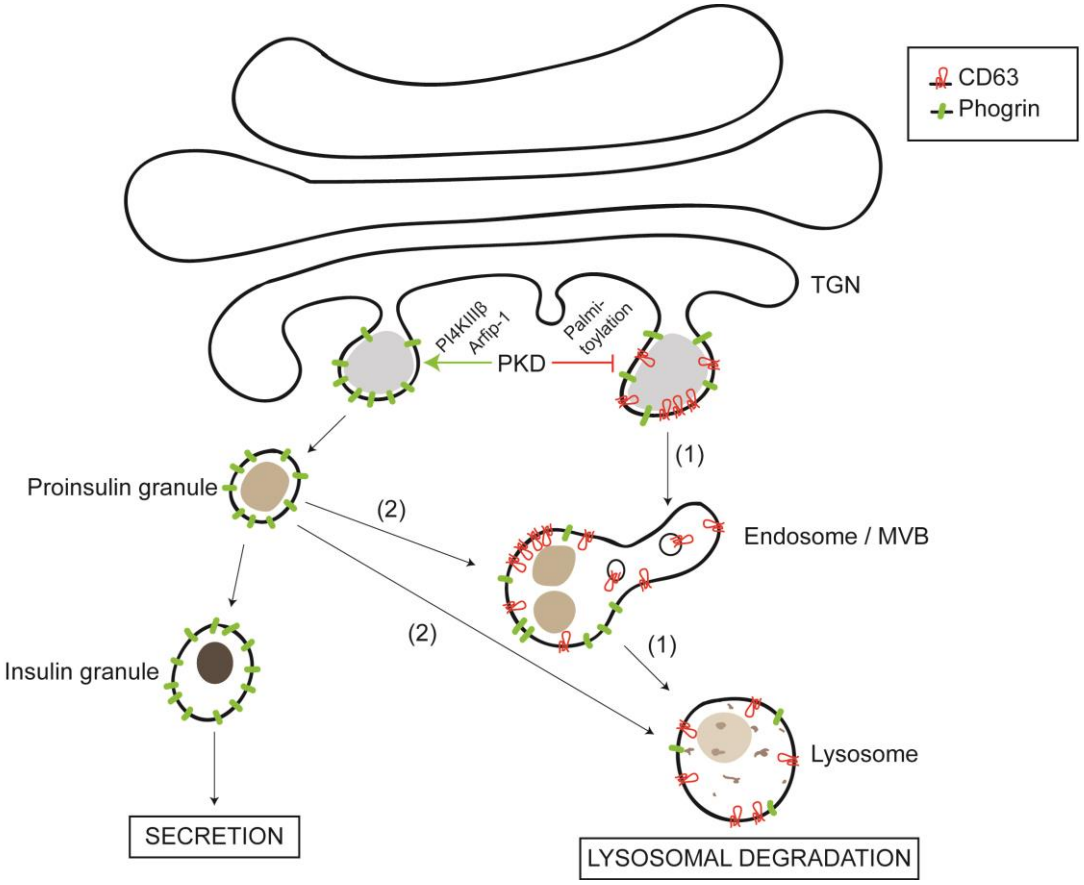

Figure 36 : Lysosomal Insulin granule degradation mechanisms model. Upon normal regulated secretion pathway, insulin granules are sorted out and separated from the TGN and mature from proinsulin granule to insulin granule. PKD was shown to play a crucial role in this process by directly phosphorylating the BAR-domain containing protein Arfaptin-1. PKD is also responsible for the PI4P membrane increase by phosphorylating the PI4KIIIβ protein which process PI3P into PI4P inducing the recruitment of many other molecular players. Under metabolic stress PKD inhibition leads to increased lysosomal insulin degradation. CD63 is targeted to the lysosome through an AP-3 dependent mechanism from the TGN to late endosome/lysosomes. Lysosomal insulin granule degradation could result from (1) sorting defect at the TGN with the co-sorting of the insulin cargo along with the lysosomal cargo leading to lysosomal degradation. Another possibility is the targeting of insulin granule directly to lysosomes (2) in a similar way of endosome/lysosome fusion.

manner. As mentioned above, Syt7 is transported to the lysosome by a CD63-dependent process in response to Syt7-palmitoylation in macrophages. A similar CD63-dependent process could take place in the context of insulin granule degradation in lysosomes. Syt7 is a promising candidate as it was found on both insulin granule and lysosomal membranes in β-cells. (Monterrat et al., 2007).

We showed that lysosomal targeting of insulin granules is controlled by PKD1. Inhibition of PKD using CID in the double knock-in cell line led to constitutive co-localisation of CD63-DsRed with Phogrin-GFP (Figure 26). PKD1 inhibition *in vivo* also led to an increased formation of GCLs (Figure 29). PKD1 was shown to mainly localise at the TGN membrane and to a smaller extent at the plasma membrane. It indirectly modifies the composition of lipids in membranes through regulating the activity of lipid-modifying enymes. PKD1 and 2 can activate PI4KIIIβ through its phosphorylation at Serine294, leading to the production of PI4P at the TGN (Hausser et al., 2005). PI(4)P was shown to be required for Arfaptin-1 recruitment to the TGN (Cruz-Garcia et al., 2013) as well as CERT and OSBP. One appealing model may involve these factors. In fact, OSBP is responsible for the transfer of sterols between membranes. An increase in sterols may recruit the PI3KIIα which interacts with CD63 and AP-3 which are key components for lysosomal targeting. Interestingly OSBP can be directly phosphorylated by PKD1, inducing its release in the cytoplasm (Malhotra and Campelo, 2011). Moreover palmitoylation of Syt7 could induce its CD63-dependent transport from the Golgi membrane to lysosomal. Palmitoylation occurs as a result of the activity of DHHC enzymes, which are highly enriched at the TGN. Screening for PKD phosphorylation consensus sites, I noticed that they were enriched in DHHC proteins suggesting a putative control of TGN palmitoylation by PKD. Identification of the molecular players involved in the targeting of the insulin granules to the CD63-positive compartments will be of great future interest. Taking advantage of our newly generated knock-in cell line, we will perform an unbiased screening approach aiming at identification of proteins involved in this process.

PKD1 silencing or inhibition led to severe insulin depletion in INS1 cells due to enhanced lysosomal insulin granule degradation (Goginashvili et al., 2015). We confirmed this finding in mice and human islets. Inhibition of PKD *in vivo* led to acceleration of diabetes in BTBR *ob/ob* mice most likely because of increased insulin loss in pancreatic β-cells. The insulin loss in CID-treated mice was coupled with increased numbers of GCL in pancreatic β-cells. In addition,

PKD1 transcription was downregulated upon onset of diabetes in mice (Figure 25). These preliminary results have to be complemented addressing possible side effects on other metabolic organs that may also contribute to acceleration of diabetes. Importantly, the gene encoding for PKD1, *PrKD1*, was identified in several genome-wide associated studies as a BMI-associated locus (Graff et al., 2013)(Locke et al., 2015)(Speliotes et al., 2010)(Wei et al., 2012) as well as a T2D-associated locus (Al Safar et al., 2013) making it a very interesting candidate. Targeting of the insulin granules to CD63-positive compartments may contribute to insulin loss and beta cell failure during diabetes. Assessment of other molecular players involved in insulin granules lysosomal degradation in the context of diabetes will be subject of future studies. GWAS studies identified *AP3S2*, the gene encoding for a subunit of the AP3 complex that for example is important for CD63 trafficking to the lysososamal compartment as a hot spot for T2D (Kooner et al., 2011).

Inhibition of PKD is deleterious in the diabetic context. The question thus raises whether its activation would be beneficial. In fact, chronic activation through deletion of its upstream inhibitor p38δ was shown to protect against insulin resistance and diabetes (Sumara et al., 2009). In collaboration with an industrial partner, we generated a specific p38δ inhibitor. We are currently on the way to characterize its effects in diabetic mice. Our industrial partner assessed the specificity and activity of the p38δ inhibitor. Their results as well as the compound structure are still confidential. Our preliminary results are quite encouraging. In obese BTBR *ob/ob* mice, which develop premature diabetes early after birth, p38d inhibition delayed diabetes onset. The total insulin content was shown to be increased in murine islets, human islets as well as islets isolated from diabetic donors (Figure 32). We did not prove yet that these beneficial effects were due to decreased targeting of insulin granules to CD63-positive compartments. Quantitiative EM analysis still needs to be done. Nevertheless, decreasing the targeting of insulin granules to the endosomal/lysosomal compartment could be an interesting new therapeutic avenue to prevent insulin loss and β-cell failure in diabetic context.

So far, my study was more focused on autophagy and indirect mTORC1 regulation by nutrient release from the CD63-positive compartments. However autophagic regulation could occur in a more direct manner. PKD1 may directly regulate macroautophagy regulators by-passing mTORC1. The central VPS34 kinase, which forms the Class III PI3K complex 1 (Figure 5), was shown to be controlled by PKD-dependent phosphorylation (Eisenberg-Lerner and Kimchi,

2012). According to this study, PKD was shown to reside in the same complex as VPS34, phosphorylating VPS34 on multiple sites including Threonine 677 promoting autophagosome formation. A phosphoproteomic study by (Franz-Wachtel et al., 2012) found that ULK1 could also be a direct target of PKD. PKD was also shown to inhibit AMPK activation by directly phosphorylating the α2 subunit at Serine 491 in muscle cells (Coughlan et al., 2016). Interestingly the α2 subunit is expressed in INS-1 cells (da Silva Xavier et al., 2000).

Recent work by Yamaguchi et al. demonstrated that a process (designated as Golgi membrane-associated degradation, GOMED) reminiscent of lysosomal degradation of insulin granules, at least in a situation when autophagy is compromised, exists in yeast. This may suggest that basic mechanisms underlying lysosomal degradation of insulin granules are evolutionary conserved. Interestingly, this process was dependent on PI4P depletion, possibly linking it to the PKD-PI4KIIIβ axis. I plan to extensively investigate this new findings and our new hypotheses in the near future.

I so far focussed on the pancreatic β-cells, but lysosomal regulation of secretory granules is certainly also very important in other islet cell types. LIMP2 levels were strikingly higher in glucagon secreting α-cells in comparison to β-cells suggesting an important role for this protein in α-cells (Figure 34). I could also demonstrate that LIMP2 localised on glucagon granules. This could indicate a role for LIMP2 in glucagon granule biogenesis/turnover or secretion. Glucagon secretion during a hyperglycaemic episode is a hallmark of diabetes. Dysregulation of glucagon homeostasis indeed was discussed as an important factor in T2D. Another possibility explaining LIMP2 co-localisation with glucagon granules could be the necessity to have LIMP2 for the specific transport of proteins to the glucagon granules. As for glucocerebrosidase, LIMP2 might be necessary for the transport of proteins needed in glucagon maturation. Glucagon is derived from the proglucagon peptide which needs to be cleaved by the specific PC1/2 enzymes. While PC1 is responsible for cleaving pro-glucagon into glucagon, PC2 generates the GLP-1 incretin. Generation of knock out cells lines and metabolic studies in total knock-out mice will potentially provide new insights onto these aspects.

Lysosomes are found in every eukaryotic cell. They were mostly considered as terminal catabolic stations that get rid of waste products and scavenge metabolic building blocks to sustain essential biosynthetic reactions during starvation. This view is now challenged and

lysosomes are increasingly regarded as a central sensing organelle controlling nutrient sensing, transcriptional regulation as well as metabolic homeostasis. (Lim and Zoncu, 2016). Their functions in different metabolic cell types including the pancreatic β-cell will provide important and fundamentally new knowledge on mechanisms underlying cellular metabolic homeostasis and thus prepare the ground for development of novel therapeutic avenues.

References

Al Safar, H.S., Jamieson, S.E., Anderson, D., Jafer, O., Fakiola, M., Tay, G.K., Blackwell, J.M., Khazanehdari, K., and Cordell, H.J. (2013). A Genome-Wide Search for Type 2 Diabetes Susceptibility Genes in an Extended Arab Family. Ann. Hum. Genet. *77*, n/a-n/a.

Alers, S., Löffler, A.S., Wesselborg, S., and Stork, B. (2011). Role of AMPK-mTOR-Ulk1/2 in the regulation of autophagy: cross talk, shortcuts, and feedbacks. Mol. Cell. Biol. *32*, 2–11.

Badman, M.K., and Flier, J.S. (2005). The gut and energy balance: visceral allies in the obesity wars. Science *307*, 1909–1914.

Banting, G., Stephens, D.J., Rous, B.A., Luzio, J.P., Reaves, B.J., Briggs, J.A.G., Gray, S.R., and Ihrke, G. (2002). Role of adaptor complex AP-3 in targeting wild-type and mutated CD63 to lysosomes. Mol. Biol. Cell *13*, 1071–1082.

Bar-Peled, L., Schweitzer, L.D., Zoncu, R., and Sabatini, D.M. (2012). Ragulator is a GEF for the rag GTPases that signal amino acid levels to mTORC1. Cell *150*, 1196–1208.

Begg, D.P., and Woods, S.C. (2013). The endocrinology of food intake. Nat. Rev. Endocrinol. *9*, 584–597.

Bento, C.F., Renna, M., Ghislat, G., Puri, C., Ashkenazi, A., Vicinanza, M., Menzies, F.M., and Rubinsztein, D.C. (2016). Mammalian Autophagy: How Does It Work? Annu. Rev. Biochem. *85*, 685–713.

Blanz, J., Zunke, F., Markmann, S., Damme, M., Braulke, T., Saftig, P., and Schwake, M. (2015). Mannose 6-phosphate-independent Lysosomal Sorting of LIMP-2. Traffic *16*, 1127–1136.

Borden, P., Houtz, J., Leach, S.D., and Kuruvilla, R. (2013). Sympathetic innervation during development is necessary for pancreatic islet architecture and functional maturation. Cell Rep. *4*, 287–301.

Brown, M.S., and Goldstein, J.L. (1986). A receptor-mediated pathway for cholesterol homeostasis. Science *232*, 34–47.

Brown, A.J., Sun, L., Feramisco, J.D., Brown, M.S., and Goldstein, J.L. (2002). Cholesterol addition to ER membranes alters conformation of SCAP, the SREBP escort protein that regulates cholesterol metabolism. Mol. Cell *10*, 237–245.

Butler, A.E., Janson, J., Bonner-Weir, S., Ritzel, R., Rizza, R.A., and Butler, P.C. (2002). Beta-cell deficit and increased beta-cell apoptosis in humans with type 2 diabetes. Diabetes *52*, 102–110.

Campbell, J.E., and Drucker, D.J. (2015). Islet α cells and glucagon-critical regulators of energy homeostasis. Nat. Rev. Endocrinol. *11*, 329–338.

Cantó, C., Gerhart-Hines, Z., Feige, J.N., Lagouge, M., Noriega, L., Milne, J.C., Elliott, P.J., Puigserver, P., and Auwerx, J. (2009). AMPK regulates energy expenditure by modulating NAD+ metabolism and SIRT1 activity. Nature *458*, 1056–1060.

Choi, S.-E., Lee, S.-M., Lee, Y.-J., Li, L.-J., Lee, S.-J., Lee, J.-H., Kim, Y., Jun, H.-S., Lee, K.-W., and Kang, Y. (2008). Protective role of autophagy in palmitate-induced INS-1 beta-cell death. Endocrinology *150*, 126–134.

Clarke, P.R., and Hardie, D.G. (1990). Regulation of HMG-CoA reductase: identification of the site phosphorylated by the AMP-activated protein kinase in vitro and in intact rat liver. EMBO J. *9*, 2439–2446.

Clee, S.M., Nadler, S.T., and Attie, A.D. (2005). Genetic and genomic studies of the BTBR ob/ob mouse model of type 2 diabetes. Am. J. Ther. *12*, 491–498.

Cotter, K., Stransky, L., McGuire, C., and Forgac, M. (2015). Recent Insights into the Structure, Regulation, and Function of the V-ATPases. Trends Biochem. Sci. *40*, 611–622.

Coughlan, K.A., Valentine, R.J., Sudit, B.S., Allen, K., Dagon, Y., Kahn, B.B., Ruderman, N.B., and Saha, A.K. (2016). PKD1 Inhibits AMPKα2 through Phosphorylation of Serine 491 and Impairs Insulin Signaling in Skeletal Muscle Cells. J. Biol. Chem. jbc.M115.696849.

Cruz-Garcia, D., Ortega-Bellido, M., Scarpa, M., Villeneuve, J., Jovic, M., Porzner, M., Balla, T., Seufferlein, T., and Malhotra, V. (2013). Recruitment of arfaptins to the trans-Golgi network by PI(4)P and their involvement in cargo export. EMBO J. *32*, 1717–1729.

Demetriades, C., Doumpas, N., and Teleman, A.A. (2014). Regulation of TORC1 in response to amino acid starvation via lysosomal recruitment of TSC2. Cell *156*, 786–799.

Donath, M.Y. (2013). Targeting inflammation in the treatment of type 2 diabetes. Diabetes Obes. Metab. *15 Suppl 3*, 193–196.

Donath, M.Y. (2014). Targeting inflammation in the treatment of type 2 diabetes: time to start. Nat. Rev. Drug Discov. *13*, 465–476.

Donath, M.Y., and Shoelson, S.E. (2011). Type 2 diabetes as an inflammatory disease. Nat. Rev. Immunol. *11*, 98–107.

Efeyan, A., Comb, W.C., and Sabatini, D.M. (2015). Nutrient-sensing mechanisms and pathways. Nature *517*, 302–310.

Egan, D.F., Shackelford, D.B., Mihaylova, M.M., Gelino, S., Kohnz, R.A., Mair, W., Vasquez, D.S., Joshi, A., Gwinn, D.M., Taylor, R., et al. (2010). Phosphorylation of ULK1 (hATG1) by AMP-activated protein kinase connects energy sensing to mitophagy. Science *331*, 456–461.

Eisenberg-Lerner, A., and Kimchi, A. (2012). PKD is a kinase of Vps34 that mediates ROS-induced autophagy downstream of DAPk. Cell Death Differ. *19*, 788–797.

Flannery, A.R., Czibener, C., and Andrews, N.W. (2010). Palmitoylation-dependent association with CD63 targets the Ca2+ sensor synaptotagmin VII to lysosomes. J. Cell Biol. *191*, 599–613.

Fowler, M.J. (2008). Microvascular and Macrovascular Complications of Diabetes. Clin. Diabetes *26*, 77.

Franz-Wachtel, M., Eisler, S.A., Krug, K., Wahl, S., Carpy, A., Nordheim, A., Pfizenmaier, K., Hausser, A., and Macek, B. (2012). Global detection of protein kinase D-dependent phosphorylation events in nocodazole-treated human cells. Mol. Cell. Proteomics MCP *11*, 160–170.

Fu, Y., and Rubin, C.S. (2011). Protein kinase D: coupling extracellular stimuli to the regulation of cell physiology. EMBO Rep. *12*, 785–796.

Fu, A., Eberhard, C.E., and Screaton, R.A. (2013). Role of AMPK in pancreatic beta cell function. Mol. Cell. Endocrinol. *366*, 127–134.

Furuta, N., Yoshimori, T., Amano, A., Noda, T., and Fujita, N. (2010). Combinational soluble N-ethylmaleimide-sensitive factor attachment protein receptor proteins VAMP8 and Vti1b mediate fusion of antimicrobial and canonical autophagosomes with lysosomes. Mol. Biol. Cell *21*, 1001–1010.

Gehart, H., Kumpf, S., Ittner, A., and Ricci, R. (2010). MAPK signalling in cellular metabolism: stress or wellness? EMBO Rep. *11*, 834–840.

Gehart, H., Goginashvili, A., Beck, R., Morvan, J., Erbs, E., Formentini, I., De Matteis, M.A., Schwab, Y., Wieland, F.T., and Ricci, R. (2012). The BAR domain protein Arfaptin-1 controls secretory granule biogenesis at the trans-Golgi network. Dev. Cell *23*, 756–768.

Gjoni, E., Brioschi, L., Cinque, A., Coant, N., Islam, M.N., Ng, C.K.-Y., Verderio, C., Magnan, C., Riboni, L., Viani, P., et al. (2014). Glucolipotoxicity impairs ceramide flow from the endoplasmic reticulum to the Golgi apparatus in INS-1 β-cells. PloS One *9*, e110875.

Goginashvili, A. (2015) Novel mechanism of fasting response in pancreatic beta cells. Thesi

Goginashvili, A., Zhang, Z., Erbs, E., Spiegelhalter, C., Kessler, P., Mihlan, M., Pasquier, A., Krupina, K., Schieber, N., Cinque, L., et al. (2015). Insulin granules. Insulin secretory granules control autophagy in pancreatic β cells. Science *347*, 878–882.

Graff, M., Ngwa, J.S., Workalemahu, T., Homuth, G., Schipf, S., Teumer, A., Völzke, H., Wallaschofski, H., Abecasis, G.R., Edward, L., et al. (2013). Genome-wide analysis of BMI in adolescents and young adults reveals additional insight into the effects of genetic loci over the life course. Hum. Mol. Genet. *22*, 3597–3607.

Guo, S., Dai, C., Guo, M., Taylor, B., Harmon, J.S., Sander, M., Robertson, R.P., Powers, A.C., and Stein, R. (2013). Inactivation of specific β cell transcription factors in type 2 diabetes. J. Clin. Invest. *123*, 3305–3316.

Gwinn, D.M., Shackelford, D.B., Egan, D.F., Mihaylova, M.M., Mery, A., Vasquez, D.S., Turk, B.E., and Shaw, R.J. (2008). AMPK phosphorylation of raptor mediates a metabolic checkpoint. Mol. Cell *30*, 214–226.

Habegger, K.M., Heppner, K.M., Geary, N., Bartness, T.J., DiMarchi, R., and Tschöp, M.H. (2010). The metabolic actions of glucagon revisited. Nat. Rev. Endocrinol. *6*, 689–697.

Habets, D.D.J., Coumans, W.A., El Hasnaoui, M., Zarrinpashneh, E., Bertrand, L., Viollet, B., Kiens, B., Jensen, T.E., Richter, E.A., Bonen, A., et al. (2008). Crucial role for LKB1 to

AMPKalpha2 axis in the regulation of CD36-mediated long-chain fatty acid uptake into cardiomyocytes. Biochim. Biophys. Acta *1791*, 212–219.

Halban, P.A., Polonsky, K.S., Bowden, D.W., Hawkins, M.A., Ling, C., Mather, K.J., Powers, A.C., Rhodes, C.J., Sussel, L., and Weir, G.C. (2014). β-cell failure in type 2 diabetes: postulated mechanisms and prospects for prevention and treatment. Diabetes Care *37*, 1751–1758.

Hardie, D.G. (2014). AMP-activated protein kinase: maintaining energy homeostasis at the cellular and whole-body levels. Annu. Rev. Nutr. *34*, 31–55.

Hausser, A., Storz, P., Märtens, S., Link, G., Toker, A., and Pfizenmaier, K. (2005). Protein kinase D regulates vesicular transport by phosphorylating and activating phosphatidylinositol-4 kinase IIIbeta at the Golgi complex. Nat. Cell Biol. *7*, 880–886.

Hirasawa, A., Tsumaya, K., Awaji, T., Katsuma, S., Adachi, T., Yamada, M., Sugimoto, Y., Miyazaki, S., and Tsujimoto, G. (2004). Free fatty acids regulate gut incretin glucagon-like peptide-1 secretion through GPR120. Nat. Med. *11*, 90–94.

Hoppe, S., Bierhoff, H., Cado, I., Weber, A., Tiebe, M., Grummt, I., and Voit, R. (2009). AMP-activated protein kinase adapts rRNA synthesis to cellular energy supply. Proc. Natl. Acad. Sci. *106*, 17781–17786.

Hu, F.B., Manson, J.E., Stampfer, M.J., Colditz, G., Liu, S., Solomon, C.G., and Willett, W.C. (2001). Diet, lifestyle, and the risk of type 2 diabetes mellitus in women. N. Engl. J. Med. *345*, 790–797.

Huang, J., and Manning, B.D. (2008). The TSC1-TSC2 complex: a molecular switchboard controlling cell growth. Biochem. J. *412*, 179–190.

Ichimura, A., Hirasawa, A., Poulain-Godefroy, O., Bonnefond, A., Hara, T., Yengo, L., Kimura, I., Leloire, A., Liu, N., Iida, K., et al. (2012). Dysfunction of lipid sensor GPR120 leads to obesity in both mouse and human. Nature *483*, 350–354.

Inoki, K., Zhu, T., and Guan, K.-L. (2003). TSC2 mediates cellular energy response to control cell growth and survival. Cell *115*, 577–590.

Ishihara, H., Wang, H., Drewes, L.R., and Wollheim, C.B. (1999). Overexpression of monocarboxylate transporter and lactate dehydrogenase alters insulin secretory responses to pyruvate and lactate in beta cells. J. Clin. Invest. *104*, 1621–1629.

Itoh, Y., Kawamata, Y., Harada, M., Kobayashi, M., Fujii, R., Fukusumi, S., Ogi, K., Hosoya, M., Tanaka, Y., Uejima, H., et al. (2003). Free fatty acids regulate insulin secretion from pancreatic beta cells through GPR40. Nature *422*, 173–176.

Jäger, S., Handschin, C., St-Pierre, J., and Spiegelman, B.M. (2007). AMP-activated protein kinase (AMPK) action in skeletal muscle via direct phosphorylation of PGC-1alpha. Proc. Natl. Acad. Sci. *104*, 12017–12022.

Jetton, T.L., Lausier, J., LaRock, K., Trotman, W.E., Larmie, B., Habibovic, A., Peshavaria, M., and Leahy, J.L. (2005). Mechanisms of compensatory beta-cell growth in insulin-resistant rats: roles of Akt kinase. Diabetes *54*, 2294–2304.

Jewell, J.L., Kim, Y.C., Russell, R.C., Yu, F.-X., Park, H.W., Plouffe, S.W., Tagliabracci, V.S., and Guan, K.-L. (2015). Metabolism. Differential regulation of mTORC1 by leucine and glutamine. Science *347*, 194–198.

Jiang, G., and Zhang, B.B. (2003). Glucagon and regulation of glucose metabolism. Am. J. Physiol. Endocrinol. Metab. *284*, E671-8.

Jørgensen, S.B., Nielsen, J.N., Birk, J.B., Olsen, G.S., Viollet, B., Andreelli, F., Schjerling, P., Vaulont, S., Hardie, D.G., Hansen, B.F., et al. (2004). The alpha2-5'AMP-activated protein kinase is a site 2 glycogen synthase kinase in skeletal muscle and is responsive to glucose loading. Diabetes *53*, 3074–3081.

Jović, M., Kean, M.J., Szentpetery, Z., Polevoy, G., Gingras, A.-C., Brill, J.A., and Balla, T. (2012). Two phosphatidylinositol 4-kinases control lysosomal delivery of the Gaucher disease enzyme, β-glucocerebrosidase. Mol. Biol. Cell *23*, 1533–1545.

Just, T., Pau, H.W., Engel, U., and Hummel, T. (2008). Cephalic phase insulin release in healthy humans after taste stimulation? Appetite *51*, 622–627.

Kahn, S.E., Zraika, S., Utzschneider, K.M., and Hull, R.L. (2009). The beta cell lesion in type 2 diabetes: there has to be a primary functional abnormality. Diabetologia *52*, 1003–1012.

Kahn, S.E., Cooper, M.E., and Del Prato, S. (2013). Pathophysiology and treatment of type 2 diabetes: perspectives on the past, present, and future. The Lancet *383*, 1068–1083.

Kantidakis, T., Ramsbottom, B.A., Birch, J.L., Dowding, S.N., and White, R.J. (2010). mTOR associates with TFIIIC, is found at tRNA and 5S rRNA genes, and targets their repressor Maf1. Proc. Natl. Acad. Sci. *107*, 11823–11828.

Kebede, M.A., Oler, A.T., Gregg, T., Balloon, A.J., Johnson, A., Mitok, K., Rabaglia, M., Schueler, K., Stapleton, D., Thorstenson, C., et al. (2014). SORCS1 is necessary for normal insulin secretory granule biogenesis in metabolically stressed β cells. J. Clin. Invest. *124*, 4240–4256.

Khan, A.H., and Pessin, J.E. (2002). Insulin regulation of glucose uptake: a complex interplay of intracellular signalling pathways. Diabetologia *45*, 1475–1483.

Kim, J., and Kim, E. (2016). Rag GTPase in amino acid signaling. Amino Acids *48*, 915–928.

Kim, J., Kundu, M., Viollet, B., and Guan, K.-L. (2011). AMPK and mTOR regulate autophagy through direct phosphorylation of Ulk1. Nat. Cell Biol. *13*, 132–141.

Kim, J., Cheon, H., Jeong, Y.T., Quan, W., Kim, K.H., Cho, J.M., Lim, Y.-M., Oh, S.H., Jin, S.-M., Kim, J.H., et al. (2014). Amyloidogenic peptide oligomer accumulation in autophagy-deficient β cells induces diabetes. J. Clin. Invest. *124*, 3311–3324.

Klionsky, D.J., Abdelmohsen, K., Abe, A., Abedin, M.J., Abeliovich, H., Arozena, A.A., Adachi, H., Adams, C.M., Adams, P.D., Adeli, K., et al. (2016). Guidelines for the use and interpretation of assays for monitoring autophagy (3rd edition). Autophagy *12*, 1–222.

Kooner, J.S., Saleheen, D., Sim, X., Sehmi, J., Zhang, W., Frossard, P., Been, L.F., Chia, K.-S., Dimas, A.S., Hassanali, N., et al. (2011). Genome-wide association study in individuals of

South Asian ancestry identifies six new type 2 diabetes susceptibility loci. Nat. Genet. *43*, 984–989.

Kruit, J.K., Wijesekara, N., Fox, J.E.M., Dai, X.-Q., Brunham, L.R., Searle, G.J., Morgan, G.P., Costin, A.J., Tang, R., Bhattacharjee, A., et al. (2011). Islet cholesterol accumulation due to loss of ABCA1 leads to impaired exocytosis of insulin granules. Diabetes *60*, 3186–3196.

Kurth-Kraczek, E.J., Hirshman, M.F., Goodyear, L.J., and Winder, W.W. (1999). 5' AMP-activated protein kinase activation causes GLUT4 translocation in skeletal muscle. Diabetes *48*, 1667–1671.

Lagouge, M., Argmann, C., Gerhart-Hines, Z., Meziane, H., Lerin, C., Daussin, F., Messadeq, N., Milne, J., Lambert, P., Elliott, P., et al. (2006). Resveratrol improves mitochondrial function and protects against metabolic disease by activating SIRT1 and PGC-1alpha. Cell *127*, 1109–1122.

Laplante, M., and Sabatini, D.M. (2009). An emerging role of mTOR in lipid biosynthesis. Curr. Biol. *19*, R1046-52.

Laplante, M., and Sabatini, D.M. (2012). mTOR signaling in growth control and disease. Cell *149*, 274–293.

Las, G., Serada, S.B., Wikstrom, J.D., Twig, G., and Shirihai, O.S. (2011). Fatty acids suppress autophagic turnover in β-cells. J. Biol. Chem. *286*, 42534–42544.

Lee, M.-S. (2014). Role of islet β cell autophagy in the pathogenesis of diabetes. Trends Endocrinol. Metab. TEM *25*, 620–627.

Levetan, C. (2010). Distinctions between islet neogenesis and β-cell replication: implications for reversal of Type 1 and 2 diabetes. J. Diabetes *2*, 76–84.

Levy, S., and Shoham, T. (2005). The tetraspanin web modulates immune-signalling complexes. Nat. Rev. Immunol. *5*, 136–148.

Li, Y., Xu, S., Mihaylova, M.M., Zheng, Hou, X., Jiang, B., Park, O., Luo, Z., Lefai, E., Shyy, J.Y.-J., et al. (2011). AMPK phosphorylates and inhibits SREBP activity to attenuate hepatic steatosis and atherosclerosis in diet-induced insulin-resistant mice. Cell Metab. *13*, 376–388.

Lim, C.-Y., and Zoncu, R. (2016). The lysosome as a command-and-control center for cellular metabolism. J. Cell Biol. *214*, 653–664.

Locke, A.E., Kahali, B., Berndt, S.I., Justice, A.E., Pers, T.H., Day, F.R., Powell, C., Vedantam, S., Buchkovich, M.L., Yang, J., et al. (2015). Genetic studies of body mass index yield new insights for obesity biology. Nature *518*, 197–206.

Luzio, J.P., Pryor, P.R., and Bright, N.A. (2007). Lysosomes: fusion and function. Nat. Rev. Mol. Cell Biol. *8*, 622–632.

Ma, X.M., and Blenis, J. (2009). Molecular mechanisms of mTOR-mediated translational control. Nat. Rev. Mol. Cell Biol. *10*, 307–318.

MACLEAN, N., and OGILVIE, R.F. (1955). Quantitative estimation of the pancreatic islet tissue in diabetic subjects. Diabetes *4*, 367–376.

Malhotra, V., and Campelo, F. (2011). PKD regulates membrane fission to generate TGN to cell surface transport carriers. Cold Spring Harb. Perspect. Biol. *3*, a005280.

Magliarelli, H. (2014) Uncovering ubiquitylation pathways in liver metabolism by a proteomic approach. Thesis

Marsin, A.S., Bertrand, L., Rider, M.H., Deprez, J., Beauloye, C., Vincent, M.F., Van den Berghe, G., Carling, D., and Hue, L. (2000). Phosphorylation and activation of heart PFK-2 by AMPK has a role in the stimulation of glycolysis during ischaemia. Curr. Biol. *10*, 1247–1255.

Marsin, A.-S., Bouzin, C., Bertrand, L., and Hue, L. (2002). The stimulation of glycolysis by hypoxia in activated monocytes is mediated by AMP-activated protein kinase and inducible 6-phosphofructo-2-kinase. J. Biol. Chem. *277*, 30778–30783.

Masters, S.L., Dunne, A., Subramanian, S.L., Hull, R.L., Tannahill, G.M., Sharp, F.A., Becker, C., Franchi, L., Yoshihara, E., Chen, Z., et al. (2010). Activation of the NLRP3 inflammasome by islet amyloid polypeptide provides a mechanism for enhanced IL-1β in type 2 diabetes. Nat. Immunol. *11*, 897–904.

Mayer, C., Zhao, J., Yuan, X., and Grummt, I. (2004). mTOR-dependent activation of the transcription factor TIF-IA links rRNA synthesis to nutrient availability. Genes Dev. *18*, 423–434.

McGee, S.L., van Denderen, B.J.W., Howlett, K.F., Mollica, J., Schertzer, J.D., Kemp, B.E., and Hargreaves, M. (2008). AMP-activated protein kinase regulates GLUT4 transcription by phosphorylating histone deacetylase 5. Diabetes *57*, 860–867.

McGirr, R., Guizzetti, L., and Dhanvantari, S. (2013). The sorting of proglucagon to secretory granules is mediated by carboxypeptidase E and intrinsic sorting signals. J. Endocrinol. *217*, 229–240.

Menon, S., Dibble, C.C., Talbott, G., Hoxhaj, G., Valvezan, A.J., Takahashi, H., Cantley, L.C., and Manning, B.D. (2014). Spatial control of the TSC complex integrates insulin and nutrient regulation of mTORC1 at the lysosome. Cell *156*, 771–785.

Merrill, G.F., Kurth, E.J., Hardie, D.G., and Winder, W.W. (1998). AICA riboside increases AMP-activated protein kinase, fatty acid oxidation, and glucose uptake in rat muscle. Am. J. Physiol. *273*, E1107-12.

Meszaros, G. (2015) CaMK1D controls beta cell mass and glucose homeostasis. Thesis.

Mihaylova, M.M., Vasquez, D.S., Ravnskjaer, K., Denechaud, P.-D., Yu, R.T., Alvarez, J.G., Downes, M., Evans, R.M., Montminy, M., and Shaw, R.J. (2011). Class IIa histone deacetylases are hormone-activated regulators of FOXO and mammalian glucose homeostasis. Cell *145*, 607–621.

Mir, S.U.R., George, N.M., Zahoor, L., Harms, R., Guinn, Z., and Sarvetnick, N.E. (2014). Inhibition of autophagic turnover in β-cells by fatty acids and glucose leads to apoptotic cell death. J. Biol. Chem. *290*, 6071–6085.

Molnár, G., Faragó, N., Kocsis, Á.K., Rózsa, M., Lovas, S., Boldog, E., Báldi, R., Csajbók, É., Gardi, J., Puskás, L.G., et al. (2014). GABAergic neurogliaform cells represent local sources of insulin in the cerebral cortex. J. Neurosci. *34*, 1133–1137.

Montane, J., Klimek-Abercrombie, A., Potter, K.J., Westwell-Roper, C., and Verchere, C.B. (2012). Metabolic stress, IAPP and islet amyloid. Diabetes Obes. Metab. *14 Suppl 3*, 68–77.

Monterrat, C., Grise, F., Benassy, M.N., Hémar, A., and Lang, J. (2007). The calcium-sensing protein synaptotagmin 7 is expressed on different endosomal compartments in endocrine, neuroendocrine cells or neurons but not on large dense core vesicles. Histochem. Cell Biol. *127*, 625–632.

Muoio, D.M., Seefeld, K., Witters, L.A., and Coleman, R.A. (1999). AMP-activated kinase reciprocally regulates triacylglycerol synthesis and fatty acid oxidation in liver and muscle: evidence that sn-glycerol-3-phosphate acyltransferase is a novel target. Biochem. J. *338 (Pt 3)*, 783–791.

Nakatogawa, H. (2013). Two ubiquitin-like conjugation systems that mediate membrane formation during autophagy. Essays Biochem. *55*, 39–50.

O'Brien, P.D., Hur, J., Hayes, J.M., Backus, C., Sakowski, S.A., and Feldman, E.L. (2014). BTBR ob/ob mice as a novel diabetic neuropathy model: Neurological characterization and gene expression analyses. Neurobiol. Dis. *73*, 348–355.

Oh, Y.S., Lee, Y.-J., Kang, Y., Han, J., Lim, O.-K., and Jun, H.-S. (2013). Exendin-4 inhibits glucolipotoxic ER stress in pancreatic β cells via regulation of SREBP1c and C/EBPβ transcription factors. J. Endocrinol. *216*, 343–352.

O'Neill, H.M., Holloway, G.P., and Steinberg, G.R. (2012). AMPK regulation of fatty acid metabolism and mitochondrial biogenesis: implications for obesity. Mol. Cell. Endocrinol. *366*, 135–151.

Osório, J. (2014). Diabetes: Protective role of autophagy in pancreatic β cells. Nat. Rev. Endocrinol. *10*, 575–575.

Otonkoski, T., Jiao, H., Kaminen-Ahola, N., Tapia-Paez, I., Ullah, M.S., Parton, L.E., Schuit, F., Quintens, R., Sipilä, I., Mayatepek, E., et al. (2007). Physical exercise-induced hypoglycemia caused by failed silencing of monocarboxylate transporter 1 in pancreatic beta cells. Am. J. Hum. Genet. *81*, 467–474.

Peden, A.A., Oorschot, V., Hesser, B.A., Austin, C.D., Scheller, R.H., and Klumperman, J. (2004). Localization of the AP-3 adaptor complex defines a novel endosomal exit site for lysosomal membrane proteins. J. Cell Biol. *164*, 1065–1076.

Pehmøller, C., Treebak, J.T., Birk, J.B., Chen, S., Mackintosh, C., Hardie, D.G., Richter, E.A., and Wojtaszewski, J.F.P. (2009). Genetic disruption of AMPK signaling abolishes both contraction- and insulin-stimulated TBC1D1 phosphorylation and 14-3-3 binding in mouse skeletal muscle. AJP Endocrinol. Metab. *297*, E665–75.

Perera, R.M., and Zoncu, R. (2016). The Lysosome as a Regulatory Hub. Annu. Rev. Cell Dev. Biol. *32*.

Peterson, T.R., Sengupta, S.S., Harris, T.E., Carmack, A.E., Kang, S.A., Balderas, E., Guertin, D.A., Madden, K.L., Carpenter, A.E., Finck, B.N., et al. (2011). mTOR complex 1 regulates lipin 1 localization to control the SREBP pathway. Cell *146*, 408–420.

Pols, M.S., and Klumperman, J. (2009). Trafficking and function of the tetraspanin CD63. Exp. Cell Res. *315*, 1584–1592.

Prentki, M., Matschinsky, F.M., and Madiraju, S.R.M. (2013). Metabolic signaling in fuel-induced insulin secretion. Cell Metab. *18*, 162–185.

Radhakrishnan, A., Goldstein, J.L., McDonald, J.G., and Brown, M.S. (2008). Switch-like control of SREBP-2 transport triggered by small changes in ER cholesterol: a delicate balance. Cell Metab. *8*, 512–521.

Ranheim, T., Dumke, C., Schueler, K.L., Cartee, G.D., and Attie, A.D. (1997). Interaction between BTBR and C57BL/6J genomes produces an insulin resistance syndrome in (BTBR x C57BL/6J) F1 mice. Arterioscler. Thromb. Vasc. Biol. *17*, 3286–3293.

Reczek, D., Schwake, M., Schröder, J., Hughes, H., Blanz, J., Jin, X., Brondyk, W., Van Patten, S., Edmunds, T., and Saftig, P. (2007). LIMP-2 is a receptor for lysosomal mannose-6-phosphate-independent targeting of beta-glucocerebrosidase. Cell *131*, 770–783.

Rivera, J.F., Costes, S., Gurlo, T., Glabe, C.G., and Butler, P.C. (2014). Autophagy defends pancreatic β cells from human islet amyloid polypeptide-induced toxicity. J. Clin. Invest. *124*, 3489–3500.

Röder, P.V., Wu, B., Liu, Y., and Han, W. (2016). Pancreatic regulation of glucose homeostasis. Exp. Mol. Med. *48*, e219.

Rong, Y., Liu, M., Ma, L., Du, W., Zhang, H., Tian, Y., Cao, Z., Li, Y., Ren, H., Zhang, C., et al. (2012). Clathrin and phosphatidylinositol-4,5-bisphosphate regulate autophagic lysosome reformation. Nat. Cell Biol. *14*, 924–934.

Rubinsztein, D.C., Mariño, G., and Kroemer, G. (2011). Autophagy and aging. Cell *146*, 682–695.

Sancak, Y., Bar-Peled, L., Zoncu, R., Markhard, A.L., Nada, S., and Sabatini, D.M. (2010). Ragulator-Rag complex targets mTORC1 to the lysosomal surface and is necessary for its activation by amino acids. Cell *141*, 290–303.

Sandoval, D., Cota, D., and Seeley, R.J. (2007). The integrative role of CNS fuel-sensing mechanisms in energy balance and glucose regulation. Annu. Rev. Physiol. *70*, 513–535.

Seino, Y., Fukushima, M., and Yabe, D. (2010). GIP and GLP-1, the two incretin hormones: Similarities and differences. J. Diabetes Investig. *1*, 8–23.

Settembre, C., Di Malta, C., Polito, V.A., Arencibia, M.G., Vetrini, F., Erdin, S., Erdin, S.U., Huynh, T., Medina, D., Colella, P., et al. (2011). TFEB links autophagy to lysosomal biogenesis. Science *332*, 1429–1433.

Shackelford, D.B., and Shaw, R.J. (2009). The LKB1-AMPK pathway: metabolism and growth control in tumour suppression. Nat. Rev. Cancer *9*, 563–575.

Sharlow, E.R., Giridhar, K.V., LaValle, C.R., Chen, J., Leimgruber, S., Barrett, R., Bravo-Altamirano, K., Wipf, P., Lazo, J.S., and Wang, Q.J. (2008). Potent and selective disruption of protein kinase D functionality by a benzoxoloazepinolone. J. Biol. Chem. *283*, 33516–33526.

Shigihara, N., Fukunaka, A., Hara, A., Komiya, K., Honda, A., Uchida, T., Abe, H., Toyofuku, Y., Tamaki, M., Ogihara, T., et al. (2014). Human IAPP-induced pancreatic β cell toxicity and its regulation by autophagy. J. Clin. Invest. *124*, 3634–3644.

da Silva Xavier, G., Leclerc, I., Salt, I.P., Doiron, B., Hardie, D.G., Kahn, A., and Rutter, G.A. (2000). Role of AMP-activated protein kinase in the regulation by glucose of islet beta cell gene expression. Proc. Natl. Acad. Sci. *97*, 4023–4028.

Sobota, J.A., Bäck, N., Eipper, B.A., and Mains, R.E. (2009). Inhibitors of the V0 subunit of the vacuolar H+-ATPase prevent segregation of lysosomal- and secretory-pathway proteins. J. Cell Sci. *122*, 3542–3553.

Speliotes, E.K., Willer, C.J., Berndt, S.I., Monda, K.L., Thorleifsson, G., Jackson, A.U., Allen, H.L., Lindgren, C.M., Luan, J. 'an, Mägi, R., et al. (2010). Association analyses of 249,796 individuals reveal 18 new loci associated with body mass index. Nat. Genet. *42*, 937–948.

Sumara, G., Formentini, I., Collins, S., Sumara, I., Windak, R., Bodenmiller, B., Ramracheya, R., Caille, D., Jiang, H., Platt, K.A., et al. (2009). Regulation of PKD by the MAPK p38delta in insulin secretion and glucose homeostasis. Cell *136*, 235–248.

Talchai, C., Xuan, S., Lin, H.V., Sussel, L., and Accili, D. (2012). Pancreatic β cell dedifferentiation as a mechanism of diabetic β cell failure. Cell *150*, 1223–1234.

Thorens, B. (2014). Neural regulation of pancreatic islet cell mass and function. Diabetes Obes. Metab. *16 Suppl 1*, 87–95.

Trayhurn, P. (2005). Endocrine and signalling role of adipose tissue: new perspectives on fat. Acta Physiol. Scand. *184*, 285–293.

Trudeau, K.M., Colby, A.H., Zeng, J., Las, G., Feng, J.H., Grinstaff, M.W., and Shirihai, O.S. (2016). Lysosome acidification by photoactivated nanoparticles restores autophagy under lipotoxicity. J. Cell Biol. *214*, 25–34.

Velikkakath, A.K.G., Nishimura, T., Oita, E., Ishihara, N., and Mizushima, N. (2012). Mammalian Atg2 proteins are essential for autophagosome formation and important for regulation of size and distribution of lipid droplets. Mol. Biol. Cell *23*, 896–909.

Wei, W.-H., Hemani, G., Gyenesei, A., Vitart, V., Navarro, P., Hayward, C., Cabrera, C.P., Huffman, J.E., Knott, S.A., Hicks, A.A., et al. (2012). Genome-wide analysis of epistasis in body mass index using multiple human populations. Eur. J. Hum. Genet. *20*, 857–862.

Weir, G.C., and Bonner-Weir, S. (2013). Islet β cell mass in diabetes and how it relates to function, birth, and death. Ann. N. Y. Acad. Sci. *1281*, 92–105.

Woods, A., Dickerson, K., Heath, R., Hong, S.-P., Momcilovic, M., Johnstone, S.R., Carlson, M., and Carling, D. (2005). Ca2+/calmodulin-dependent protein kinase kinase-beta acts upstream of AMP-activated protein kinase in mammalian cells. Cell Metab. *2*, 21–33.

Wu, N., Zheng, Shaywitz, A., Dagon, Y., Tower, C., Bellinger, G., Shen, C.-H., Wen, J., Asara, J., McGraw, T.E., et al. (2013). AMPK-dependent degradation of TXNIP upon energy stress leads to enhanced glucose uptake via GLUT1. Mol. Cell *49*, 1167–1175.

Xu, G., Chen, J., Jing, G., and Shalev, A. (2012). Preventing β-cell loss and diabetes with calcium channel blockers. Diabetes *61*, 848–856.

Yabe, D., and Seino, Y. (2011). Two incretin hormones GLP-1 and GIP: comparison of their actions in insulin secretion and β cell preservation. Prog. Biophys. Mol. Biol. *107*, 248–256.

Yamaguchi, H., Arakawa, S., Kanaseki, T., Miyatsuka, T., Fujitani, Y., Watada, H., Tsujimoto, Y., and Shimizu, S. (2016). Golgi membrane-associated degradation pathway in yeast and mammals. EMBO J. *35*, 1991–2007.

Yang, J., Carra, S., Zhu, W.-G., and Kampinga, H.H. (2013). The regulation of the autophagic network and its implications for human disease. Int. J. Biol. Sci. *9*, 1121–1133.

Yang, T., Espenshade, P.J., Wright, M.E., Yabe, D., Gong, Y., Aebersold, R., Goldstein, J.L., and Brown, M.S. (2002). Crucial step in cholesterol homeostasis: sterols promote binding of SCAP to INSIG-1, a membrane protein that facilitates retention of SREBPs in ER. Cell *110*, 489–500.

Young Oh, Talukdar, S., Bae, E.J., Imamura, T., Morinaga, H., Fan, W., Li, P., Lu, W.J., Watkins, S.M., and Olefsky, J.M. (2010). GPR120 is an omega-3 fatty acid receptor mediating potent anti-inflammatory and insulin-sensitizing effects. Cell *142*, 687–698.

Zhang, C.-S., Jiang, Li, M., Zhu, M., Peng, Y., Zhang, Y.-L., Wu, Y.-Q., Li, T.Y., Liang, Y., Lu, Z., et al. (2014). The lysosomal v-ATPase-Ragulator complex is a common activator for AMPK and mTORC1, acting as a switch between catabolism and anabolism. Cell Metab. *20*, 526–540.

Zhang, Y.-L., Guo, H., Zhang, C.-S., Lin, S.-Y., Yin, Z., Peng, Y., Luo, H., Shi, Y., Lian, G., Zhang, C., et al. (2013). AMP as a low-energy charge signal autonomously initiates assembly of AXIN-AMPK-LKB1 complex for AMPK activation. Cell Metab. *18*, 546–555.

Annexes

INSULIN GRANULES

Insulin secretory granules control autophagy in pancreatic β cells

Alexander Goginashvili,[1] Zhirong Zhang,[1] Eric Erbs,[1] Coralie Spiegelhalter,[1] Pascal Kessler,[1] Michael Mihlan,[1] Adrien Pasquier,[1] Ksenia Krupina,[1] Nicole Schieber,[2] Laura Cinque,[3] Joëlle Morvan,[1] Izabela Sumara,[1] Yannick Schwab,[2] Carmine Settembre,[3,4] Romeo Ricci[1,5]*

Pancreatic β cells lower insulin release in response to nutrient depletion. The question of whether starved β cells induce macroautophagy, a predominant mechanism maintaining energy homeostasis, remains poorly explored. We found that, in contrast to many mammalian cells, macroautophagy in pancreatic β cells was suppressed upon starvation. Instead, starved β cells induced lysosomal degradation of nascent secretory insulin granules, which was controlled by protein kinase D (PKD), a key player in secretory granule biogenesis. Starvation-induced nascent granule degradation triggered lysosomal recruitment and activation of mechanistic target of rapamycin that suppressed macroautophagy. Switching from macroautophagy to insulin granule degradation was important to keep insulin secretion low upon fasting. Thus, β cells use a PKD-dependent mechanism to adapt to nutrient availability and couple autophagy flux to secretory function.

Upon feeding, the pancreatic β cell catabolizes nutrients to secrete insulin. Conversely, insulin secretion decreases upon fasting (*1*). A shortage of nutrients also induces macroautophagy (hereafter referred to as "autophagy"). During autophagy, cellular components are sequestered into autophagosomes and degraded upon targeting to lysosomes (autolysosomes). Resulting catabolites maintain cells in a metabolically active state and ensure cell survival (*2*). However, catabolism of nutrients could also trigger insulin release, which should be avoided during fasting. Autophagy might thus be a bad strategy for a β cell to cope with nutrient deprivation. Both induction and lack of induction of autophagy have been reported in fasted β cells (*3, 4*). We thus wanted to assess the importance of autophagy in fasted β cells.

Microtubule-associated protein 1 light chain 3 B (LC3B) incorporates into membranes of autophagosomes (*5*). Unexpectedly, INS1 cells (a rat insulinoma–derived β cell line) exogenously expressing LC3B tagged with green fluorescent protein (GFP) (LC3B-GFP) deprived of serum and amino acids or glucose (Glc), but not of serum alone, decreased LC3B-GFP puncta (fig. S1, A to C). Conversely, starved human embryonic kidney (HEK) 293 cells increased LC3B-GFP puncta (fig. S1, D and E) (*6*). INS1 cells endogenously expressing LC3B-GFP ($INS1^{LC3B\text{-}GFPendo}$ cells) (fig. S2, A to C) treated without or with bafilomycin A1 (BafA1), which blocks autolysosomal degradation of LC3B (*7*), decreased LC3B-GFP puncta upon starvation (Fig. 1A and fig. S2, D to F). Tandem RFP-GFP–tagged LC3 (ptfLC3; RFP, red fluorescent protein) allows for discrimination of yellow fluorescent autophagosomes and red fluorescent autolysosomes (*8*). Multiple RFP-GFP puncta were converted into RFP-only puncta upon the onset of starvation. A reduction in RFP puncta and no reappearance of RFP-GFP puncta were observed over time (fig. S3, A and B). Correlative light and electron microscopy (CLEM) confirmed their autophagic origin (Fig. 1B). Moreover, lipidated autophagosomal LC3B (LC3B-II) decreased in starved INS1 cells in the absence and presence of BafA1 (Fig. 1C). In contrast, starvation increased LC3B-II in HEK293 cells (fig. S4). p62 binds polyubiquitinylated substrates for targeting to autophagosomes (*9*). p62 was moderately increased during starvation, independent of BafA1 (Fig. 1C). p62 puncta clustered and increased in size (fig. S5A). Accordingly, p62/LC3B-GFP colocalization was decreased, indicating suppressed autophagy-dependent clearance of p62. ATG16L1 binds to preautophagosomes (*10*). ATG16L1- and ATG16L1/LC3B-GFP–positive puncta moderately decreased upon starvation (fig. S5B). Quantitative electron microscopy (QEM) confirmed reduced autophagic compartments in β cells of starved murine primary islets (fig. S6). Moreover, in LC3B-GFP–expressing mice (*11*), autophagosomes decreased in β cells upon fasting (Fig. 1D and fig. S7). What about other secretory cells, in which nutrients do not act as secretagogues? In contrast to β cells, primary murine plasma cells induced autophagy upon starvation, whereas secretion of immunoglobulin G was reduced (fig. S8, A and B). Thus, nutrient-sensing β cells appear to use a distinct mechanism to overcome shortage of nutrients.

Targeting of secretory granules (SGs) to lysosomes might be an alternative strategy (*12*). Lysosomal Lamp1 and SG protein Phogrin colocalized close to the Golgi upon starvation in INS1 cells. Lysosomal inhibitors (LIs) increased their colocalization (fig. S9, A to C). QEM, immunogold labeling, and CLEM revealed abundant granule-containing lysosomes (GCLs) (fig. S10, A to D). We next used density gradients to purify GCLs (see supplementary materials and methods). Upon starvation, Phogrin- and lysosomal Lamp2-positive signals shifted to heavier fractions containing GCLs. LC3B was almost undetectable in shifted fractions, suggesting independence of GCLs from autophagy (Fig. 2A). Accordingly, starvation did not increase LC3B-GFP/Phogrin colocalization (fig. S11). Moreover, inactivation of autophagy did not change the amount of GCLs in starved cells (fig. S12, A and B).

Secretory granules are generated at the Golgi. Proinsulin, a marker for nascent SGs (*13*), markedly decreased upon starvation (Fig. 2B). Its reduction was partially restored by LIs. Abundant GCLs were confirmed ex vivo by QEM of starved primary murine islets (Fig. 2C and fig. S13A). In fasted GFP-LC3B–expressing mice, Lamp2 and proinsulin/insulin [(Pro)insulin] colocalization increased, whereas there was no increase in LC3B-GFP/(Pro)insulin colocalization (Fig. 2D and fig. S13, B and C). Thus, β cells employ starvation-induced nascent granule degradation (SINGD) instead of autophagy during fasting.

Lysosome-derived amino acids induce translocation of mechanistic target of rapamycin (mTOR) complex 1 (mTORC1) to lysosomal membranes, mTORC1 activation (*14, 15*), and subsequent suppression of autophagy (*16–18*). The mTOR inhibitors rapamycin and torin 1 increased the number of LC3B-GFP puncta in starved INS1 cells (Fig. 3A). Moreover, starvation localized mTOR to Phogrin/Lamp1-positive puncta close to the Golgi (Fig. 3B). mTORC1 suppresses starvation-induced autophagy through phosphorylation of Unc-51–like kinase 1 (ULK1) (*19*). Indeed, phospho-ULK1 remained high upon starvation and was abolished by rapamycin, whereas mTORC1-mediated phosphorylation of S6K1 (*20*) diminished during starvation (Fig. 3C). Accordingly, S6K1 phosphorylation was shown to require higher mTOR activity than ULK1 phosphorylation (*21*). Moreover, starvation led to formation of large phospho-ULK1 puncta that colocalized with Lamp1/Phogrin (fig. S14, A and B). Thus, nutrient depletion leads to induction of SINGD that locally activates mTOR to suppress autophagy.

Fasting suppresses both insulin secretion and autophagy. Would insulin secretion increase if autophagy is induced upon starvation? Keeping autophagy high by rapamycin precluded suppression of insulin secretion in INS1 cells (fig. S15). We next used tat-beclin1 (*22*) to specifically trigger autophagy in β cells of murine primary islets upon nonstimulatory Glc (fig. S16, A and B). Tat-beclin1 increased insulin secretion

[1]Institut de Génétique et de Biologie Moléculaire et Cellulaire (IGBMC), INSERM, CNRS, Université de Strasbourg, 67404 Illkirch, France. [2]Cell Biology and Biophysics Unit, European Molecular Biology Laboratory (EMBL), 69117 Heidelberg, Germany. [3]Dulbecco Telethon Institute and Telethon Institute of Genetics and Medicine (TIGEM), 80131 Naples, Italy. [4]Medical Genetics, Department of Medical and Translational Science Unit, Federico II University, Via Pansini 5, 80131 Naples, Italy. [5]Nouvel Hôpital Civil, Laboratoire de Biochimie et de Biologie Moléculaire, Université de Strasbourg, 67091 Strasbourg, France.
*Corresponding author. E-mail: romeo.ricci@igbmc.fr

to levels comparable with those observed upon stimulatory Glc (fig. S16C). Potassium channel closure that evokes calcium influx and exocytosis of SGs (*1*) was required, as the potassium channel activator diazoxide abolished this effect (fig. S16D). Insulin secretion was also potentiated by tat-beclin1 in murine islets at stimulatory Glc, which was blocked by diazoxide (fig. S16, E and F). Tat-beclin1 also increased insulin secretion from ex vivo fasted human islets (Fig. 3D and fig. S17, A and B). Thus, SINGD-mediated suppression of autophagy is important to keep insulin secretion low during fasting.

Protein kinase D (PKD) controls insulin SG biogenesis at the Golgi (*23*, *24*). Thus, PKD inactivation could have an effect on the turnover of nascent SGs. Indeed, inhibition of PKD decreased the amount of proinsulin (Fig. 4A). Proinsulin biosynthesis was unchanged in PKD1-depleted cells (fig. S18, A and B). However, accumulation of newly formed insulin was decreased, suggesting enhanced degradation of de novo synthesized insulin (fig. S18C). QEM and immunogold analyses revealed abundant GCLs in the Golgi area (Fig. 4B and fig. S19, A and B), which was further corroborated by subcellular fractionation (fig. S19C). PKD inhibition increased Phogrin/Lamp1 colocalization, which was more prominent upon LI treatment (fig S19, D to F). Phogrin/LC3B-GFP colocalization remained unchanged (fig. S20). mTOR largely colocalized with Lamp1 (Fig. 4C), and phospho-ULK1 was increased (Fig. 4D) in PKD1-depleted cells. PKD1 knockdown decreased accumulation of LC3B-II in the presence of BafA1 (fig. S21A). Moreover, PKD inhibition decreased LC3B-GFP puncta in absence and presence of BafA1 (fig. S21B).

If PKD controls SINGD, its activity should be regulated by nutrients. PKD activity at the Golgi decreased upon starvation (fig. S22, A and B). Loss of the p38δ kinase leads to activation of PKD in β cells (*23*). GCLs were markedly decreased in β cells of ex vivo fasted *p38δ* knockout ($p38\delta^{-/-}$) islets (Fig. 4E and fig. S23A). Accordingly, (Pro)insulin/Lamp2 colocalized to a lesser extent in β cells of fasted $p38\delta^{-/-}$ mice (fig. S23, C and D), suggesting that high PKD activity prevents SINGD. In contrast, autophagic compartments were increased in fasted $p38\delta^{-/-}$ β cells, indicating that SINGD-dependent suppression of autophagy was diminished (Fig. 4E and fig. S23B). Thus, PKD is a major regulator of SINGD and autophagy in β cells.

Altogether, inactivation of PKD evokes SINGD, localized activation of mTOR, and suppression of autophagy, which is critical to prevent insulin release during fasting. On the other hand, PKD activity is required for SG biogenesis (Fig. 4F). Because the nascent SGs are preferentially secreted (*25*), SINGD-mediated suppression of autophagy may represent an optimal strategy to counteract insulin secretion, at the same time providing sufficient nutrients. Because SINGD-mediated suppression of autophagy depends on abundant nascent SGs, their depletion will probably derepress autophagy without increasing insulin release. Timing when depletion occurs may vary substantially depending on the models and protocols used and may thus explain previously

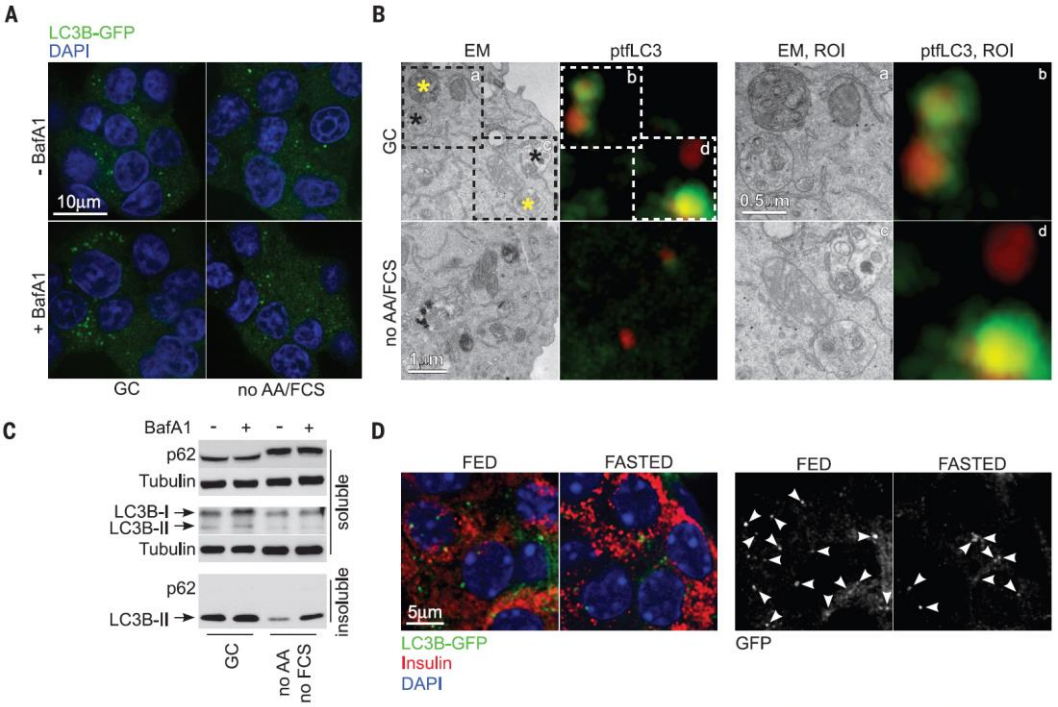

Fig. 1. Nutrient depletion suppresses autophagy in β cells. (**A**) LC3B-GFP puncta in INS1$^{LC3B\text{-}GFPendo}$ cells under growing culture (GC) and no amino acids and fetal calf serum (AA/FCS) for 1 hour in the absence and presence of BafA1 (10 nM). DAPI, 4′,6-diamidino-2-phenylindole. (**B**) CLEM of ptfLC3-expressing INS1 cells under GC and no AA/FCS for 2 hours. Regions of interest (ROI) are indicated with labeled dashed squares. Yellow and black asterisks indicate autophagosomes and autolysosomes, respectively. EM, electron microscopy. (**C**) Immunoblot of LC3B and p62 using soluble and insoluble fractions of lysates of INS1 cells under GC and no AA/FCS for 1.5 hours, nontreated or treated with 1 nM BafA1 for the last hour of incubation. Glyceraldehyde-3-phosphate dehydrogenase (GAPDH) served as a loading control. (**D**) Immunofluorescence (IF) of LC3B-GFP puncta (white arrowheads) and insulin (red) in β cells in islets of fed and fasted LC3B-GFP–expressing mice. The nuclei were stained with DAPI.

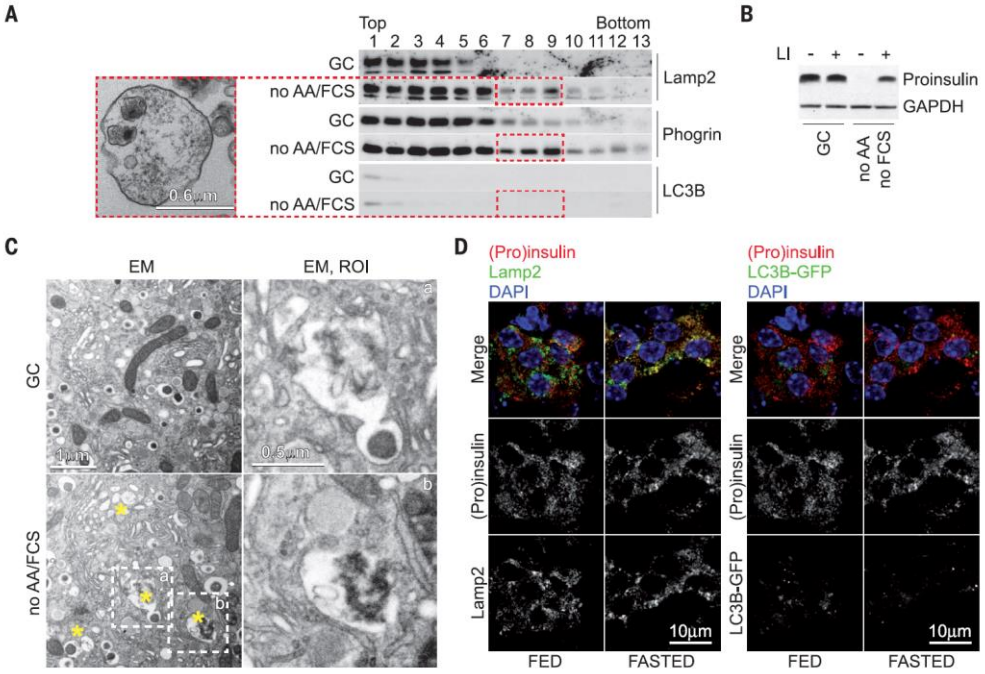

Fig. 2. Nutrient depletion induces SINGD in β cells. (**A**) Immunoblot of Lamp2, Phogrin, and LC3B using lysates of indicated fractions from INS1 cells under GC and no AA/FCS for 30 min. EM of GCLs in shifted fractions is indicated by red dashed boxes. (**B**) Immunoblot of proinsulin using lysates of INS1 cells treated or not with LIs under GC and no AA/FCS for 6 hours. GAPDH was served a loading control. (**C**) EM of Golgi areas in primary murine islets under GC and no AA/FCS for 2 hours. Yellow asterisks indicate GCLs. ROI are indicated with dashed squares. (**D**) IF of (Pro)insulin and Lamp2 (left) and (Pro)insulin and LC3B-GFP (right) in β cells in islets of fed and fasted LC3B-GFP expressing mice. The nuclei were stained with DAPI.

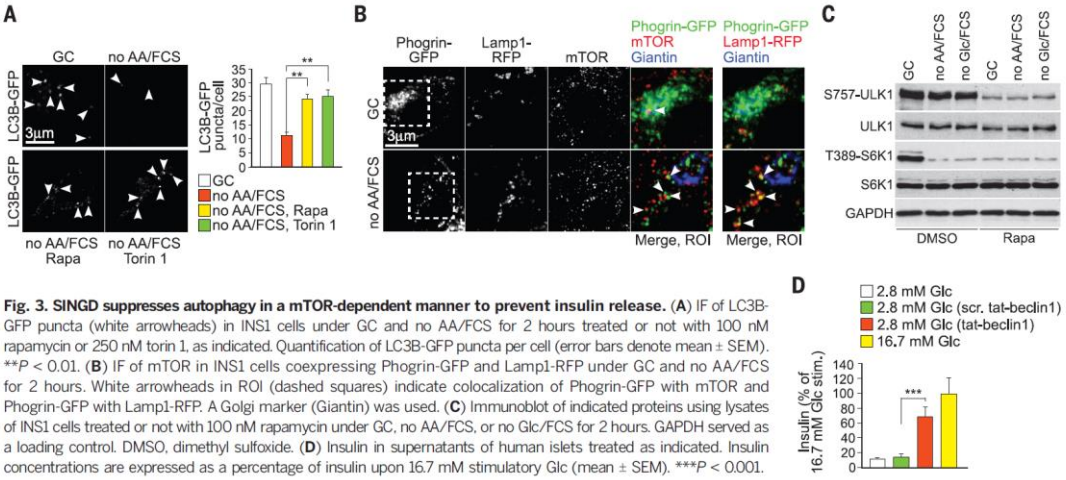

Fig. 3. SINGD suppresses autophagy in a mTOR-dependent manner to prevent insulin release. (**A**) IF of LC3B-GFP puncta (white arrowheads) in INS1 cells under GC and no AA/FCS for 2 hours treated or not with 100 nM rapamycin or 250 nM torin 1, as indicated. Quantification of LC3B-GFP puncta per cell (error bars denote mean ± SEM). $^{**}P < 0.01$. (**B**) IF of mTOR in INS1 cells coexpressing Phogrin-GFP and Lamp1-RFP under GC and no AA/FCS for 2 hours. White arrowheads in ROI (dashed squares) indicate colocalization of Phogrin-GFP with mTOR and Phogrin-GFP with Lamp1-RFP. A Golgi marker (Giantin) was used. (**C**) Immunoblot of indicated proteins using lysates of INS1 cells treated or not with 100 nM rapamycin under GC, no AA/FCS, or no Glc/FCS for 2 hours. GAPDH served as a loading control. DMSO, dimethyl sulfoxide. (**D**) Insulin in supernatants of human islets treated as indicated. Insulin concentrations are expressed as a percentage of insulin upon 16.7 mM stimulatory Glc (mean ± SEM). $^{***}P < 0.001$.

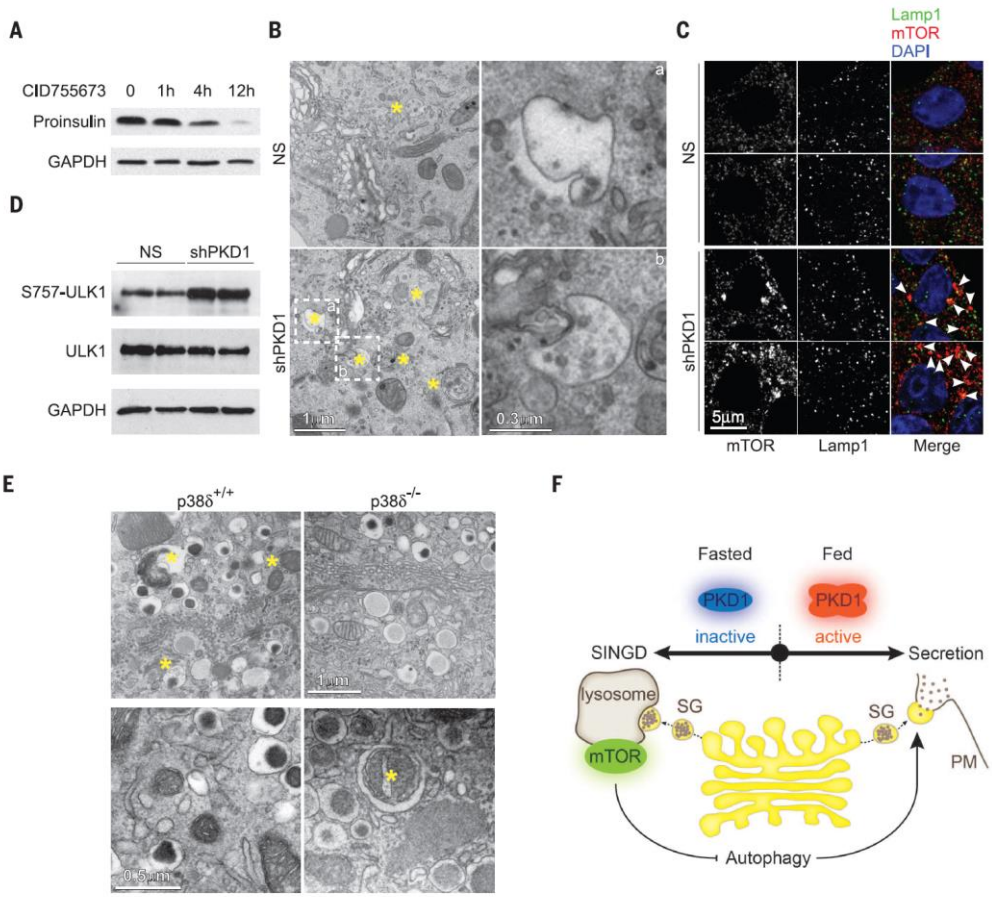

Fig. 4. PKD controls SINGD. (**A**) Immunoblot of proinsulin using lysates of INS1 cells treated with CID755673 for the indicated times. GAPDH served as a loading control. (**B**) EM of Golgi areas in nonsilenced (NS) and PKD1-depleted (shPKD1) INS1 cells. Yellow asterisks indicate GCLs. ROI are indicated with dashed squares. (**C**) IF of mTOR and Lamp1 in nonsilenced and PKD1-depleted INS1 cells. White arrowheads indicate colocalization of mTOR with Lamp1. Nuclei were stained with DAPI. (**D**) Immunoblot of indicated proteins using lysates of nonsilenced and PKD1-depleted INS1 cells. GAPDH served as a loading control. (**E**) (Top) EM of Golgi areas of fasted β cells in primary islets of $p38\delta^{+/+}$ and $p38\delta^{-/-}$ mice. Yellow asterisks indicate GCLs. (Bottom) EM of cytoplasm of fasted β cells in primary islets of $p38\delta^{+/+}$ and $p38\delta^{-/-}$ mice. The yellow asterisk indicates an autophagosome. (**F**) Model linking SINGD, secretion, and autophagy. PM, plasma membrane.

described inconsistencies (*3*). Accordingly, prolonged fasting of mice can induce autophagy in β cells (*26*). Our model could also explain the regulation of autophagy despite constitutively high adenosine monophosphate–activated protein kinase activity in β cells (*27*).

Our data show that triggering autophagy results in increased secretion of insulin. Although this should be avoided during fasting, it may be beneficial when insulin demands are high; for example, after a meal or in diabetes (*28*). The positive correlation between autophagy and insulin secretion may suggest an involvement of autophagy in postprandial insulin release, probably going beyond the widely established housekeeping role of autophagy.

REFERENCES AND NOTES

1. P. Rorsman, M. Braun, *Annu. Rev. Physiol.* **75**, 155–179 (2013).
2. J. D. Rabinowitz, E. White, *Science* **330**, 1344–1348 (2010).
3. C. Ebato *et al.*, *Cell Metab.* **8**, 325–332 (2008).
4. R. Singh, A. M. Cuervo, *Cell Metab.* **13**, 495–504 (2011).
5. I. Tanida, T. Ueno, E. Kominami, *Int. J. Biochem. Cell Biol.* **36**, 2503–2518 (2004).
6. Y. Kabeya *et al.*, *EMBO J.* **19**, 5720–5728 (2000).
7. A. Yamamoto *et al.*, *Cell Struct. Funct.* **23**, 33–42 (1998).
8. S. Kimura, T. Noda, T. Yoshimori, *Autophagy* **3**, 452–460 (2007).
9. G. Bjørkøy *et al.*, *J. Cell Biol.* **171**, 603–614 (2005).
10. N. Fujita *et al.*, *Mol. Biol. Cell* **19**, 2092–2100 (2008).
11. N. Mizushima, A. Yamamoto, M. Matsui, T. Yoshimori, Y. Ohsumi, *Mol. Biol. Cell* **15**, 1101–1111 (2004).
12. R. E. Smith, M. G. Farquhar, *J. Cell Biol.* **31**, 319–347 (1966).
13. D. F. Steiner, D. Cunningham, L. Spigelman, B. Aten, *Science* **157**, 697–700 (1967).
14. R. Zoncu *et al.*, *Science* **334**, 678–683 (2011).
15. Y. Sancak *et al.*, *Science* **320**, 1496–1501 (2008).
16. L. Yu *et al.*, *Nature* **465**, 942–946 (2010).
17. C. Betz, M. N. Hall, *J. Cell Biol.* **203**, 563–574 (2013).
18. S. G. Kim, G. R. Buel, J. Blenis, *Mol. Cells* **35**, 463–473 (2013).
19. J. Kim, M. Kundu, B. Viollet, K. L. Guan, *Nat. Cell Biol.* **13**, 132–141 (2011).

20. R. B. Pearson *et al.*, *EMBO J.* **14**, 5279–5287 (1995).
21. S. A. Kang *et al.*, *Science* **341**, 1236566 (2013).
22. S. Shoji-Kawata *et al.*, *Nature* **494**, 201–206 (2013).
23. G. Sumara *et al.*, *Cell* **136**, 235–248 (2009).
24. H. Gehart *et al.*, *Dev. Cell* **23**, 756–768 (2012).
25. G. Gold, M. L. Gishizky, G. M. Grodsky, *Science* **218**, 56–58 (1982).
26. K. Fujimoto *et al.*, *J. Biol. Chem.* **284**, 27664–27673 (2009).
27. G. A. Rutter, G. Da Silva Xavier, I. Leclerc, *Biochem. J.* **375**, 1–16 (2003).
28. M.-S. Lee, *Trends Endocrinol. Metab.* **25**, 620–627 (2014).

ACKNOWLEDGMENTS

We thank H. de F. Magliarelli, H. Gehart, O. Sumara, G. Sumara, N. Djouder, E. Hafen, R. J. Loewith, J. Klumperman, E. Polishchuk, R. Polishchuk, and all current members of the Ricci laboratory for critical scientific inputs. We thank A. Hausser for providing G-PKDrep-live, G. Rutter for providing Phogrin-GFP, J. Hutton (deceased) and H. Davidson for an antibody against Phogrin, and J. Klumperman for an antibody against Lamp1. We thank M. Koch, N. Messaddeq, and C. Ruhlmann for support in imaging; N. Mizushima for providing GFP-LC3 transgenic mice; and P. Halban and J.-I. Miyazaki for sharing the MIN6B1 cell line. This work was supported by a European Research Council (ERC) starting grant (ERC-2011-StG, 281271-STRESSMETABOL) and a European Foundation for the Study of Diabetes/Lilly European Diabetes Research Programme grant. A.G. and Z.Z. were supported by the ERC grant, M.M. was supported by a fellowship of the Deutsche Forschungsgemeinschaft, A.P. was supported by an IGBMC Ph.D. fellowship, K.K. was supported by a fellowship (Bourse Régionale de Recherche from region Alsace and INSERM), I.S. was supported by the Action Thématique et Incitative sur Programme (ATIP)–Avenir program, L.C. and C. Spiegelhalter were supported by a Telethon Grant, and N.S. and Y.S. were supported by EMBL internal funding. A.G. and R.R. have applied for a patent that protects autophagy-inducing molecules to increase insulin release.

SUPPLEMENTARY MATERIALS

www.sciencemag.org/content/347/6224/878/suppl/DC1
Materials and Methods
Figs. S1 to S23
References (*29*–*36*)

9 November 2014; accepted 5 January 2015
10.1126/science.aaa2628

Résumé en français

Pour fonctionner correctement, tout système a besoin d'énergie. Chez les organismes vivants, les nutriments représentent la principale source d'énergie. Les nutriments les plus communs pour notre organisme sont le glucose et sucres dérivés, les acides aminés et les lipides (Efeyan et al. 2015). Pour les êtres humains, ces nutriments sont issus de la nourriture provenant de notre alimentation. Chez tous les organismes l'absence de nutriment est délétère voir à long terme létale, c'est pourquoi chaque espèce vivante a développé des mécanismes pour détecter et stocker les nutriments, afin d'assurer leur présence et disponibilité pour l'organisme quel que soit la situation. En période d'abondance, les nutriments peuvent être stockés. Au contraire, en période de faible apport, comme lors d'un jeun, les réserves de nutriments préalablement stockées peuvent être réquisitionnées. Les organismes unicellulaires étant directement exposés aux nutriments venant de leur environnement, la régulation des nutriments se limitent chez eux à l'échelle cellulaire. Chez les organismes complexes, toutes les cellules ne sont pas en contact avec l'environnement extérieur et l'apport en nutriments aux différentes cellules doit se faire par un système de circulation. Les organismes supérieurs ont développés des organes spécialisés ayant pour fonction d'assurer l'apport en nutriments aux autres organes/cellules n'ayant pas les capacités de stockage et ne pouvant pas réquisitionner les nutriments pendant les périodes de mise à jeun. Cela implique un niveau de régulation supplémentaire à l'échelle de l'organisme. Chez les humains, les nutriments et l'homéostasie énergétique sont régulés principalement par des signaux hormonaux induisant de multiples voies de signalisation chez les cellules ciblées. La dérégulation de ces mécanismes est à l'origine de nombreuses maladies métaboliques, qui représentent à l'heure actuelle un problème de santé de plus en plus grave dans nos sociétés. L'introduction développera dans un premier temps les mécanismes impliqués dans la détection des nutriments et le stockage au niveau de l'organisme chez les mammifères. L'attention sera ensuite portée vers les mécanismes impliqués sur la régulation des nutriments à l'échelle cellulaire. La troisième partie de l'introduction détaillera la régulation des nutriments chez les cellules pancréatiques béta. La dernière partie de l'introduction portera sur l'implication du dérèglement de ces mécanismes dans la pathologie du diabète de type 2. Les résultats avec les conclusions seront ensuite présentés après avoir posé la problématique de cette thèse.

I) Détection et homéostasie du glucose à l'échelle de l'organisme

Chez les mammifères, les nutriments sont extraits de la nourriture dans la voie gastro-intestinale. Après avoir été digérés en petite molécules par les enzymes digestives, les nutriments passent la barrière intestinale et arrivent dans le sang où ils peuvent être transportés et distribués aux différents organes. Afin d'assurer son fonctionnement, l'organisme doit maintenir une distribution stable des nutriments même lorsque les apports extérieurs sont faibles. Il est donc important de stocker les nouveaux nutriments absorbés après consommation de nourriture afin de pouvoir les utiliser plus tard quand la nourriture se fait plus rare. Plusieurs organes comme les tissus adipeux, les muscles et le foie sont capables de stocker les nutriments lorsque l'organisme se nourrit, et de mobiliser ces nutriments lors des périodes de mise à jeun. Les nutriments sont délivrés aux organes par le sang, ce qui permet de détecter leurs niveaux et les niveaux énergétiques à différents niveaux. La régulation de l'homéostasie énergétique se fait par un réseau de régulation comprenant plusieurs organes périphériques comme les intestins, le foie, le cerveau, les muscles, les os, les tissus adipeux et le pancréas. En plus des lipides, des protéines ou des vitamines, la régulation des niveaux de glucose chez les mammifères et les humains est critique, et a donc était largement étudiée. La dérégulation des niveaux de glucose caractérise de nombreuses maladies métaboliques comme le diabète, une maladie métabolique menant à de sérieuses complications.

Le niveau sanguin de glucose, aussi appelé la glycémie, doit être gardé à des niveaux constants. Chez les humains, la glycémie optimale, ou euglycémie, est comprise entre 70mg/dL et 100mg/dL avant prise alimentaire. Une glycémie supérieure à 100mg/dL est appelée hyperglycémie. Une glycémie inférieure à 70mg/dL est appelée hypoglycémie. Après une prise alimentaire, le corps est exposé à une phase hyperglycémique et les niveaux de glucose sanguin doivent être diminués. A l'inverse, lors d'une période prolongée de mise à jeun, la glycémie doit être augmentée. Depuis près d'un siècle, il a été démontré que le retrait du pancréas entrainait une sévère hyperglycémie et le diabète, ce qui a mené à la conclusion que cet organe était absolument crucial dans le maintien d'une glycémie normale.

Le pancréas est composé de deux parties, le partie exocrine, qui représente environ 98% de l'organe et est responsable de la sécrétion d'enzyme de digestion dans la voie gastro-intestinale. Les 1-2% restant de l'organe est composée par la partie endocrine constituée par les ilots pancréatiques, aussi appelée ilots de Langerhans, qui sécrètent des hormones de régulation majeurs dans le sang. Les ilots pancréatiques sont composés par 5 types cellulaires différents sécrétant des hormones spécifiques : les cellules alpha secrètent le glucagon, les cellules béta co-sécrètent l'insuline, l'amyline et le C-peptide, les cellules gamma secrètent le polypeptide

pancréatique, les cellules delta sécrètent la somatostatine et les cellules epsilon sécrètent la ghrelin (Röder et al, 2016).

L'homéostasie du glucose est contrôlée par principalement deux hormones : l'insuline et le glucagon. Lors d'hyperglycémie, les cellules pancréatiques beta sécrètent de l'insuline dans le sang. L'insuline stimule la capture du glucose dans le foie, les muscles et les tissus adipeux. L'insuline promeut aussi la conversion du glucose en glycogène, un produit de stockage pour le court-terme, dans le foie par un procédé appelé glycogénèse. Par ces actions combinées, l'insuline diminue les taux de glucose sanguins. A l'opposée, l'hypoglycémie inhibe la sécrétion d'insuline et induit la sécrétion du glucagon dans le sang par les cellules alpha. Le glucagon stimule la conversion du glycogène en glucose par un procédé appelé glycogénolyse et la synthèse *de novo* de glucose par gluconeogénèse dans le foie, ce qui permet la restauration de l'euglycémie (Figure 1). Une description plus détaillée de l'action de ces deux hormones sur les différents organes périphériques est faite dans cette thèse.

Pour résumer, les ilots pancréatiques sont centraux dans la régulation de l'homéostasie du glucose. Leurs interactions complexes et réciproques avec les autres organes par des signaux hormonaux, des neuropeptides et des cytokines permettent à l'organisme de réagir de manière adaptée aux changements des niveaux de nutriments et d'utiliser de manière optimale les énergies stockées dans les organes de stockages lors des périodes de faibles apports en nutriments. La prochaine partie introduit très brièvement les différents mécanismes de détections et régulation des nutriments connus agissant non plus au niveau de l'organisme mais au niveau cellulaire.

II) Détection et homéostasie des nutriments à l'échelle de cellulaire

Une fois que les nutriments sont distribués aux cellules grâce au système vasculaire, ils sont utilisés et transformés par la cellule pour en tirer de l'énergie. La détection par la cellule des nutriments peut se faire par différents moyens comme par exemple l'attachement direct de la molécule à son détecteur, ou par des mécanismes indirects reposant sur la détection de molécules substituts renvoyant aux niveaux d'abondance des nutriments (Efayan et al, 2015). Les niveaux de lipides et de glucose sont plutôt détectés par des senseurs spécifiques directs. Un autre moyen pour la cellule de réguler son activité en fonction des ressources disponible est de sentir les niveaux d'énergie, issus de la dégradation des nutriments. Lors de l'épuisement des niveaux d'énergie, la cellule peut sentir cette baisse et réagir de manière adaptée en diminuant les mécanismes cellulaires les plus énergivores et en favorisant l'activation des mécanismes permettant la génération d'énergie. Un des acteurs majeurs pour cette régulation

est le complexe protéique AMPK, qui détectent les variations des niveaux des molécules énergétiques AMP/ADP/ATP. Au contraire, lors de phases riches en nutriments, les cellules adaptent leur métabolisme pour s'étendre et proliférer. Un des acteurs majeurs impliqué dans cette adaptation est le complexe protéique mTORC1 qui favorise l'activation des mécanismes impliqués dans la croissance et la prolifération, mécanisme gourmands en énergie, et au contraire inhibe les mécanismes de sauvegarde et de stockage de l'énergie. Lors d'une mise à jeun prolongée, les cellules peuvent aussi déclencher un processus d'auto-cannibalisme cellulaire appelée autophagie afin de générer de nouveaux nutriments. Il est intéressant de noter qu'un type d'organelle est commun à ces mécanismes de détections et régulations cellulaire des nutriments : les lysosomes. Les lysosomes sont des organelles acides impliqués dans la dégradation des composants cellulaires, et jouent un rôle majeur dans l'autophagie. De plus l'activité des complexes AMPK et mTORC1 peut être régulée à la membrane des lysosomes ce qui place les lysosomes au centre de la régulation cellulaire des nutriments. Chaque mécanisme de régulation cellulaire est décrit en détail dans la thèse. Ces mécanismes sont communs à la plupart des cellules eucaryotes, nous souhaitions savoir si ces mécanismes s'appliquaient aussi pour des cellules spécialisées dans la régulation des nutriments à l'échelle de l'organisme comme les cellules béta.

III) Les nutriments contrôlent l'action des cellules béta

Les cellules pancréatiques béta dépendent fortement du métabolisme de leurs nutriments pour activer leur fonction principale : la sécrétion de l'insuline. Pour cette raison le métabolisme du glucose dans les cellules béta exerce des fonctions uniques (Prentki et al, 2013). Par exemple, a l'opposé de la plupart des cellules, les cellules pancréatiques beta peuvent activer le métabolisme du glucose sans avoir besoin de stimulations hormonales ou neuronales extracellulaires additionnelles : la seule présence du glucose entraine son métabolisme dans les cellules béta. L'activité de l'AMPK a déjà était largement étudié dans les cellules béta dans le début des années 2000. Récemment l'inhibition de l'autophagie a été impliquée dans la mise en échec des cellules béta lors de stress métaboliques. En effet, sa fonction de maintenance est nécessaire aux cellules béta pour faire face à la production massive de granule d'insuline pour répondre aux stress métabolique tel que l'obésité et la résistance à l'insuline. En effet, la délétion de gènes autophagiques cruciaux dans les ilots pancréatiques *in vivo* a mené à l'augmentation de l'apparition du diabète chez des modèles animaux (Lee, 2014). De plus l'inhibition de l'autophagie par l'activation dépendante au palmitate de mTORC1 favorise la mort des cellules béta (Choi et al., 2008). Enfin l'autophagie est importante pour retirer la

formation des IAPP, un facteur important dans l'apparition du diabètes chez les humains (Rivera et al., 2014) (Kim et al., 2014) (Shigihara et al., 2014) (Osório, 2014). Du fait de leur rôle unique dans l'homéostasie du glucose à l'échelle de l'organisme, les cellules béta n'utilisent pas les mêmes voies métaboliques que la plupart des cellules pour générer leur énergie. Par exemple, lors de leur développement, les cellules pancréatiques béta inhibent l'expression de l'enzyme lactate dehydrogenase (LDH), qui convertie le lactate en pyruvate, et le transporteur de monocarboxylate (MCT1 aussi connu sous le nom SLC16A1) à la membrane plasmique, qui permettent conjointement le transport du lactate et du pyruvate à l'intérieur des cellules. La faible expression de la MCT et de la LDH permettent de rendre la réponse de sécrétion d'insuline spécifique seulement au glucose et non au pyruvate et lactate, ce qui permet d'empêcher la sécrétion d'insuline lors d'efforts physiques, générateurs de lactate et pyruvate. En effet une sécrétion d'insuline inappropriée lors d'un effort physique pourrait entrainait une phase d'hypoglycémie à l'échelle de l'organisme. Notre équipe a découvert un nouveau mécanisme cellulaire similaire, spécifique et nécessaire aux cellules béta, leur permettant de faire face à un manque en nutriment sans enclencher la sécrétion d'insuline (Goginashvili et al 2015).

La plupart des cellules de mammifères déclenchent l'autophagie lors d'une mise à jeun et la baisse de l'apport en nutriments par le milieu extérieur. Nous avons découvert qu'au contraire les cellules béta employaient un mécanisme différent. A la place de l'autophagie, les cellules beta à jeun induisent la dégradation de leurs nouveaux granules d'insuline (les granules d'insuline naissants) à proximité de l'appareil de Golgi par fusion directe avec les lysosomes, un phénomène que nous avons appelé Starvation-Induced Nascent Granule Degradation (SINGD). Ce processus est indépendant des mécanismes moléculaires typique impliquée pour l'autophagie. De façon surprenante, l'activité de l'autophagie semble être très élevée en conditions riche en nutriments. En effet, le nombres d'autophagosomes, les vésicules à double membranes responsables de l'englobement des composants devant être dégradés par autophagie, était très élevé chez les cellules beta sous conditions riche en nutriments, et baissait dramatiquement lors de la mise à jeun des cellules (Goginashvili et al 2015). Ceci peut s'expliquer par la nécessité d'avoir un mécanisme de maintenance efficace dans les cellules lorsqu'elles doivent générer de grande quantité d'insuline. De plus nous avons aussi observé que le déclenchement de l'autophagie favorisait la sécrétion d'insuline même sous des niveaux de glucose équivalent à une phase hypoglycémique. Cette observation explique la raison pour laquelle l'autophagie n'est pas utilisée par les cellules béta lors d'une baisse en apport en

nutriment, afin d'éviter la sécrétion inappropriée des granules d'insuline qui serait extrêmement dommageable à l'échelle de l'organisme lors une période de mise à jeun (Goginashvili et al 2015). En dégradant leurs granules d'insuline naissants, ceux préférentiellement sécrétés, les cellules pancréatiques béta peuvent regagner des nutriments, et ainsi maintenir leur homéostasie énergétique, sans sécréter d'insuline. Nous avons aussi montré que le SINGD activait le complexe mTORC1 ce qui menait à l'inhibition de l'autophagie. Au niveau des mécanismes moléculaires, nous avons observé que la diminution des nutriments s'accompagnait par la diminution de l'activité d'une autre kinase, la protéine kinase D (PKD) au niveau de l'appareil de Golgi et que l'inactivation de la PKD déclenchait la mise en place du SINGD. Par conséquent, les cellules béta emploient un mécanisme dépendant de la PKD pour s'adapter aux niveaux de nutriment disponibles tout en couplant les flux de l'autophagie avec leur fonction de sécrétion.

La protein kinase D1 (PKD1) est une kinase sérine/thréonine dépendante de la voie calcium/calmoduline qui peut s'attacher aux membranes lipidiques du Trans-Golgi Network (TGN) ainsi qu'à la membrane plasmique. Il a été montré que son activité était dépendante de la kinase p38delta qui peut directement l'inhiber par la phosphorylation de sa sérine 397 et 401 (Sumara et al., 2009). Suite à la délétion du gène codant pour la p38delta, La PKD1 est activée de manière chronique, ce qui entraine l'augmentation des niveaux totaux d'insuline et des niveaux de sécrétion d'insuline en réponse au glucose (Sumara et al., 2009). Il est intéressant de constater que la protéine p38delta est seulement exprimée dans le pancréas (Sumara et al. 2009). La PKD1 peut aussi réguler la formation de vésicules de transport au TGN en augmentant l'activité de protéines modifiant les lipides comme la Phosphatidylinositol 4 kinase beta (PI4KIIIbeta), qui convertit les PI en PI4P au TGN (Hausser et al., 2005). De plus l'activité de PKD1 impacte directement la formation des granules d'insuline par le contrôle qu'elle exerce sur la protéine Arfaptine 1, une protéine permettant la séparation des granules d'insuline du TGN seulement après leur pleine maturation. Il est intéressant de noter qu'arfaptine 1 est aussi recruter au TGN par la présence de PI4P (Cruz-Garcia et al., 2013). Il a été montré que le silencing de PKD1 ou son inhibition sont dommageable pour la sécrétion d'insuline et le contenu total d'insuline dans les cellules béta. (Sumara et al. 2009)(Goginashvili et al 2015). Lors d'une mise à jeun, il a été montré que l'activité de PKD1 baissait de manière remarquable en parallèle aux niveaux de l'autophagie dans les cellules béta. Parce qu'il a été montré que les niveaux de SINGD et de l'activité de PKD1 jouaient tous les deux un rôle sur le nombre des granules d'insuline lors d'une mise à jeun, nous souhaitions savoir si un mécanisme similaire

pouvait se dérouler de manière inappropriée lors de troubles métaboliques tel que le diabète de type 2, ou le dérèglement des niveaux d'insuline et du fonctionnement des cellules béta ont un impact critique.

IV) Le diabète de type 2 et les cellules pancréatique béta

Le diabète est une maladie métabolique caractérisée par une hyperglycémie chronique résultant d'une faible action de l'insuline, d'une faible sécrétion ou de la combinaison des deux. L'hyperglycémie chronique mène à de nombreuses complications incluant les rétinopathies, les néphropathies, les neuropathies ainsi que des altérations macrovasculaires (Fowler, 2008). Alors que le diabète de type 1 (DT1) est principalement causé par la destruction auto-immune des cellules pancréatiques béta, le diabète de type 2 (DT2) est un déséquilibre métabolique caractérisé par une hyperglycémie dans un contexte de résistance à l'insuline et un manque relatif d'insuline (Kumar et al, 2015). Le DT2 est une maladie multifactorielle ayant des origines génétiques et environnementales (Hu et al., 2001). L'obésité et le mode de vie sédentaire sont fortement liés avec l'apparition de cette maladie. En parallèle à l'augmentation de la prévalence de l'obésité à l'échelle mondiale, la prévalence du DT2 augmente aussi et il y a maintenant plus de 370 millions de patients diabétiques diagnostiqués dans le monde. le DT2 est caractérisé par plusieurs causes métaboliques, les principaux étant la dysfonction des cellules béta et la résistance à l'insuline des tissus périphériques (Kahn et al., 2013). La résistance périphérique à l'insuline est une condition physiopathologique dans laquelle les tissus périphériques, comme les muscles, le foie et les tissus adipeux échouent à répondre correctement à l'action normale de l'insuline en capturant le glucose sanguin (Meszaros, 2015 thèse). La résistance à l'insuline est fortement liée à l'obésité et à l'augmentation des graisses à l'intérieur de l'organisme. Elle dépend de mécanismes extrinsèques comme les adipokines, les taux plasmatiques élevés d'acide gras libre et les cytokines pro-inflammatoires mais aussi de mécanismes intrinsèques provoqués par une accumulation anormale des lipides intracellulaires, le stress oxidatif, le dysfonctionnement des mitochondries et le stress du Réticulum endoplasmique (Trayhurn, 2005). Cependant la résistance à l'insuline ne peut pas être considérée comme l'unique facteur favorisant l'apparition du DT2. En effet, la plupart des personnes obèses et insulino-résistantes ne deviennent pas diabétiques. Les patients obèses ne deviennent diabétiques que si leur cellules pancréatiques béta échouent à fournir les quantités d'insuline nécessaires (Weir et Bonner-Weir, 2013). La résistance à l'insuline induit d'abord une phase de compensation caractérisée par une augmentation de la masse et de la fonction des cellules béta par la prolifération des cellules existantes et/ou de la néogenèse, la formation *de*

novo de cellules pancréatiques beta (Levetan, 2010). La compensation à la résistance à l'insuline est aussi accomplie par une augmentation de capacité de sécrétion des cellules béta menant à des phénotype hyperinsulinémiques, l'augmentation des concentration plasmatiques de l'insuline (Jetton et al., 2005). En opposition aux individus pré-diabétiques insulino-résistants, la masse des cellules pancréatiques béta est grandement diminuée chez les patients diabétiques terminaux en raison de l'échec des cellules béta (Maclean and Ogilvie, 1955)(Butler et al., 2002).

L'échec des cellules béta a longtemps était considéré comme résultant de la perte et la mort des cellules béta (Halban et al., 2014). Bien que cela soit le résultat final, de nombreux mécanismes peuvent mener à cette perte des cellules béta. Le point de vue classique où l'apoptose est la responsable principale de la perte des cellules béta est de plus en plus discuté et complémenté par d'autre concepts. Par exemple il a été montré que les cellules béta pouvaient subir simultanément une dé-différentiation en cellules alpha, delta ou gamma par l'inhibition de l'action de facteurs de transcription clé dans le maintien de l'identité des cellules béta (Talchai et al., 2012).

V) But du projet

Nos travaux précédents ont révélé qu'en réponse à une mise à jeun, les cellules béta induisaient le ciblage des granules d'insuline naissants vers les lysosomes. Ce nouveaux processus a pour conséquence d'induire la diminution des niveaux d'insuline dans les cellules béta et d'inhiber l'autophagie, deux processus retrouvés pendant le DT2. Nous souhaitions savoir si ce processus pouvait aussi être augmenté de manière inappropriée lors de situations de stress métaboliques et pendant un DT2 menant à la mise en échec des cellules béta.

VI) Le ciblage des granules d'insuline vers des compartiments positifs pour CD63 est augmenté chez les cellules pancréatiques béta en condition diabétiques

Le SINGD est caractérisé par la dégradation lysosomale des granules d'insuline, de l'activation locale de mTORC1 et l'inhibition de la PKD1. Afin de savoir si un processus similaire au SINGD se déroule pendant le DT2, nous avons décidé d'évaluer ces caractéristiques dans différents modèles de diabètes. Je me suis d'abord concentré sur le modèle déjà bien établi des souris *ob/ob* déficientes pour la leptine dans le fond génétique BTBR (Clee et al., 2005)(O'Brien et al., 2014)(Xu et al., 2012). Les souris *ob/ob* sont homozygotes pour une mutation sur le gène *leptin* menant à la perte de fonction de la protéine leptine, ce qui entraine un phénotype d'hyperphagie accompagné d'une prise rapide de poids et une obésité morbide. La souche en fond génétique BTBR est caractérisée par une résistance à l'insuline remarquable

(Ranheim et al. 1997). La combinaison de la mutation ob et du fond génétique BTBR résulte en une obésité sévère et un diabète avancé chez les souris BTBR *ob/ob* en moins de 8 semaines. L'analyse par microscopie électronique d'ilots pancréatique a confirmé la baisse du nombre des granules d'insuline chez les souris diabétiques en comparaison aux souris contrôles. Il est important de noter que le nombre de lysosomes contenant des granules d'insuline (LCGs) était fortement augmenté par au moins un facteur 2 chez les cellules pancréatiques béta des souris diabétiques en comparaison à des souris contrôles de même âge et sexe. Le paradigme dans le domaine est que la perte des granules d'insuline en conditions diabétiques est due à leur sursécrétion en dehors des cellules en conséquence de l'hyperglycémie chronique. Notre observation suggère la possibilité que l'augmentation de la dégradation des granules d'insuline puisse aussi contribué à la perte des granules d'insuline lors du DT2.

Afin de mieux caractériser les changements au niveau des compartiments lysosomaux, nous avons réalisé une analyse par immunofluorescence sur des ilots pancréatiques provenant de ces souris avec des anticorps ciblant les quatre marqueurs de lysosomes principaux : LAMP1, LAMP2, CD63 et LIMP2, en co-marquant les granules d'insuline. Ce premier criblage a révélé que le signal de CD63 était grandement augmenté dans les cellules pancréatiques béta provenant d'ilots de souris BTBR *ob/ob* en comparaison aux contrôles. Les analyses par RT-qPCR et Western Blots ont révélé que l'expression de CD63 était de fait augmentée dans les ilots provenant des souris diabétiques en comparaison aux ilots de souris contrôles. Afin de mieux évaluer la localisation de CD63 en relations avec les granules d'insuline, nous avons ensuite utilisé la lignée de cellules pancréatiques béta INS1-E dérivée d'un insulinome de rat. Afin de reproduire *in vitro* des conditions diabétiques, nous avons soumis ces cellules à des environnements glucolipotoxiques avec des milieux contenant des concentrations élevés de glucose et d'acide gras libre comme décrit précédemment. (Gjoni et al., 2014)(Oh et al., 2013. En accord avec nos premières observations sur les ilots diabétiques, les niveaux de signal de CD63 étaient augmentés sous conditions glucolipotoxiques en comparaison aux contrôles. CD63 co-localisait fortement avec les granules d'insuline à proximité de l'appareil de Golgi sous conditions glucolipotoxiques en comparaison aux contrôles, ce qui indique un ciblage potentiel des granules d'insuline vers les compartiments positif à CD63. Afin de mieux comprendre les dynamiques induisant la co-localisation entre les structures positive à CD63 et les granules d'insuline, nous avons décidé de générer à l'aide de la technologie CRISPR-Cas9 une lignée cellulaire INS1 double knock-in marquant de manière endogène CD63 et la protéine membranaire des granules d'insuline phogrin avec respectivement le tag DsRed et GFP. Après

vérification de la bonne génération de notre outil nous avons soumis cette nouvelle lignée cellulaire à des conditions glucolipotoxiques. De nouveaux nous avons observé une augmentation de la colocalisation entre les compartiments positifs à CD63 et les granules d'insuline. Une quantification non-biaisée a été effectuée en utilisant des coefficients de corrélation de Pearson basée sur une analyse utilisant des seuils d'intensité de signal déterminée de manières automatiques. Ensemble ces résultats confirment notre première observation et suggère que le mécanisme de dégradation lysosomale des granules d'insuline pourrait être augmenté lors d'un DT2.

Lors de notre étude précédente nous avons trouvé que la dégradation lysosomale des granules d'insuline en réponse à une privation de nutriments inhibait aussi l'autophagie par une voie dépendante à mTORC1. Nous nous sommes donc demandé si le ciblage augmenté des granules d'insuline vers les compartiments positifs à CD63 sous conditions diabétiques était accompagnée par une inhibition de l'autophagie. De fait il a été montré que la suppression de l'autophagie était impliquée dans l'échec des cellules béta. J'ai donc souhaité évaluer les niveaux de l'autophagie lors de conditions diabétiques. J'ai évalué les flux autophagiques en mesurant les niveaux cellulaires de la protéine p62 sur des ilots pancréatiques provenant de souris diabétiques ou contrôles. La protéine p62 est une protéine adaptatrice qui s'attache aux agrégats protéiques polyubiquitinés et à la protéine LC3-II présente à la membrane des autophagophores. La fusion entre l'autophagosome et les lysosomes entraine la dégradation de p62. L'analyse des niveaux de p62 donne donc des informations importantes quant aux niveaux des flux autophagiques. Les niveaux de p62 étaient augmentés dans les ilots provenant des souris diabétiques en comparaison aux contrôles ainsi que dans les cellules INS1 soumises aux conditions glucolipotoxiques en comparaison aux conditions contrôles. Afin d'évaluer la formation des autophagosomes, nous avons utilisé une lignée cellulaire INS1 knock-in exprimant LC3 fusionné avec GFP (Goginashvili et al., 2015). Cette lignée cellulaire permet de visualiser en temps réel la protéine LC3B. Dans cette lignée cellulaire la formation des autophagosomes peut être détectée sous forme de points fluorescents. En comptant le nombre de points nous avons observé que le nombre d'autophagosomes était diminué en réponse à un traitement prolongé en conditions glucolipotoxiques en comparaison aux contrôles. L'analyse par immunoblot en utilisant des anticorps contre LC3 a confirmé cette première observation. De plus, le blocage de la fusion entre les lysosomes et les autophagosomes en utilisant l'inhibiteur d'autophagie et de lysosomes Bafilomycine A1 a aussi montré une diminution des

niveaux de LC3-II en conditions glucolipotoxiques en comparaison aux contrôles. Nous en avons conclu que le ciblage des granules d'insuline aux lysosomes est associé à une diminution des flux autophagiques, ce qui contribue ensemble à l'échec des cellules béta. Notre étude montre que la formation des LCGs coïncide avec une réduction globale de l'autophagie, ce qui suggère que l'autophagie n'est pas la voie première pour la dégradation des granules d'insuline lors d'un diabète.

Afin de mieux évaluer la dégradation lysosomale des granules en comparaison à l'autophagie, nous avons traité nos cellules double knock-in CD63-DsRed/Phogrin-GFP avec de la Bafilomycine A1. La Bafilomycine A1 est un composé qui en plus d'inhiber la fusion entre les autophagosomes et les lysosomes inhibe l'acidification des lysosomes en bloquant la pompe à proton vATPase, empêchant la dégradation des composants à l'intérieur des lysosomes. Le traitement pendant 4h avec de la Bafilomycine A1 a mené une colocalisation remarquable entre CD63 et phogrin en comparaison aux contrôles. Ce résultat nous permet de conclure qu'une quantité importante des granules d'insuline peut être potentiellement ciblée et dégradée par les lysosomes d'une manière indépendante de l'autophagie. Les lysosomes sont des centres de détection des nutriments pour la cellule. La dégradation de l'insuline dans les lysosomes devrait en principe relâcher des nutriments qui peuvent recruter mTORC1. Nous avons donc décidé d'évaluer le recrutement de mTORC1 à la membrane des compartiments positifs à CD63 et savoir 'il était augmenté en conditions glucolipotoxiques en comparaison aux contrôles.

Sous conditions glucolipotoxiques, une forte augmentation du recrutement de mTORC1 aux structures positives à CD63 est observée. Le recrutement de mTORC1 à la membrane des lysosomes entraine son activation. Par conséquent, l'augmentation de l'activité de mTORC1 peut contribuer à l'inhibition de l'autophagie. Ensemble ces résultats indiquent que le ciblage des granules d'insuline aux compartiments positifs à CD63 est augmenté pendant un stress glucolipotoxique et que cela recrute mTORC1 à la membrane lysosomale entrainant sans doute son activation et l'inhibition de l'autophagie. Pour déterminer l'importance de CD63 pour l'homéostasie des granules d'insuline nous avons décidé de silencer CD63 dans les cellules INS1 et d'évaluer les niveaux d'insuline après un choc gluclolipotoxiques.

Après vérification de l'efficacité du silencing induite par notre pool de siARN par immunofluorescence, nous n'avons pas détectée de différence notable entre les cellules traitées

avec un si-contrôle ou les cellules traitées avec le pool de siARN ciblant CD63. Cependant, lorsque les cellules knock-down ont été soumises à un stress glucolipotoxiques le silencing de CD63 permettait le maintien des niveaux d'insuline en comparaison aux cellules traitées avec in si-control. De plus l'analyse par immunofluorescence en utilisant des anticorps spécifiques pour l'insuline a révélé que le knock down de CD63 induisait le retour des granules d'insuline à la membrane en comparaison aux cellules contrôles sous conditions glucolipotoxiques. Ensemble ces résultats indiquent que CD63 contribue à la dégradation des granules d'insuline.

Comme introduit précédemment, le mécanisme SINGD est contrôlé par la kinase PKD1. Nous souhaitions donc savoir si PKD1 pouvait avoir un impact sur notre processus lors d'un DT2.

VII) L'inhibition de PKD contribue à la mise en échec des cellules béta lors d'un diabète

L'analyse par Western blot sur des lysats provenant d'ilots pancréatiques de souris diabétiques ou contrôle a révélé que l'expression de PKD était diminuée chez les ilots diabétiques en comparaison aux contrôles. De plus l'analyse par RT-qPCR nous a montré que des 3 membres de la famille des PKD, PKD1 était la plus abondante. De manière importante, la transcription de PKD1 était réduite par 2 fois en comparaison aux ilots provenant de souris contrôles. De manière similaire l'analyse par western blot sur des lysats provenant de cellules traitées sous conditions glucolipotoxiques a aussi révélé une diminution dans les niveaux d'expression des PKD. Etant donné que les conditions glucolipotoxiques induisent la colocalisation entre les compartiments positifs pour CD63 et les granules d'insuline, et en même temps diminue l'expression de PKD1, nous nous sommes demandé si l'activité de PKD1 était impliquée dans le ciblage des granules d'insuline vers les lysosomes.

Nous avons évalué le rôle de l'activité de PKD1 en utilisant l'inhibiteur spécifique des PKD, CID755673 (Sharlow et al., 2008). Notre laboratoire a montré que le traitement des cellules INS1 avec l'inhibiteur CID mène à la perte d'insuline via l'augmentation de leur dégradation lysosomale (Goginashvili et al., 2015). Nous avons confirmé la perte d'insuline chez les ilots pancréatiques murins et humains sous traitement avec CID. Je voulais ensuite savoir si l'inhibition de PKD menait à une augmentation du ciblage des granules d'insuline vers les compartiments positifs à CD63. Pour cela, nous avons traitées les cellules double knock-in CD63-DsRed/Phogrin-GFP avec du CID ou DMSO comme contrôle. En comparaison aux

contrôles, nous avons observé une augmentation de colocalisation entre CD63 et phogrin lors du traitement avec CID.

Afin de déterminer si CD63 était impliqué dans la voie de dégradation lysosomale des granules d'insuline dépendante à la PKD, nous avons effectué un knock-down de CD63 sur des cellules exprimant de manière chronique des shARN ciblant la PKD1. L'analyse par western blot de ces cellules a révélé une restauration des niveaux d'insuline chez les cellules INS1-shPKD1 traitée avec siARN CD63 en comparaison aux cellules INS1-shPKD1 seulement traitées avec des si-control. Ce résultat indique que CD63 agit en aval de PKD1 pour la dégradation lysosomale.

Nous voulions ensuite évaluer l'impact de l'inhibition de PKD1 *in vivo* dans un contexte diabétique. Pour cela nous avons implantée des pompes osmotiques Alzet® contenant du CID ou le solvant seul comme control dans des souris diabétique BTBR *ob/ob.* Le traitement au CID a accéléré l'apparition du diabète de manière remarquable en comparaison aux souris contrôles. Cette accélération était accompagnée par une perte de poids importante, une sécrétion d'insuline diminuée en réponse au glucose, ainsi qu'une baisse totale de la quantité d'insuline dans les cellules pancréatiques béta chez les souris traitées au CID. Afin de mieux comprendre la raison de la perte d'insuline chez les cellules pancréatiques béta nous avons réalisé une analyse quantitative par microscopie électronique des cellules pancréatiques beta. Une augmentation importante des LCGs a été observée pour les cellules pancréatiques béta provenant des souris traitées en comparaison aux souris contrôles ce qui indique que la perte d'insuline chez les cellules béta est la conséquence d'une dégradation lysosomale augmentée. Pour résumer nous avons trouvé que les niveaux de PKD1 étaient diminués lors d'un diabète chez les souris ou un stress glucolipotoxiques chez les cellules INS1. L'inhibition de la PKD mène à l'augmentation du ciblage des granules d'insuline vers les lysosomes et les compartiments positifs à CD63. L'inhibition *in vivo* de PKD entraine une accélération de l'apparition du diabète chez les souris BTBR *ob/ob* suite à l'augmentation des LCGs et à la perte de l'insuline chez les cellules pancréatiques beta. Au contraire, il a été montré que l'activation de la PKD était bénéfique pour lutter contre le diabète (Sumara et al., 2009). Nous souhaitions donc évaluer l'impact que pourrait avoir l'activation de la PKD lors d'un DT2.

VIII) L'activation de la PKD mène à la restauration des niveaux d'insuline et une homéostasie du glucose améliorée chez les souris.

L'activation de la PKD1 dans les souris knock-out p38delta induit la baisse de la dégradation lysosomale des granules d'insuline (Goginashvili et al., 2015). Nous nous sommes donc demandé si l'inhibition de la p38delta, résultant en l'activation de PKD1, par voie pharmacologique pouvait être bénéfique dans un contexte diabétique. Grâce à la collaboration avec un partenaire industriel, nous avons généré un composé (dénommé RA) avec un fort pouvoir d'inhibition spécifique de la p38delta. Nous avons vérifié que l'inhibition de la p38delta induisait bien une activation de la PKD sur des ilots pancréatiques humains en comparaison à des ilots traités avec le solvant seul. Afin de tester notre composé en conditions diabétiques nous avons répété les implantations avec les pompes osmotiques cette fois-ci avec le composé RA. Nous avons observé un ralentissement clair dans l'apparition des symptômes diabétiques chez les souris BTBR *ob/ob* traitées avec RA en comparaison aux souris traitées avec la solution contrôle. Nous avons aussi mesuré la sécrétion d'insuline en réponse à une stimulation au glucose avec ou sans traitement au RA sur des ilots pancréatiques provenant de patient non diabétiques. Le RA n'induit pas d'effet sur la sécrétion en réponse au glucose. Cependant les ilots traités pour 48h avec le RA présentaient des niveaux d'insuline totaux plus élevés en comparaison aux ilots contrôles. Ce résultat a été confirmé par analyse immunoblot. Ensemble ces résultats suggèrent une implication de la dégradation lysosomale des granules d'insuline lors de la mise en échec des cellules béta pendant le DT2 et donnent de nombreuses évidences quant aux conséquences bénéfiques du ciblage de ce processus dans les cellules béta en tant que nouvelle approche thérapeutique pour le traitement du DT2.

Adrien PASQUIER

Lysosomal degradation of insulin granules promotes β-cell failure in type 2 diabetes

Résumé

Notre équipe a récemment découvert l'importance du ciblage des granules d'insuline aux lysosomes lors d'une mise à jeun chez les cellules pancréatiques β. Le diabète de type 2 (TD2) est caractérisé par la résistance à l'insuline couplé au dysfonctionnement des cellules β-et à leur perte. Je souhaitais évaluer le ciblage des granules d'insuline aux lysosomes dans le contexte diabétique. Grâce à un modèle murin, nous avons trouvé que le nombre des lysosomes contenant des granules d'insuline était augmenté chez les cellules β-provenant de souris diabétiques en comparaison aux contrôles. Ceci était accompagné par l'augmentation des niveaux de la protéine lysosomale CD63. Parce que PKD1 contrôle le ciblage des granules d'insuline aux lysosomes lors d'une mise à jeun, nous nous sommes demandé si PKD1 était importante lors d'un diabète de type 2. Dans nos modèles, les niveaux de PKD1 étaient diminués en conditions diabétiques en comparaison aux contrôles. De plus, l'inhibition de PKD1 entrainait l'augmentation du ciblage des granules d'insuline aux lysosomes et accélérait l'apparition du diabète dans notre modèle murin. Nous souhaitions ensuite savoir si l'activation de PKD1 dans les cellules pancréatiques β-pouvait être avantageuse dans un contexte diabétique. De fait, grâce à l'utilisation d'un composé spécifique, nous avons pu montrer que l'activation de PKD1 menait à l'augmentation des niveaux d'insuline sur des ilots pancréatiques humains et ralentissait l'apparition du diabète dans notre modèle murin. Pour conclure, j'ai aussi débuté la caractérisation des lysosomes sur d'autres types cellulaires des ilots pancréatiques. Nous avons observé que LIMP2, une autre protéine lysosomale, était fortement exprimée chez les cellules pancréatiques α.

Résumé en anglais

Our team recently uncovered the importance of the targeting of insulin granules to the lysosomal compartments in pancreatic β-cells during fasting. Type 2 Diabetes (T2D) is characterised by insulin resistance coupled with pancreatic β-cell failure which account for both β-cells dysfunction and β-cells death. I wanted to assess the targeting of insulin granule to the lysosomes in the context of T2D. Using murine diabetic model, we found that the number Granule-containing Lysosomes was enhanced in diabetic β-cells in comparison to controls. This was accompanied by an increase in the level of the lysosomal protein CD63. Because PKD1 controls the targeting of insulin granule to the lysosomes during fasting, I wondered if PKD1 was important during T2D. PKD1 levels were decreased in our diabetic models in comparison to controls. Moreover inhibition of PKD1 led to enhanced targeting of the insulin granules to the lysosomes and accelerated apparition of diabetes in our murine model. I also tested if activation of PKD1 in pancreatic β-cells could be beneficial in the context of diabetes. Indeed using a specific compound, we showed that PKD1 activation led to an increase in insulin levels and delayed onset of diabetes in our murine model. My work thus uncovered mechanisms underlying a fundamentally new process in β-cells with potential implications for novel therapeutic directions in T2D. Finally, I started to assess lysosomes in another pancreatic islets cell type. I found that LIMP2, another lysosomal membrane protein, was specifically highly expressed in the pancreatic α-cells.